HR Wallingford

CHANNEL PROTECTION
Turbulence downstream of structures

by M Escarameia and R W P May

Report SR 313
April 1992

Address: **Hydraulics Research Ltd,** Wallingford, Oxfordshire OX10 8BA, United Kingdom.
Telephone: 0491 35381 International + 44 491 35381 Telex: 848552 HRSWAL G.
Facsimile: 0491 32233 International + 44 491 32233 Registered in England No. 1622174

This report describes work funded by the Department of the Environment under Research Contract No 7/6/163. It is published on behalf of the Department of the Environment, but any opinions expressed in this report are not necessarily those of the funding Department. The work was carried out in the Research Department of HR Wallingford headed by Dr. W.R. White. The nominated project officers were Dr. R. Thorogood for DoE and Dr. W.R. White for HR Wallingford.

ABSTRACT

An experimental study, funded by the Department of the Environment, was made of the stability of riprap and concrete blocks for channel protection in highly turbulent environments.

An extensive literature review on riprap sizing formulae is presented in this report as well as some general background on turbulence generated downstream of hydraulic structures. It was found that the existing guidelines do not apply to highly turbulent flows and that the nominal stone size given by the different equations can vary as much as four times. This refers both to normal turbulent flows ie. natural, straight channels and to highly turbulent flows, ie. downstream of structures. In terms of weight the predictions vary by a factor of up to 64. Therefore any uncertainties may have major economic consequences.

Tests were carried out with six different stone sizes (D_{50} varied between 4.6 and 11.8mm) on a flat bed, and various turbulence levels. Tests were also performed with riprap placed on slopes of 1V:2.5H and 1V:2H to assess bank revetment stability. An Izbash-type equation for sizing riprap under normal and high turbulence conditions was obtained from the analysis of the test results. This equation incorporates a stability coefficient which quantitatively takes into account the turbulence level. The same equation was found to apply both to riprap on a flat bed and on bank slopes. No additional slope factor is required to define the stability of riprap on banks.

The performance of granular and synthetic filters was also investigated for riprap on a flat bed. The tests showed that a sand filter determined according to the usual Terzaghi rules destabilised the armour layer in highly turbulent environments. The performance of riprap incorporating a geotextile was approximately as good as the riprap without the granular filter.

The second part of the study was concerned with the stability of concrete blocks on a flat bed and on slopes of 1:2.5 and 1:2 as an alternative material to riprap. It was found that the same type of equation proposed for the design of riprap can be applied to concrete blocks on a flat bed and on slopes of 1:2.5 (or flatter). The thickness of the concrete blocks given by the equation is 75% of the size of riprap required for the same flow conditions.

LIST OF SYMBOLS

A	Coefficient in Jansen's equation; constant in Appendix B
a	Maximum linear dimension of a particle
B	Crest length
B_1	Coefficient in PIANC's equation
b	Intermediate dimension of a particle
C	Coefficient in Maynord's equation; stability coefficient in eqn (20)
C_1	Coefficient in Izbash's equation
C'	Coefficient in eqn (22)
c	Minimum dimension of a particle
D	Nominal particle size
D_n	Size of the equivalent cube $(= (\frac{M}{\rho s})^{1/3})$
D_s	Diameter of the equivalent sphere $(= (6\frac{M}{\pi \rho s})^{1/3})$
D_x	Dimension of stone which exceeds dimension of x% of the stones by weight
d_2	Theoretical tailwater depth
E	Constant in Appendix B
e	Voids ratio $(= V_v/V_s)$
Fr	Froude number of flow $(= U/(gy_o)^{0.5})$
Fr2	Froude number of flow $(= U/(gP)^{0.5})$
g	Acceleration due to gravity
H	Crest height
h	Height of a point (x, y, z) above a horizontal datum
J	Stability coefficient in eqn (24)
K	von Karman constant
K_h	Depth factor in Pilarczyk's equation (1990)
K_s	Slope factor in Pilarczyk's equation (1990)
K_T	Turbulence factor in Pilarczyk's equation (1990)
k_g	Permeability of a geotextile
k_s	Nikuradse's roughness height
L	Stability coefficient in eqn (25)
M_x	Mass of stone greater than that of stones in x% of the mixture by mass
m	Slope gradient in Appendix B
O	Opening size of a geotextile
P	Hydraulic depth defined as the flow area divided by the surface width
p	Pressure
r	Relative turbulence intensity in Pilarczyk's equation (1984)
S_f	Shape factor of stone $(= \frac{c}{(a\ b)^{0.5}})$
s	Specific gravity of stone
TI	Turbulence intensity $(= \frac{rms\ u}{\overline{u}})$
t	Time

LIST OF SYMBOLS (CONT'D)

U	Mean flow velocity in the channel
U_d	Depth-averaged velocity
u	Streamwise velocity component
u_m	Maximum velocity
u_*	Shear velocity
V	Instantaneous velocity
V_b	Mean velocity near the bed
V_s	Volume of solids
V_v	Volume of voids
v	Cross stream velocity component
W	Weight
W_x	Weight of stone greater than that of stones in x% of the mixture by weight
w	Vertical velocity component
y	Height above the bed
y_o	Total flow depth
z_o	"Roughness height"
α	Bank slope
β	Angle in the equation of the Department of Transport of State of California
γ	Coefficient in Pilarczyk's equation (1984)
γ_r	High turbulence factor in Pilarczyk's equation (1984)
Δ_m	Relative density of protection unit in Pilarczyk's equation (1990)
δ	Thickness of boundary layer
ν	Kinematic viscosity
ρ	Density of water
σ	Standard deviation
τ	Shear stress
ϕ	Internal friction angle of the stone; stability factor in Pilarczyk's equation (1990)
ψ_s	Shields parameter $\left(= \frac{\tau}{\rho\, g\, (s-1) D} \right)$
Ω	Factor for reduced stability of stones on banks
$'$	Fluctuation around the mean
$\bar{x}$	Time-averaged value of quantity x
rms	Root mean square value

$$\nabla^2 = \frac{\partial^2}{\partial x^2} + \frac{\partial^2}{\partial y^2} + \frac{\partial^2}{\partial z^2}$$

CONTENTS page

CONTENTS (CONT'D) page

CONTENTS (CONT'D)

FIGURES

PLATES

CONTENTS (CONT'D)

APPENDICES

1 INTRODUCTION

Flows downstream of structures such as gates, weirs and stilling basins can be highly turbulent and the velocity distributions very non-uniform. Channel protection is therefore normally required to prevent, or at least limit, the extent of scour produced by the flow on the river bed and banks. Riprap is one of the most widely used forms of flexible protection for natural and artificial watercourses. However, it was found from a survey carried out recently by HR Wallingford for a CIRIA project on channel protection (Hemphill and Bramley, 1989) that, despite a considerable amount of past research, many of the available design methods give widely-varying predictions of stable stone sizes. Such uncertainties can have major economic consequences: a typical difference of 30% in predicted stone size can increase the weight of the stone by a factor of 2.2.

The objectives of this research project were:

1 to carry out experimental work on riprap stability in high turbulence flows downstream of hydraulic structures, and

2 to investigate low-cost alternatives to riprap for channel protection.

The ultimate aim of this study was to produce guidelines for the design of stable protection of channels. This could be achieved by developing rational design formulae that relate the stability of a revetment to the local flow conditions and the degree of turbulence. Existing guidelines such as the ones given by the US Bureau of Reclamation are based on limited data and do not take quantitative account of highly turbulent flows. Current research being carried out by the US Army Corps of Engineers is concerned with the use of riprap for protection of stream banks against current attack; their work is applicable where uniform flow conditions in a channel determine the velocities around its perimeter.

It was also the purpose of this study to investigate the performance of filters in channel revetments to assess their suitability for highly turbulent environments. Where adequate supplies of stone are not available, the use of riprap for channel protection can be prohibitive. Although several low-cost alternatives have been tried (eg concrete blocks, gabion mattresses and semi-rigid systems), no rational criteria for their design have been developed so far. Basic research work was also needed in this area to determine their suitability and compare their performance with riprap. However, several of the possible low-cost revetments do not perform well in highly turbulent environments due to their low flexibility. It was therefore decided to test the performance of loose, solid concrete blocks, both on a flat bed and on banks of two different slopes.

Funding for this study was provided by the Construction Directorate of the Department of the Environment and the work was carried out between April 1989 and March 1992.

2 TURBULENCE

2.1 General concepts

Turbulence can be described as a process whereby the energy of an 'orderly' steady flow is converted into the random kinetic energy of eddies of decreasing sizes down to the molecular level. At this level the energy is transferred in the form of heat (Yuen and Fraser, 1979). The fluid particles move in extremely irregular paths producing instantaneous changes in the velocity direction and intensity. Due to the random nature of turbulent flows it is usual to consider the instantaneous velocity V (and other quantities such as the pressure) as the sum of two terms:

$$V = \overline{V} + V' \tag{1}$$

where

$\overline{V}$ is the time-averaged velocity responsible for

the transport of fluid particles and V' represents turbulent fluctuations around the mean.

The turbulent fluctuations introduce considerable additional shear stresses by increasing the momentum exchange rate when compared with laminar flow. As the flow paths are so erratic in turbulent flows, the velocity components in the three orthogonal directions (u, v and w) can assume similar importance. These components figure in the Navier-Stokes (N-S) equations for turbulent flows (see, for example, Tennekes and Lumley, 1972) as can be seen in the following three-dimensional form of the N-S equation in the x direction:

$$\frac{\partial \overline{u}}{\partial t} + \overline{u}\,\frac{\partial \overline{u}}{\partial x} + \overline{v}\,\frac{\partial \overline{u}}{\partial y} + \overline{w}\,\frac{\partial \overline{u}}{\partial z} = -\frac{\partial}{\partial x}\left(\frac{p}{\rho} + gh\right)$$

$$+\upsilon\nabla^2\,\overline{u} - \left[\frac{\partial \overline{u'u'}}{\partial x} + \frac{\partial \overline{u'v'}}{\partial y} + \frac{\partial \overline{u'w'}}{\partial z}\right] \qquad (2)$$

additional stress components
due to turbulence

For the definition of these variables refer to the list of symbols at the beginning of this report.

For the study of turbulent flows it is obviously important to assess the role of turbulent velocity fluctuations in relation to the time-averaged velocity, since these fluctuations can be larger than the average value. This can be done by determining the turbulence intensities, defined as:

$(\overline{u'^2})^{1/2}/\overline{u}$, $(\overline{v'^2})^{1/2}/\overline{u}$ and $(\overline{w'^2})^{1/2}/\overline{u}$

in the x, y and z direction, respectively. The numerators of these ratios give the standard deviation from the mean and are commonly known as the rms values. In fact, according to the definition, the standard deviation is given by:

$$\sigma = \left[\frac{1}{T}\,\lim_{T\to\infty}\int_0^T (V-\overline{V})^2 dt\right]^{1/2} = (\overline{V'^2})^{1/2} \qquad (3)$$

Turbulent flows are common in most engineering problems and, in particular downstream of hydraulic structures, where high velocity and pressure fluctuations usually impose considerable stress on the channel bed and banks. The type and extent of the protection required is very dependent on the level of turbulence and will be discussed in the next sections.

2.2 Turbulence produced in hydraulic jumps

Considerable research has been carried out to characterise turbulence downstream of structures such as weirs, sluice gates and spillways, where a hydraulic jump is formed to establish the transition from a supercritical to a subcritical flow (see Fig 1). The majority of these studies has been orientated towards the measurement and analysis of pressure forces, induced by the turbulent flow, on concrete slabs of stilling basins. This has been done in order to predict and, if possible, prevent excessive vibrations, cavitation erosion and the occurrence of damage in joints of slabs.

The highly turbulent nature of hydraulic jumps, which is in fact responsible for the dissipation of a considerable part of the energy of the supercritical flow, has been studied by several authors. Many of these studies have dealt with the analysis of pressure fluctuations beneath hydraulic jumps to determine their rms values and their frequency distribution (see, for example, Narayanan, 1978 and Lopardo et al, 1984). In most cases the analysis is confined to stilling basins; very little information is available on the characterisation of turbulence in areas downstream of stilling basins which may still require some protection. Campbell (1966) focused on the protection required for river beds and banks submitted to various levels of turbulence. The levels of turbulence considered were the levels expected in straight channels and energy dissipators such as small stilling basins. Small stilling basins were defined as having a length three times the theoretical tailwater depth d_2 or greater, and a design depth equal to d_2. 'Small turbulent basins' was the name given to basins with lengths smaller or equal to 2.5 times d_2 and a tailwater depth less than d_2. The stone weight and equivalent diameters necessary to protect the river bed are given on a chart. Campbell stresses, however, that these criteria are not suitable for large energy dissipation which should be studied in physical models.

3 CHANNEL PROTECTION-PREVIOUS STUDIES

3.1 Initiation of particle movement

The initiation of threshold movement can be taken as the beginning of the failure process of a river protection revetment. A shear stress is exerted on the bottom of the channel as a result of the water current action and determines the slope of the vertical velocity profile along the depth of the flow. Lift and drag forces are therefore present in this process. In turbulent flows the magnitude, direction and point of application of these forces are random quantities, fluctuating around their mean values. Even the laminar sublayer, normally considered to be dominated by viscosity, is affected by high energy eddies coming from the main turbulent flow. These generate 3-D high- and low-speed velocity bursts in the laminar sublayer (Raudkivi, 1990). On the other hand, the main flow is also influenced by the burst of low momentum fluid coming from the sublayer. This contributes to a local deceleration of the flow and generates more eddies. Rock protection revetments can start to move not only due to the shear force produced by the primary water current but also to the impulse drag exerted by a passing eddy or to a local decrease in pressure which generates uplift forces.

A number of factors can influence the initiation of particle motion, some of them due to the geotechnical characteristics of the rock, some to the layout of the revetment and others to the hydraulic features of the flow. Included in the geotechnical characteristics of the rock are the size, the specific weight, the surface roughness, the gradation and the porosity of the rockfill. The particle shape, defined by a suitable shape factor, may also be included in this group. Some tests have shown that flatter stones have a lower threshold velocity than standard quarry stone. However, tests performed at the Delft Hydraulics Laboratory, The Netherlands, with coarse particles showed no direct relationship between shape and threshold velocity for particles with the same nominal size (Pilarczyk, 1984). The effect of the gradation seems to be pronounced only for wide particle gradations: the finer particles are eroded first by the flow thus leaving a layer of coarser grains which prevents further scour. Associated with the gradation is the range of porosities that can be achieved for a particular rockfill. It seems probable that the higher the degree of compaction (ie the lower the porosity) the higher is the rock stability. However no systematic studies are known to have been carried out on this topic. One possible reason for this is that river protection downstream of hydraulic structures is normally done by dumping riprap on the river bed, so no mechanical compaction takes place.

3.2 Riprap design formulae

Since riprap is undoubtedly the most common material used as river bed protection, several guidelines on grading have been developed over the years based on experience as well as on common sense. These design criteria normally refer to the gradation in terms of stone weight rather than its dimension, to the thickness of the riprap blanket and to the ratio between the maximum and minimum dimensions of each block. An example of the lower and upper limits for grading riprap is given by Hemphill and Bramley (1989):

$$W_{100}/W_{50} = 2 \text{ to } 5$$
$$W_{85}/W_{50} = 1.7 \text{ to } 3.3 \qquad (4)$$
$$W_{15}/W_{50} = 0.1 \text{ to } 0.4$$
$$W_{85}/W_{15} = 4 \text{ to } 12$$

where W_x is the weight of the stone that is greater than that of x% of the stones by weight. Angular shaped stones are preferred to round stones because of increased stability, and the maximum dimension of each particle should not exceed three times the minimum dimension. Regarding the thickness of the riprap blanket, it can be taken to be at least 1 to 1.5 times the maximum diameter of the largest stones or twice the average diameter (Keown et al, 1977).

As an introductory note to the following literature review, it should be pointed out that, as expected, the design equations show a dependence of the stone size on a power of either the mean flow velocity U or the velocity near the bed V_b. However, the authors do not always make it clear which value of velocity is used in the different equations. Vague terms such as "local critical velocity" or "average critical velocity" were found in the literature search, and some uncertainty arises as to what definition of velocity has been adopted by the authors.

Raudkivi (1990) suggests the following simple relationship* as a first approach to sizing riprap protection on horizontal beds:

$$D_s = 0.0413\ V^2_b \qquad (5)$$

where

V_b = velocity near the bed, and
D_s = diameter of the equivalent sphere of specific gravity 2.65.

This author also developed a relationship combining the Manning-Strickler formulae with the Shields threshold criteria for unidirectional flow with the Shields parameter equal to 0.04 and specific gravity of stones of 2.65 (Raukdivi, 1990):

$$D = 4.5 \times 10^{-3}\ U^3/y_o{}^{0.5} \qquad (6)$$

* All equations given in this report are in SI units unless otherwise stated (eg the dimensions of the stone diameter are in metres and the flow velocity in m/s).

where

D = nominal size of the stone
y_o = flow depth, and
U = mean flow velocity

Peterka (1964) combining existing equations, laboratory results and prototype observations produced a curve for sizing riprap downstream of stilling basins. The curve gives an estimate of the stable size of most of the stones in a well graded mixture. His results can assume the following mathematical form:

$$D = 0.0376\ V_b^2 \qquad (7)$$

where

D = stone diameter, and
V_b = velocity near the bed

Peterka points out, however, that the curve is only tentative and therefore liable to modification resulting from further tests or more extensive field observations.

For the design of bank riprap subjected to currents moving parallel to the banks, Searcy (1967) recommends the use of two charts adapted from the Hydraulic Design Criteria, US Corps of Engineers (see Fig 2). It is a trial and error method which requires a first estimate of the stone size, the value of the total flow depth and the mean velocity. Then one of the charts allows the conversion of the average velocity in the channel into the velocity at stone level. This velocity is entered in the second chart which will give the equivalent spherical diameter (or weight) of stone for various bank slopes. For flow depths greater than 10ft the method suggests to reduce by 60% the observed flow depth when using the first chart. The resulting stone size is then considered to be stable not only at the toe of the bank but also closer to the water surface. However, the transition between these two different procedures is not absolutely clear.

The Department of Transportation of the State of California (1970) recommends the use of the following expression for the design of rock armour in slopes under current attack (note that this equation is in ft-s units):

$$W = \frac{0.00002 V_b^6 \, s \, \text{cosec}^3\,(\beta-\alpha)}{(s-1)^3} \qquad (8)$$

where

W = minimum weight in lb of outside stone for no damage; two thirds of stone should be heavier

V_b = stream velocity in ft/s to which the bank is exposed (assumed to be the velocity near the bed)

s = specific gravity of stone

β = 70° for randomly place rubble

α = face slope

Where no accurate velocity data are available V_b can be taken as 2/3 of the average stream velocity for parallel flow tangential to bank; for impinging flow against curved banks V_b can be taken as 4/3 of the average stream velocity. Where wave action dominates over current action the Department of Transportation of the State of California recommends the formulae used for shore protection schemes.

An experimental study of riprap stability in decelerating flow (as opposed to uniform flow) was carried out by Maynord (1978) using stone sizes with D_{50} between 7.9 and 11.3 mm, a bottom slope of 0.008 and various bank slopes. The following relationship was obtained:

$$D_{50}/y_o = CFr^3 \qquad (9)$$

where

y_o = water depth
Fr = Froude number of flow = $U/(gy_o)^{0.5}$
U = mean channel velocity
g = acceleration due to gravity
C = coefficient dependent on the channel geometry (straight or curved) and on location of riprap (bottom or slope). Different factors of safety can also be included in this coefficient.

For straight channels and bottom riprap, or slopes 1V:3H or flatter incipient motion conditions led to C = 0.22; for slopes 1V:2H incipient motion conditions led to C = 0.26. Maynord pointed out that in decelerating flows intense and irregular vorticity is generated which can resemble the turbulence downstream of a hydraulic structure. Hence the values of C refer to relatively high levels of turbulence. However, it should be noted that the experimental procedure used by this author only produced the additional turbulence associated with expansion in decelerating flows.

More recently, Maynord et al (1989) proposed another expression which is suitable for design of riprap in low turbulent environments, ie straight open channel flows. Unlike his previous equation, which was based on the Shields criterion and on the Manning-Strickler resistance equations, this expression was derived using dimensional analysis:

$$D_{30}/y_0 = C' \left(\left(\frac{1}{s-1} \right)^{0.5} \frac{U_d}{(g y_o)^{0.5}} \right)^{2.5} \qquad (10)$$

According to Maynord the velocity to be used should be both representative of the flow conditions at the bed and easy to estimate. The local average velocity (or depth averaged velocity) fulfils these two requirements, and was therefore adopted. The characteristic size of stone used in this equation is D_{30} to account for variations in riprap gradation. Maynord found that the coefficient C' remained constant for different stone gradations if D_{30} was adopted instead of the more commonly used D_{50} or D_{90}. The coefficient C' is equal to 0.30 for both flat beds and slopes less than or equal to 1V:2H.

Based on studies of river closure by transverse dumping of rock, Izbash and Khaldre (1970) developed a relationship which can be used not only for 'normal' turbulence flows but also for flows downstream of hydraulic structures such as culverts. The diameter of the equivalent spheres

$$D_{s50} = \left(\frac{6M_{50}}{\pi \rho s}\right)^{1/3}$$ can be found using:

$$D_{s50} = C_1 \frac{V_b^2}{g(s-1)\Omega} \qquad (11)$$

where

V_b = velocity near the bed

s = specific weight of stone

C_1 = coefficient variable with the level of turbulence

C_1 = 0.35 low turbulence (ie normal river flow)

C_1 = 0.68 partially developed turbulent boundary layer (ie higher turbulence levels)

Ω = factor that allows for the reduced stability of particles on a sloping bank

$$\Omega = \left(1-\frac{\sin^2\alpha}{\sin^2\phi}\right)^{1/2}$$

where α is the bank slope, and ϕ is the internal friction angle of the stone. Izbash did not include this factor in his equation. However, several authors have used it when quoting Izbash's equation, based on tractive-force criteria for design of stable channels.

A similar equation for riprap sizing is suggested by Jansen et al (1979), also taking into account the level of turbulence in the flow but this time using the mean flow velocity U:

$$D_s = \frac{A}{(s-1)} \frac{U^2}{2g} \frac{1}{1 - \frac{\sin^2\alpha}{\sin^2\phi}} \tag{12}$$

where D_s is the diameter of spherical particles and all the other symbols have the same meaning as in Izbash's formula. Based on investigations carried out by the US Bureau of Reclamation, Jansen et al recommend the following values for A:

A = 0.2 minor turbulence
A = 0.5-0.7 normal turbulence
A = 1.4 major turbulence

Pilarczyk (1984) recommends a general stability formula, valid for stones with specific gravity between 2.6 and 2.7:

$$D=\gamma \frac{U^3}{Y_o^{0.5}} \tag{13}$$

where

D = equivalent diameter of the average weight of stones W_{50}

U = critical velocity, believed to be equivalent to the mean flow velocity

y_o = water depth

γ = numerical coefficient

- γ = 0.005 - horizontal bottom with no bed roughness discontinuity and uniform flow (limited stone transport)
- γ = 0.010 - bottom protection for limited stone transport, construction phases of

a dam or sill with B/H >5 (where B is crest length and H crest height)

γ = 0.015 - bottom protection for absolute rest of stone or a sill with B/H < 5.

This method suggests that the value of the critical velocity be reduced by a factor γ_r to account for high turbulence such as that generated in hydraulic jumps. This factor is given by:

$$\gamma_r = \frac{1.45}{1+3r}$$

where

r = represents the relative turbulence intensity and can take the values

r = 0.15 for uniform flow over a rough bed

r = 0.3 to 0.35 immediately downstream of stilling basins.

A precise definition of the relative turbulence intensity r is not given by Pilarczyk but it can be seen that a value of r of 15% results in γ_r = 1. Values of r above 15% correspond to turbulent conditions superimposed on the "normal" turbulence of natural streams. It seems reasonable to assume that a value of r equal to 0.15 corresponds to an rms of the velocity fluctuation of 15% of the mean.

Using the Shields critical velocity approach, Pilarczyk (in PIANC, 1987) produced a formula which also takes into account the level of turbulence. This formula, however was developed only for turbulence levels as high as the ones generated by bends:

$$\frac{D_{n50}}{y_o} = \left[\frac{U_d}{B_1 [g(s-1)\Omega\ \psi_s\ y_o]^{0.5}} \right]^{2.5} \tag{14}$$

where

D_{n50}	=	size of equivalent cubes (> 1 mm; non cohesive)
U_d	=	depth integrated flow velocity
Ω	=	as defined before $(\Omega = (1 - \frac{\sin^2\alpha}{\sin^2\phi})^{0.5})$
s	=	specific weight of stone
Y_o	=	depth of flow at the toe of the banks
ψ_s	=	Shields parameter
		ψ_s = 0.03 no movement
		ψ_s = 0.04 start of instability
		ψ_s = 0.06 movement
B_1	=	coefficient dependent on the turbulence level in the channel
		B_1 = 8-10 minor turbulence (e.g. uniform flow, smooth bed, laboratory flumes)
		B_1 = 7-8 normal turbulence of rivers and channels
		B_1 = 5-6 major turbulence (e.g. outer bends, local disturbances)

The grain size Dn_{50} is defined as $(\frac{M_{50}}{\rho s})^{1/3}$ where M_{50} represents the mass of the stone that is greater than that of 50% of the stones by weight; ρ is the fluid specific gravity and s the stone specific gravity. Stability of these blocks would not be guaranteed in areas of high turbulence where uplift forces may occur.

Recently Pilarczyk (1990) presented a more general equation for the design of channel protection materials, which can be applied not only for the design of riprap but also of gabions and mattresses. In fact this author provides the only equation known for design of mattresses formed by concrete blocks subjected to currents and turbulence. The formula includes a number of factors to take into account the turbulence level, the nature of the velocity profile (fully developed boundary layer as opposed to a partially developed one), the exposure to the flow of the protection materials, and the position of the materials on the bed or the banks:

$$\Delta_m D_n = \phi K_T \frac{0.035}{\Psi_{cr}} K_h K_s^{-1} \frac{U_d^2}{2g} \qquad (15)$$

where

D_n - thickness of protection unit

For rock, $D_n = (\frac{M_{50}}{\rho s})^{1/3}$ = 50% value

of the mass distribution curve of the stone, or $D_n = 0.85\ D_{50}$.

For mattresses and gabions, D_n is average thickness

Δ_m - relative density of protection unit

For rock, $\Delta_m = (\rho_s - \rho_w)/\rho_w$

For mattresses, $\Delta_m=(1-n)(\rho_s-\rho_w)/\rho_w$

n = porosity

K_h - depth factor

$K_h = \frac{2}{(log12\ y_o/k_r)^2}$ for logarithmic velocity profile

$k_r = D_n$ for concrete blocks

$k_r = 2\ D_n$ for rock

$K_h = (\frac{Y_o}{D_n})^{-0.2}$ for partially developed velocity profile

ψ_{cr} - critical shear stress parameter

ψ_{cr} = 0.035 for rock

ψ_{cr} = 0.06-0.10 for gabions

K_T - turbulence factor

K_T = ⅔ for low turbulence, uniform flow

K_T = 1.0 for normal turbulence in rivers

K_T = 2.0 for high turbulence, local disturbances and outer bends of rivers. This value should only be used when the velocity used in the equation is the mean average velocity, instead of the local mean velocity.

K_s - slope factor (defined as Ω)

ϕ - stability factor

ϕ = 1.25 for exposed edges of loose units

ϕ = 1.0 for exposed edges of mattresses

ϕ = 0.75 for continuous protection of loose units

ϕ = 0.50 for continuous protection by mattresses

U_d - depth averaged flow velocity

The relationship between the bottom velocity and the mean velocity for a rough turbulent flow can be obtained by the following equation (Rouse, 1950):

$$V_b/U = \frac{1}{0.68\log(y_o/k_s)+0.71} \qquad (16)$$

where

V_b = velocity near the bed

U = mean flow velocity

y_o = water depth

k_s = Nikuradse's roughness height

Uncertainty normally arises when trying to estimate the value of k_s in terms of a suitable particle size in the above equation. Pilarczyk (in Closure of Tidal Basins, 1984) suggests k_s = 1 to 2 D_{50} for uniform size and k_s = 1 to 2 D_{90} for non-uniform graded sediment. This is supported by Raudkivi (1967) who stresses that the value of k_s varies considerably with the actual type/state of the mobile bed. Armouring can occur on natural beds of well-graded material thus increasing the roughness value.

Another relationship between V_b and U is given by the Waterways Experiment Station - WES - (in Ramos, 1990):

$$V_b/U = \frac{0.71}{0.68\log(y_o/D_s) + 0.71} \tag{17}$$

where

D_s = size of the equivalent sphere $\quad (D_s = (\frac{6M}{\pi\rho s})^{1/3})$

and all the other symbols have the same meaning as in equation (16).

Assuming that $k_s = D_s$, it can be seen that this equation differs from equation (16) by a factor of 0.71. However, no apparent justification was found for this discrepancy. Having been derived from the early work on pipe resistance carried out by Nikuradse and by Prandtl, equation (16) seems therefore to be more reliable.

It can be seen from the literature review that most relationships give the nominal stone size, D, proportional to V to the power 2 to 3 (V either being the mean flow velocity or the critical velocity at stone level). The equations where $D \alpha V^2$ are in accordance with Brahms incipient motion formula which gives the critical velocity as $V_{cr} = kW^{1/6}$, where k is an empirical constant and W is the particle weight (see, for example, Raudkivi, 1967). Since $W \alpha D^3$ it follows that $D \alpha V_{cr}^2$. For high velocity flow conditions it is apparent that inadequate velocity estimates can greatly affect the size of riprap required to protect channels downstream of structures. Furthermore, all the relationships presented that take into account the influence of turbulence levels only define these levels qualitatively. Hence considerable subjective judgement is involved in the process.

Two graphs have been produced relating the Froude number (Fr) to the ratio between the stone size and the total water depth (D/y_o) - Figs 3 and 4. They allow a comparison of the different equations presented in the literature review. Since the Froude number is usually defined using the mean flow velocity, U, the equations where the critical velocity is given in terms of the velocity near the bed, V_b, had to be modified. Equation (16) was therefore adopted for the relationship between V_b and U. As mentioned earlier, it is not certain which nominal stone size should be used for the roughness height k_s. For the present comparison it was decided to take $k_s = D_{50}$. It must be stressed, however, that the value of k_s has a marked effect on the ratio V_b/U. For example, considering the range of $D/y_o = 0.01$ to 0.1, a value of $k_s = 2D_{50}$ would correspond to an increase of 11 to 17% in the ratio V_b/U, when compared to $k_s = D_{50}$. The procedure using equation (16) was followed for the equations proposed by Izbash, Raudkivi (equation (5)), Peterka and the chart proposed by Searcy.

Since the equation due to Maynord et al (1989) is expressed in terms of D_{30} instead of D_{50}, it needed to be altered to be compared with the other equations. In Maynord's tests D_{30}/D_{50} ranged from 0.60 to 0.93. For the present comparison it seems reasonable to assume that $D_{30} = 0.70\ D_{50}$. This relationship was therefore substituted in equation (10).

The first graph (Fig 3) refers to equations obtained under normal turbulence conditions: equations (5), (6), (10), (11), (12), (13), (14), (15) and Searcy's work.

The second graph (Fig 4) refers to equations obtained under high turbulence conditions: equations (7), (9), (11), (12), (13), (14) and (15). It was found that equation (15) for partially developed flow plotted similarly to equation (14), ie Pilarczyk's most recent equation seems to be mainly an extension of his previous equation to allow the design of gabions and mattresses. It should be noted once again that Maynord's equation (1978) was derived for turbulence generated by decelerating flow and not for turbulence downstream of structures. Similarly, Pilarczyk's equation (1987) refers only to turbulence generated by bends. As for Izbash's equation, it can be argued that the coefficient for high turbulence was obtained for isolated stones placed on top of a triangular shaped rockfill structure. This situation somewhat differs from that of a rockfill bed placed downstream of a stilling basin, for example. Campbell's chart (mentioned in section 2.2) is based on two equations which are similar in type to Izbash's equation. It was found that Campbell's equation for "small stilling basins" corresponds to a coefficient C_I of 1.0 ; the equation for "small turbulent stilling basins" corresponds to a coefficient of 1.37. The fact that most of the formulae in Figure 4 do not apply to highly turbulent flows only emphasises the need for research in this area.

The comparison of the two graphs shows that, as expected, bigger stone sizes are required to protect against higher levels of turbulence. This is apparent from the shift of the curves to the left in Figure 4, ie lower Froude numbers for the same stone size. The widely varying predictions of the stone size given by the different equations can also be seen in Figures 3 and 4. For example, for a mean velocity U = 1.88 m/s and a water depth y_o = 1m, the nominal stone size can vary as much as four times, from 0.021m to 0.076m under normal turbulence or from 0.046m to 0.180m under high turbulence. In terms of weight, the predictions vary by a factor of up to 64.

4 EXPERIMENTAL SET-UP

4.1 Test rig

The tests were carried out in an existing 2.4m wide by 28m long flume fitted with three pumps having a total capacity of 0.5m^3/s. In order to obtain a wider range of velocities and tailwater depths it was decided to reduce the width of the channel from 2.4m to 1.21m. An adjustable sluice gate was designed and installed in the flume to produce a hydraulic jump with associated turbulence upstream of the test section. The tailwater depths were controlled by means of a flap gate and a valve at the downstream end of the flume. Model materials representing different sizes of riprap were placed in a 2.60m long test section. Figure 5 and Plate 1 show the general layout of the flume.

The transition between the smooth surface flume bed and the test section was achieved by a 1.74m long reach of stone fixed with glue to wooden boards placed on the flume bed. The purpose of the fixed stone reach was twofold: firstly, to act as a transition between a smooth and a rough surface; and secondly, to prevent excessive scour produced by unrealistically high turbulence levels upstream of the test section. Otherwise the formation of scour holes and bars would most probably affect the levels of turbulence in the test section. The upstream end of the fixed stone reach was placed 1.4m downstream of the sluice gate and stone sizes varied from test to test but were always smaller than, or equal to, the sizes that were being tested.

The tests to study stability of riprap on banks required a different arrangement of the flume. A sloping bank was introduced on one side of the 1.21m wide test section, with the vertical wall of the flume on the opposite side. This simulated half of a symmetrical trapezoidal channel, and allowed observations through the perspex windows of the flume. Two banks with slopes of 1:2 and 1:2.5 (V:H) were studied separately in the flume, and a transition was included to allow a gradual change between the rectangular section upstream of the sluice gate, and the trapezoidal section at the testing reach. The banks were simulated by wooden boards; wire mesh was fixed to the wooden boards to increase their roughness and hence better simulate the adhesion of the riprap or concrete blocks to the underlying soil.

4.2 Instrumentation

Discharges were measured by a Crump weir downstream of the flume which was calibrated at the beginning of the tests. Two devices were installed to measure water levels in the flume : a simple scale, upstream of the sluice gate, and a micrometer screw point gauge, downstream of the test section. The accuracy of the point gauge is approximately 0.0003m.

Point values of instantaneous flow velocity in the test section were measured by a three-component ultrasonic Minilab current meter (Plate 2) positioned 1.0m downstream of the end of the fixed stone reach. The meter calibration was checked independently against a Braystoke current meter which was also used to measure mean velocities just above the flume bed, upstream of the sluice gate. Preliminary tests with the ultrasonic current meter showed that it required regular monitoring of the offset signals at zero flow velocity conditions. This can be accounted for by the sensitivity of this type of equipment to temperature changes and to the presence of air bubbles or particles in the water. Therefore the probe's offsets were recorded regularly during the tests. A number of checks of the local averaged velocities given by the ultrasonic probe were also carried out during the testing using a miniature propeller meter. A summary of the components and system specifications of the ultrasonic probe can be found in Appendix A.

4.3 Model materials

4.3.1 Riprap

Various sizes of stones were selected for the tests and their grading curves and specific gravity were obtained. Three different angular stones with D_{50} between 4.6 and 11.8mm were used in the tests (Figs 6 to 8) as well as three different round stones with D_{50} between 7.3 and 9.3mm (figs 9 to 11). In this study the angular materials were identified by the letter A and the round materials by the letter R.

A sample of each of the stones was weighed into groups and grading curves in terms of weight were produced. This enabled the calculation of average spherical and cubic diameters (D_s and D_n, respectively) required by some of the existing formulae. The shape factor of each material was also determined in order to assess any possible influence of the shape on riprap stability. This factor was defined as (see Pilarczyk, 1984):

$$S_f = \frac{c}{(ab)^{0.5}} \tag{18}$$

where a, b and c are the maximum, intermediate and minimum linear dimensions of the three mutually perpendicular axes. These dimensions were measured with a micrometer with an accuracy of approximately 0.05mm. Values of the nominal stone size D_{15}, D_{50}, D_{85}, the specific gravity, the M_{15}, M_{50}, M_{85}, M_{100} masses and the shape factor for each model material are listed in Table 1.

Regarding the grading of the model materials, it was found that the stone used in the tests broadly conformed with the guidelines recommended by Hemphill and Bramley (1989) and mentioned in section 3.2. Stone sizes 11.8mmA, 7.3mm R and 9.3 R, however, were not within the recommended limits for they were too uniform.

As can be seen from Table 1, the angular stones tested had higher shape factors (S_f) than the round stones. In both cases, however, the values were below the typical value for quarry stone of 0.7. This indicates that the round stones were relatively flatter than the angular ones and that neither were as blockish in shape as full-size quarry stone. It was also found that the maximum dimension of some of the particles in every sample exceeded three times the minimum dimension. These differences are difficult to avoid because quarry stone is obtained by excavation and blasting while the gravels used in the present study had been subject to more abrasion and erosion.

4.3.2 Concrete blocks

Alternatives to riprap can include gabion mattresses, randomly placed bricks or concrete cubes, gunny bags (geotextile bags filled with bricks) and mattresses of interlocking or cabled precast-concrete blocks. The last type was selected for testing because such blocks are being increasingly used in the UK and abroad ; reasons include economy, lack of suitable stone, ease of construction and visual appearance. Since most types of concrete blocks used for protection are proprietary, the design of such a scheme is normally done according to the particular manufacturer's guidelines. As mentioned in Section 3.2, only one equation that is suitable for the design of concrete block protection was found in the literature search for this study.

There are many types of proprietary concrete blocks, and these differ in size and thickness, and in the shape of the cut-outs and interlocks.

However, the most important parameter affecting stability is the net weight per unit area of a block. Therefore, in order to obtain general results, the present tests were carried out with solid blocks of a cement mortar having a specific weight of 2330kg/m^3 and dimensions 0.030m x 0.030m x 0.008m. The proportions of cement, sand and water were chosen such that the specific weight of the blocks was close to the specific weight of concrete. Also, the thickness of the blocks, 0.008m, was chosen so that their stability would be comparable with that of the gravel used in the riprap tests.

The blocks were obtained by pouring the cement mixture into plastic moulds especially fabricated for that purpose. The moulds were then placed on a vibrating table in order to reduce the air content of the final product and thus increase its density.

4.4 Data acquisition and method of analysis

The point velocity measurements from the three-component current meter were logged automatically into a Compaq Deskpro 286e micro-computer fitted with a differential analogue input board (AIP-24). The data acquisition board was used to convert voltage signals into digital signals read by the computer. This 24 channel board was also equipped with three filters to reduce interference by high frequency noise.

Records of 4096 point velocity measurements for each of the three directions (main stream, across the flume and vertical) were collected at a frequency of 12.5Hz.

A program, DATAEDIT, developed at HR to remove spurious peaks from data files was then run with the data collected during the tests. In spite of the filters already mentioned, spurious peaks may occur in a record. They are mainly due to the following causes: high frequency electrical interference by other equipment, possible power instability and the occasional passing of air bubbles between the sensors of the probe. This last cause was particularly likely to occur at measurements near the water surface in high turbulence tests where the flow was very aerated. This fact and the somewhat bulky shape of the probe, restricted the maximum and the minimum depths of water at which measurements could be taken. The program DATAEDIT, by also providing a visualization of the velocity records, showed that the data were random in nature.

Another program PCTURB, also developed at HR, was then applied to calculate time-averaged velocity components, rms values and turbulence intensities in the three orthogonal directions. Values of the shear velocity and shear stress for each test were calculated by means of program TURBCALC. For the calculation of these quantities the velocity profile was assumed to be logarithmic and the temperature of the flow was taken into account in the determination of the water density and viscosity. The output of this program also included the Froude and Reynolds numbers of the flow. Appendix B is a summary of the theory behind the procedure used to calculate the bed shear stress from a number of measured mean velocities at various heights above the bed. The uncertainties regarding the positioning of the bed level were overcome by a procedure included in the program.

This procedure consisted of the introduction of datum levels which were repetitively fitted until the best correlation between Z_0 and u_* was obtained (Z_0 is the roughness height and u_* the shear velocity). The program also allowed to neglect some points of the velocity profile in order to achieve a better correlation coefficient with the assumed logarithmic profile. This feature is particularly important for tests with a partially developed boundary layer, where the shape of the velocity profile differs from a logarithmic curve.

4.5 Test procedure

4.5.1 Riprap on bed

The rock materials were placed in the flume and levelled to obtain a flat bed at the beginning of each test. The amount of material used was weighed before hand so that the voids ratio, e, of the mobile bed could be determined. This quantity is defined as $e = \frac{V_v}{V_s}$, where V_v = volume of voids (V_v = total volume - volume of solids) and V_s = volume of solids.

Values of the voids ratio varying from 0.4 for stone size 4.6mmA to approximately 1 for stone size 9.3mmR were obtained. Note that these values were obtained without any compaction, the rock simply being dumped into the mobile bed reach of the flume and levelled afterwards. An indication of the reduction in e with compaction was obtained by manually compacting a small amount of material. This showed that values of e of the order of 0.30 to 0.50 could be achieved for all stone sizes.

Two types of test were carried out in this study: with normal turbulence, ie no hydraulic jump, and with higher turbulence. In the normal turbulence tests the sluice gate upstream of the test section was kept fully open so that it would not interfere with the flow. The initiation of stone movement was obtained by either increasing the flow discharge or lowering the tailwater gate. The procedure adopted in the high turbulence tests was first to adjust the sluice gate opening so that the resulting hydraulic jump was used as a turbulence generator in the test section. It should be noted that the jump was always produced upstream of the test section. The tailwater gate was then gradually lowered until initiation of stone movement was observed, whilst maintaining the hydraulic jump away from the mobile bed.

Since the criteria for initiation of movement can be rather subjective, measures were taken to follow the same criteria in all the tests performed. Therefore, it was decided to mark a rectangular area on the mobile bed in the vicinity of the ultrasonic probe which was positioned 1.0m downstream of the end of the fixed stone reach (see Fig 5). This area extended from 0.10m upstream of the position of the probe to 0.10m downstream of it (see Plate 2 for example).

The threshold of movement was reached when a fixed number of stones would roll on the marked area during a fixed period of time. This procedure was thought to be objective and to enable different experimenters to carry out the tests. The motion of stones was easily observed through the transparent window on one side of the flume.

Once the flow conditions had stabilised and the threshold of movement had been reached, measurements of velocity in the three orthogonal directions were taken with the ultrasonic probe. All measurements were carried out at the test section, in the marked area. In the beginning of this study the velocity measurements were taken along verticals on the centreline of the flume and at half width between the flume axis and its right and left walls. Later it was decided that measurements along the flume centreline were sufficient to characterize the flow because the values of the mean local velocity did not vary considerably with the transverse position.

The Braystoke current meter, which was permanently positioned upstream of the sluice gate, was used to measure values of the free stream velocity, taken as a reference velocity. The flow discharge, the water temperature, the upstream and the tailwater levels were recorded both at the beginning and at the end of each test. For reasons already pointed out, the offset probe signals at zero velocity were also recorded before and after each test (see Section 4.2).

Care was taken to level the mobile bed again after each test. Approximately the same amount of stone and degree of compaction were used in all tests of a particular stone size.

4.5.2 Riprap on bank

The tests were carried out with flow conditions set in a similar way as for bed riprap. The measurements were taken at three points: a point on the bank corresponding to half flow depth (whenever feasible); the toe of the bank; and on the horizontal bed at the mid point between the toe of the bank and the side wall.

Due to the introduction of the transition, the measuring section had to be placed further downstream when compared with the bed riprap tests. Measurements were taken with the Braystoke current meter along the flume to obtain an estimate of the development of the boundary layer. The measuring section was selected downstream of the point where the near-bottom velocity (at approximately 10% of the water depth) no longer varied with distance, ie where the boundary layer seemed to be fully developed. It should be noted, however, that since the development of the boundary layer depends on the flow conditions and on the stone size, the state of development varied from test to test.

4.5.3 Concrete blocks

Tests with concrete blocks also involved measurements on the channel bed and on the bank, and the setting of flow conditions was the same as for riprap. However, the threshold of movement of individual blocks was difficult to identify because the loss of one block caused rapid and progressive movement of others. Therefore the limit of stability was re-defined to be the occurrence of significant damage to the protection scheme. Measurements of the flow conditions at this limit were restricted to only one point near the bed because of the speed of failure and the need to protect the delicate ultrasonic current meter. However, full velocity profiles were usually measured at conditions somewhat below those at failure.

The blocks were laid by hand on the bed or banks over a fine layer of sand so as to form a continuous mattress (Plate 5). A few tests were carried out with staggered blocks to assess the possible increase in stability associated with this layout (see Plate 8). The flatness of the surface formed by the concrete blocks was assessed at the beginning of the tests. The maximum departure from the mean level was ±1mm, or approximately ±6% of the thickness of the blocks.

5 RIPRAP ON BED

5.1 Preliminary tests

A number of preliminary tests was carried out prior to the study partly to test the equipment but mainly to obtain an indication of the levels of turbulence to be expected. Tests were run over a 'smooth' bed and over round stone with D_{50} = 7.7mm for different values of discharge. It should be noted that the bed of the flume, which corresponded to a Manning coefficient, n, of approximately 0.013, was considered smooth by comparison with the riprap materials.

Measurements at various heights above the bed were made of velocity and turbulence intensity TI, defined as $(\overline{V'^2})^{0.5} / \overline{u}$ (where V' is the fluctuation in any velocity component and u is the streamwise velocity component at the same level). Turbulence intensities of the order of 6% in the stream direction near the bed were obtained for velocities of around 0.25m/s over a smooth bed, whereas values of the order of 12% were obtained for flow over a rough bed. These tests were performed with naturally developed turbulence, ie the sluice gate was fully open, thus not affecting the flow in the flume. These flow conditions will hereafter be referred to as normal turbulence and will provide a base condition for studying the effect of the additional turbulence downstream of structures.

5.2 Riprap

5.2.1 Normal and high turbulence tests

The first stage of the study involved the measurement of instantaneous flow velocities over a flat, rough bed for various discharges, water depths and turbulence levels. As mentioned before most of the measurements were taken at the centreline of the flume, at a fixed distance from the sluice gate. Values of velocity were recorded at different heights above the bed by successively moving the probe from a position at the bed to the closest position to the water surface that could be recorded (see limitations mentioned in Section 4.4). When the bottom of the instrument was touching the bed, the centre of the measurement volume was 17.5mm above the bed. The number of points obtained for each velocity profile depended on the water depth and on the aeration of the flow, which itself depended on the level of turbulence generated at the sluice gate.

For this series of tests the riprap material was placed on the floor of the flume in a 45mm thick layer, ie no underlayer of a different material was present. Tests were carried out for all the stone sizes (both angular and round) and for normal and high turbulence conditions. The results regarding normal turbulence are summarized in Table 2 (angular stone) and Table 3 (round stone), while the results regarding high turbulence are summarized in Tables 4 to 9.

The tables show that the turbulence intensities (TI_u and TI_v) in the longitudinal and transverse directions assumed fairly similar values, whereas the turbulence intensities in the vertical direction (TI_w) were much lower. However, the transverse component was generally smaller than the longitudinal one. Values of TI_u varying between 9 and 13% were measured near the bed for normal turbulent conditions, and between 11 and 32% for highly turbulent conditions. Figure 12 displays three plots of the relationship between the turbulence intensities in the three orthogonal directions and the non-dimensional depth y/y_o for stone size 9.7mmA. Plots drawn for other stone sizes had a similar output. It is apparent from Figure 12 that TI_u varies much more markedly with the relative water depth than TI_v and TI_w. A similar result was obtained by Anwar and Atkins (1980) using a hot-film anemometer and an electromagnetic current meter in steady flows over a smooth bed.

From comparison of Tables 2 and 3 with Tables 4 to 9 it is noticeable that considerably lower values of turbulence intensities were present in the normal turbulence tests.

As mentioned before, all the tests were generally carried out with flow conditions such that the threshold of stone movement was reached. Although some stones did move, the overall rate of transport was not normally sufficient to cause scour holes to form. This latter situation would not be acceptable because it would lead to erosion of the underlying material and collapse of the protective rock blanket, particularly if high turbulence levels were involved. Some tests were performed in order to estimate the margin of safety between the point of threshold of motion and the point of failure of the rock protection.

Stone of sizes 7.3mm R and 9.3mm R were used in these tests which showed that for constant water depth an increase of about 20% in the flow discharge would lead to scouring under normal turbulent conditions. It was not possible to reach a result for higher levels of turbulence because the hydraulic jump, formed at the sluice gate, would respond to an increase in the discharge by moving downstream towards the test section. The instability of the jump on a flat bed is a well-known phenomenon which is, in practice, overcome by the introduction of baffle piers and end sills in stilling basins. Where such devices are not present, even a slight increase in the discharge may greatly enhance the scouring process.

A graph was produced of turbulence intensities in the mean flow direction against transverse turbulence intensities for normal flow conditions (Fig 13). Values corresponding to the smooth bed tests were also plotted in this figure. It can be seen that for very low turbulence levels, ie near the water surface, TI_v apparently becomes higher than TI_u. This phenomenon was not detected for flow over riprap, possibly because such low levels of turbulence were not reached in this case.

An experimental study carried out by Wang (1991) on the distribution of longitudinal turbulence intensities of flow over a gravel-bed showed that this distribution greatly depends on the relative roughness y_o/k_s. He used gravel size 8-10mm glued to the bottom of the flume, fully rough turbulent flows, and y_o/k_s variable between 1.36 and 6.00. The turbulent intensities were defined as $(\overline{u'^2})^{0.5} / u_*$ where u_* is the shear velocity.

Although a definition of the roughness height k_s is not given, it can be assumed to be equal to D_{50} of the gravel. Wang plotted his results against y/y_o and compared them with the curve suggested by Nezu and Rodi (1986) for smooth channels:

$$\frac{(\overline{u'^2})^{0.5}}{u_*} = 2.26\exp(-0.88\frac{y}{y_o}) \qquad (19)$$

Wang's results corresponding to $y_o/k_s < 4.0$ fell below Nezu and Rodi's curve whereas a good agreement with this curve was found for results corresponding to $4.0 \leq y_o/k_s \leq 6.0$. A similar plot was produced with the results of the present study (normal turbulence) - Figure 14. As in Wang's tests the turbulence intensity $(\overline{u'^2})^{0.5} / u_*$ seems to become constant for low values of y/y_o. For y/y_o approximately greater than 0.2, the distribution of the longitudinal turbulence intensity can be fitted by an equation of the type presented by Nezu and Rodi. The results of a test on the smooth bed were also plotted in Figure 14 to compare with Nezu and Rodi's equation. It can be seen that although the smooth bed points do not coincide with Nezu and Rodi's equation, they plot generally above the rough bed cases as an exponential curve.

5.2.2 Shape effect

As mentioned before, the tests were conducted with three different angular stones and three different round stones. This should allow some conclusions to be drawn regarding the effect of particle shape on the stability of riprap material. Stone sizes 9.7mmA and 9.3mmR are the most suitable for comparison because they had similar mean sizes and grading curves and differed principally in particle shape. For normal turbulence, the angular stone was found to withstand a higher bottom velocity (V_b = 0.930 m/s) than the round stone (V_b = 0.730 m/s). However, the shear velocity obtained in the two cases was very similar, of the order of 0.1m/s. No conclusion could be drawn regarding higher levels of turbulence since different tests gave contradictory results. The generally accepted notion that round stone is less stable than angular stone does not seem to apply to highly turbulent flows. It should be noted, however, that although the 9.3mmR size stone was round (ie it did not have any sharp edges) its shape factor S_f (eqn (18)) was similar to the 9.7mmA size stone (see Table 1). Hence the shape effect found by comparing these two materials can only be considered a 'surface shape effect'.

A graph was produced to investigate the effect of shape on the velocity profile. Figure 15 presents the relationship between the velocity at 10% of the total water depth and the mean flow velocity. Stones with different shape factors S_f do not show different relations between mean and bed velocities. This supports the conclusion drawn at the Delft Hydraulics Laboratory, The Netherlands, that for the same nominal size, higher shape factors does not necessarily mean more stable stone (see Section 3.1).

5.3 Filters

5.3.1 Granular filter

Several authors have recommended guidelines for the design of granular filters in terms of the best grading and thickness to ensure the stability of the armour layer (eg Stephenson, 1979, Span et al, 1981, and Charlton, 1983, Petersen, 1986, Hemphill and Bramley, 1981). The number of layers to adopt depends mainly on the size and type of the base material and on the availability of filter material. Very fine base materials will normally require more than one layer of filter.

A comparative analysis of the different criteria suggested by the above mentioned authors led to the following conclusions:

1. To assure internal stability of any filter layer, $D_{60} < 10\ D_{10}$;
2. To assure stability of the armour layer (top layer),

   $D_{85f} \geq 0.25\ D_{15a}$
   $D_{50f} \geq 0.14\ D_{50a}$
   $D_{15f} \geq 0.14\ D_{15a}$

   Where subscript a denotes armour layer and f filter.

3. The thickness of each layer should not be less than approximately 15cm, less than the diameter corresponding to W_{100} or less than 1.5 the diameter corresponding to W_{50}. Since

placement of riprap under water presents considerable difficulty, the thickness of the layers should be increased by 50% when placed under water, according to the US Corps of Engineers (in Petersen, 1986).

Tests were performed with an armour layer of stone size 4.6mmA and thickness 25mm, placed on top of a layer of sand 20mm thick. The grading curve of the sand used is shown in Figure 16 ; its specific gravity was 2.62 and D_{50} = 0.72mm. The overall thickness of the mobile bed was the same as in tests of riprap without any filter layer.

The purpose of the tests was to investigate the effect of an underlaying granular filter on the stability of the armour layer. Failures of riprap protection have occurred that may be due to inadequate filter layers (although designed according to the well-known Terzaghi criteria), rather than to insufficient size of the stone in the armour layer (CIRIA, 1987). The materials used in these tests were chosen in order to comply with the requirements indicated above. Table 10 lists the results obtained in these tests. Scour holes were found to form at the upstream end of the mobile bed during tests carried out with high levels of turbulence (approximately for $TI_u > 17\%$ at bed level). Comparing these tests with the tests done with stone size 4.6mmA and no granular base the following was observed:

1. Scour started to develop at the upstream end of the test section and a bar was formed just downstream;

2. As the test proceeded, the scour holes and bars increased in size, eventually reaching the measuring point and the bottom of the flume;

3. For similar Froude numbers of the flow, much higher TI are obtained under these conditions than for a single layer blanket. These high values are associated with an increase in the rms values which are possibly due to the formation of a scour hole and bar at the measuring point;

4. For lower turbulence intensities the sand base layer seems to increase the stability of the armour layer - the threshold of motion was achieved at a higher discharge.

The scouring process seems to be related to uplift forces acting in the sand layer. This process can be briefly described as follows: the sand is lifted up by the fluctuating forces; by penetrating into the voids of the armour layer stones, the particles of sand reduce its stability ; the scouring of this layer begins and once the sand layer is exposed, the scouring develops very rapidly; complete failure of the riprap blanket then occurs.

The results of the tests suggest that sand complying with the Terzaghi-based requirements nevertheless performs poorly as a filter material in highly turbulent environments. The same conclusion was reached at the US Bureau of Reclamation : it was decided to avoid using sand as an underlying filter material in riprap river protection downstream of Grand Coulee Dam where velocities and turbulence levels were usually very high. This proved to be successful (in CIRIA, 1987).

5.3.2 Synthetic filter

The functional requirements of a synthetic filter are essentially the same as those for granular filters, ie permeability to water under various

flow conditions and prevention of migration by particles in the base soil.

Guidelines for the design of synthetic filters (or filters incorporating geotextiles) have been produced by a number of authors, such as Stephenson (1979), Pilarczyk (1984), POWELL et al (1985) and PIANC (1987).

In PIANC (1987) a geotextile is defined as a synthetic filter whose main function in a revetment is to act as a filter medium between the coverlayer and the subsoil. Besides their filtering properties, geotextiles are flexible, which allows them to deform and still remain intact, and resistant to tension and tear.

A filter cloth was selected for the tests in accordance with the guidelines suggested by the authors mentioned above. This geotextile was a non-woven fabric with the commercial name of TERRAM NP4 and the following specifications:

k_g = 0.09m/s
O_{90} = 0.05mm

The tests were carried out with a sand base with D_{50} = 0.72mm on top of which the filter cloth was placed. A layer of stone size 4.6mmA was then placed over the geotextile. To enable a comparison of the performance of the granular and the synthetic filters, the thickness used for the stone layer was the same in both cases. Also, the tests were carried out with flow discharges, flow depths and gate openings similar to the ones used in tests of the granular filter and in tests with a single-layer of stone size 4.6mmA. Table 11 lists the results obtained in these tests. Unlike what happened in the tests with a granular filter, no major scouring was observed in tests with the geotextile. At the end of most tests, however, small scour holes were observed at the upstream right corner of the mobile bed but these holes did not reach the measuring point. The performance of the riprap incorporating a geotextile was, thus, found to be approximately as good as the single layer riprap. However, it was also found that a small increase in the discharge in test T47 produced extensive scouring at the upstream end of the mobile bed, followed by lifting of the geotextile which resulted in the complete collapse of the riprap revetment. Such sudden failure had not been observed with a single-layer of riprap.

6 RIPRAP ON BANK

The stability of a particle resting on a bank under current attack depends on the balance between two destabilizing forces and the resistance to motion offered by the particle. This resistance force is the product of the component of the particle's weight normal to the slope and the coefficient of friction, which is defined as the tangent of the particle's angle of repose. The destabilizing forces are the tractive force induced by the flow and the component of the particle's weight that tends to cause the particle to roll down the slope. At the threshold of movement the resistance force equals the force tending to cause motion.

An important ratio for design purposes is the tractive-force ratio (see, for example Chow, 1973). This is the ratio between the unit tractive force that causes impending motion on a sloping surface, and the one that causes impending motion on a flat bed: $\Omega = (1 - \frac{\sin^2\alpha}{\sin^2\phi})^{0.5}$.

As can be seen in the riprap design formulae presented in Section 3.2, several authors include the above ratio in their equations (equations (11), (14) and (15)). Equation (8), suggested by the Department of Transportation of the State of California, does not take into account the angle of repose of the stone; instead, another angle, α, is introduced which depends on the material and technique used to protect the bank. Maynord (1978) - equation (9) - includes the influence of the slope in the coefficient C; he found that the slope effect was negligible for slopes 1V:3H or flatter. Later Maynord et al (1989) suggested that the slope effect could be neglected for slopes 1V:2H or flatter.

6.1 Slope 1:2

Tables 12 to 14 summarize the results obtained with angular stones placed on a bank of slope 1:2 and on the adjacent section of flat bed. Measurements were taken at three points: a point on the bank corresponding to half flow depth; the toe of the bank; and on the horizontal bed at the mid point between the toe of the bank and the side wall. However, only measurements at the toe and on the bank were included in the tables. Since the results at the toe for test S6 were not reliable, the ones obtained at mid-channel were, instead, included in Table 12. For the measurements taken on the bank, the probe was positioned such that the depth of water at that point would be half the total flow depth. Contrary to what was expected, the beginning of stone instability did not always occur on the bank; in some tests carried out with stone size 11.8mmA the stone was first seen to move on the bed of the flume. In most of the tests, however, instability was observed either at the toe, or on the bank at locations where the water depth was greater than approximately 2/3 of the total water depth.

As can be seen in Tables 12 to 14, higher values of TI_u (and in some cases also higher TI_v) were obtained on the bank than at the toe for most of the tests carried out. This results from a generally lower mean streamwise velocity and bigger velocity fluctuations at the bank. It was also found that in most high turbulence tests the rms values of the vertical velocity component increased as one approached the water surface.

For all tests involving slopes, the Froude number of the flow was calculated in two different ways, as can be seen for example in Tables 12 to 14. The first method is the one adopted for the flat bed case, ie $Fr = U/(g\ y_o)^{0.5}$, where y_o is the total flow depth and U is the section-mean velocity. The second method calculates Fr2 using a flow depth defined as the area of the cross section divided by the width of the water surface. This second method, which gives higher values of the Froude number for trapezoidal areas than the first method, is more representative of the flow conditions where slopes are involved.

6.2 Slope 1:2.5

Tables 15 to 17 summarize the results obtained with angular stones placed on a bank of slope 1:2.5 and on the adjacent section of flat bed. As for tests with slope 1:2, the probe was positioned on the bank such that the water depth above it would be approximately half the total flow depth. In most tests the threshold of movement was found to occur on the bank, just above the toe in some cases. It was also found that, as for slope 1:2, the turbulence intensity in the streamwise direction assumed higher values on the bank than at the toe. This was only noticeable for high turbulence tests.

In some of the tests done with stone size 4.6mmA it was not possible to calculate reliably the value of the shear velocity u_* (see Table 15). In fact, the values of flow velocity for tests S28, S28A and S29 presented a marked S-shape profile which deviated considerably from the assumed logarithmic profile. S-shape profiles were found by other researchers in flows over rough beds and low water depths. It is not clear why this type of profile occurred only for the smallest stone size tested and for water depths above 0.250m.

7 CONCRETE BLOCKS

7.1 Flat bed

The tests with concrete blocks on a flat bed were carried out with the blocks placed on an approximately 30mm thick underlayer of 0.72mm sand, which was the same as used in the granular filter tests (see Section 5.3.1). As mentioned before, measurements at bed level were taken when the blocks started to fail but, in most tests, measurements were also taken before the point of failure was reached. This was done in order to obtain velocity profiles, since these could not be measured once failure occurred (see Section 4.5.3). Because the movement of blocks was a sudden occurrence that could have damaged the probe, it was difficult to judge the right moment to measure the velocity profile near failure. In the majority of the tests this was done at a flow rate fairly well below that which ultimately caused failure.

Plate 5 shows the typical layout of the blocks before a test run and Plate 6 illustrates the catastrophic collapse of the blocks at the end of test C29; strong scouring of the underlayer can be observed. Plate 6 also shows the miniature propeller meter that was used during tests C29 and C30 as a replacement for the ultrasonic probe, which was malfunctioning at the time when these tests were performed. Only mean values of velocity were recorded with the miniature propeller meter and therefore no values of turbulence intensity could be measured. The results of tests involving the failure of blocks on the flat bed are summarized in Table 18.

7.2 Slopes 1:2.5 and 1:2

The banks were constructed with the same sloping wooden boards as used in the equivalent riprap tests (Chapter 6). Wire mesh was fixed to the boards to increase adhesion and covered with a thin layer of 0.72mm sand. The blocks were then placed on the slope, normally in chequerboard-fashion (or stack bond). The horizontal floor of the channel was filled with riprap of size 9.7mmA, the concrete blocks occupying only the banks (see, for example, Plate 7). Along the toe of the bank a small wooden batten was fixed normal to the bed to provide support for the concrete blocks. The blocks were therefore restricted from sliding down the slope on to the flat bed.

In most tests failure was found to occur near the toe of the bank but the number of blocks lifted up varied from test to test. The results of the tests can be found in Table 18. One test (C13) was performed with staggered blocks (stretcher bond) on a slope of 1:2.5 to investigate the effect of a different layout on the stability of the blocks (see Plate 8). It was found that, for a similar water depth, staggered blocks were stable under a higher velocity than blocks having the normal layout (compare tests C10 and C13 in Table 18). The value of velocity measured in test C10 was 0.787m/s whereas in test C13 it was equal to 0.813m/s. This corresponds to an increase of approximately 5%.

8 ANALYSIS OF TEST RESULTS

8.1 Riprap

8.1.1 <u>Comparison of results with existing formulae</u>

It was decided to start the analysis of test results by comparing them with the equations presented in Section 3.2. The results of the present study for the flat bed case were plotted over the curves recommended by the different authors and shown in Figures 3 and 4. A graph (Fig 17) was then produced with the results of high turbulence tests in comparison with the curves that showed the best agreement with them. These curves corresponded to equations proposed by Izbash and by Pilarczyk (1987). Campbell's equation for small stilling basins was also plotted in Figure 17. Two curves corresponding to Pilarczyk's equation using a turbulence coefficient B_l equal to 5 were plotted: one using a critical shear stress parameter ψ = 0.04 and the other using ψ = 0.06. Since the stability criterion adopted in the testing was that of particle movement, better agreement was expected with the equation using ψ = 0.06, and this proved to be the case. Campbell's equation for small stilling basins, which is similar in type to Izbash's equation, shows a good agreement with the experimental results ; the only difference between the two equations concerns the value of the coefficient C_l. Pilarczyk's curve for ψ = 0.04 and Izbash's curve can be considered as envelopes to the test results for the flat bed.

In spite of some experimental scatter, either the Pilarczyk or the Izbash-type equation could be taken as the basis of the analysis. Subsequent analysis involving not only the flat bed case but also the two slopes studied, showed that the scatter of results was larger for a Pilarczyk-type equation than for an Izbash-type equation. This was found to be mainly due to the depth factor introduced in Pilarczyk's equation. It should be noted again that Pilarczyk uses the mean velocity in the vertical (or depth averaged velocity U_d)

while Izbash uses the velocity near the bed V_b. This means that the plot of Izbash's equation in Figure 17 contains the assumption about the relation between U_d and V_b which was given by equation (16). This assumption affects the goodness of fit in Figure 17.

As mentioned in Section 3.2, Pilarczyk in his 1990 equation considers two types of velocity profile: one described by a logarithmic distribution (fully developed profile) and another described by a power function (partially-developed profile). In the present study both types were identified but the partially-developed profiles occurred much more frequently. For illustration purposes, the two types and their agreement with a logarithmic distribution are shown in Figure 18. A third type, S-shape profile, was also found to occur in some tests at the toe and on the bank of slopes (Fig 18). As mentioned in Section 6.2, the reasons for the occurrence of such profiles are not clear but appear to be related to separation or retardation of flow near slopes.

The analysis was carried out using the size of equivalent cubes D_{n50} for the characteristic dimension of stone, as defined by Pilarczyk (see Section 3.2). Since the values of mass for the different stone sizes had been determined in the present study (see Table 1), the various D_{n50} could be directly used in the analysis. However, when D_{n50} is not known, it is possible to use the following equivalences to relate the known stone dimensions with D_{n50} and D_s: $D_{n50} = 0.909\ D_{50}$ and $D_s = 1.13\ D_{50}$. The relationship obtained between D_{n50} and D_{50} agrees well with Stephenson's recommendations of $D_{n50} \approx 0.90\ D_{50}$ (Stephenson, 1977). It should be noted however, that because these equivalences were obtained for the set of stones tested, they may not be general.

Due to the uncertainties regarding the representation of the velocity profile, the analysis of the test results described in the next section was based on an Izbash-type equation, using the equivalent cube as the characteristic stone dimension.

8.1.2 Analysis of results based on an Izbash-type equation

The well-known Izbash equation, presented in Section 3.2, shows strong dependence of the stone size on the bottom velocity but, like the other equations, the turbulence coefficient is only qualitatively defined. The aim of the present analysis was to try to quantify the turbulence coefficient in terms of the turbulence intensity in the streamwise direction, TI_u. For that purpose, Izbash's equation was re-arranged such that a factor C defined as $C = \frac{D_{n50}(s-1)2g}{V_b^2}$ could be

plotted against TI_u. In order to standardise the results, both the "bottom" velocity V_b and the corresponding turbulence intensity TI_u were determined at a height above the bed equal to 10% of the water depth y_o. This reference level was partly determined by the size of the ultrasonic current meter, which prevented measurements being made much closer to the bed when flows were shallow. However, the 0.1 y_o level is suitable for several reasons: it is close enough to the bed for conditions to be representative of those experienced by the protection layer; errors or uncertainties in vertical position have much less effect on measurements at this level than at points closer to the bed where the velocity profile is much steeper; and thirdly, it is a suitable level for taking near-bed measurements in small-scale physical models. The relationship between C and TI_u (hereafter just referred to as TI) is shown in Figure 19. Results of flat bed tests and results of velocity measurements at the toe of the banks are plotted in this figure, using the values tabulated in Tables 19 to 21. U_d in the tables refers to the depth averaged velocity calculated from each velocity profile obtained in the tests. It is apparent in Figure 19 that C increases with TI for turbulence intensities above 10%, approximately. For lower values, C assumes a constant value of about 0.36. This finding shows that the adoption of a constant value for high levels of turbulence is not a good representation of reality. Izbash's formula assumes spherical particles and velocity at the bed. Using the logarithmic velocity profile due to Nikuradse (which leads to equation (16)) it can be shown that Izbash's coefficient for normal turbulence is equivalent to approximately 0.33. This agrees well with the value of C = 0.36 obtained for normal turbulence in the present study. However, Izbash's formula for higher turbulence may lead to underestimation of stone size if the turbulence intensity exceeds approximately 13%. In spite of the experimental scatter (which is to be expected in turbulence studies), it was possible to fit a linear equation to the results of the tests with a correlation coefficient of about 0.90: C = 12.3 TI -0.87 for TI > 10% approximately.

It is also noticeable in Figure 19 that the results of tests with riprap on slopes are mixed in with the results for flat beds. There is therefore no need to analyse the two sets of data separately (at least for slopes up to 1:2, as tested here). This appears to contradict the general use of the stability factor Ω discussed in Chapter 6, but may be a result of analysing the results in terms of the bottom velocity at the toe of the bank. Although the slope reduces the stability of the stones, local velocities on the bank are likely to be smaller than at the toe. Maynord et al (1989) also found a similar effect in their study.

A best-fit equation in terms of bottom velocity for the results of the present study is as follows:

$$D_{n50} = C \frac{1}{s-1} \frac{V_b^2}{2g} \tag{20}$$

where C is a stability coefficient that varies with turbulence

C = 0.36 for TI ≤ 10%

C = 12.3 TI -0.87 for 10% < TI ≤ 30%

$$TI = \frac{rms\ u}{V_b}$$ at 10% of the water depth.

For safe design of riprap it is recommended to adopt for the definition of C the envelope curve represented by the dashed line in Figure 19. This line was drawn parallel to the best fit line so as to include all the experimental points that indicated higher values of D_{n50} than given by the best fit line. As can be seen in the figure, the envelope line is valid for the whole range of turbulence intensities studied, ie 5% ≤ TI ≤ 30%.

The safe design equation for riprap is then given by:

$$D_{n50} = (12.3\ TI - 0.20)\ \frac{1}{s-1}\ \frac{V_b^2}{2g} \qquad (21)$$

for TI ≥ 5%

The analysis so far described involved the value of V_b at 10% of the total water depth. However, it would be useful for design purposes if the bed velocity could also be related to the depth averaged velocity because U_d is more likely to be known than V_b. Since the ratio V_b/U_d will be affected by the relative roughness of the bed, it was decided to investigate the relationship between V_b/U_d and the non-dimensional ratio y_o/D_{n50}. Three plots were produced for the cases of the flat bed (Fig 20), the 1:2.5 slope (Fig 21) and the 1:2 slope (Fig 22). A power curve with the equation

$$V_b/U_d = 0.52\ (y_o/D_{n50})^{0.14} \qquad (22)$$

was found to fit the results for the flat bed satisfactorily. This same equation also fitted the results for the 1:2.5 slope quite well but a poor agreement was found for points at the toe of the steeper slope of 1:2. In Figure 22 the points corresponding to measurements taken half way between the toe of the bank and the side wall of the channel were also plotted. They have a better agreement with the power curve. This suggests that the flow velocity in the corner formed by the bank and the bed begins to be significantly reduced by resistance effects when the slope of the bank reaches about 1:2 or steeper.

Figure 23 is essentially equivalent to Figure 19 except that the bottom velocity V_b is replaced by the depth averaged velocity U_d and C becomes a new parameter C′. In Figure 23 only the results that showed a good agreement with equation (22) were plotted, ie the flat bed case and slope 1:2.5. Using the relationship between V_b/U_d and y_o/D_{50} given by equation (22), C′ was defined as

$$C' = 3.7 \frac{2g(s-1)D_{n50}}{U_d^2} (D_{n50}/y_o)^{0.28} \quad (23)$$

The variation of the measured values of C′ with the turbulence intensity is shown by the plot in Figure 23.

In comparison with Figure 19, more scatter is apparent for the reasons explained above. Nevertheless, a reasonable fit can be found between C′ and TI in the form of the following linear equation for the flat bed and the 1:2.5 data: $C' = 0.26$ for $TI \leq 10\%$ and $C' = 13.9\,TI - 1.13$ for $10\% < TI \leq 30\%$, with a correlation coefficient of 0.89.

This result leads to an alternative best-fit equation based on the mean (depth-averaged) velocity above the toe:

$$D_{n50} = J \frac{1}{s-1} \left(\frac{y_o}{D_{n50}}\right)^{0.28} \frac{U_d^2}{2g} \tag{24}$$

where

J - stability coefficient that varies with turbulence

$J = 0.075$ for $TI \leq 10\%$

$J = 3.75\ TI - 0.30$ for $10\% < TI \leq 30\%$

Note that the exponent 0.28 derives from the relationship between V_b and U presented by equation (22).

The stable stone size can be explicitly obtained by the following best-fit equation:

$$D_{n50} = L \left(\frac{1}{s-1}\right)^{0.78} y_o^{0.22} \left(\frac{U_d^2}{2g}\right)^{0.78} \tag{25}$$

where

$L = 0.13$ for $TI \leq 10\%$

$L = (3.75\ TI - 0.30)^{0.78}$ for $10\% < TI \leq 30\%$

An envelope line (represented by a dashed line) was also plotted in Figure 23, following the same criteria adopted for Figure 19. The resulting equation for safe design of riprap in terms of the depth-averaged velocity is as follows:

$$D_{n50} = [(3.75TI-0.090)\frac{1}{(s-1)}\frac{U_d^2}{2g}]^{0.78}y_o^{0.22} \quad (26)$$

for TI ≥ 5%

8.2 Concrete blocks - analysis of results

In order to investigate the effect of side slope on the stability of the concrete blocks, sets of tests were carried out with similar flow depths and gate openings. For example, tests C10 and C17 and tests C7 and C22 are directly comparable. As can be seen in Table 18, the tests corresponding to the 1:2 slope (C17 and C22) show higher values of turbulence intensity (measured at 0.1 y_o above the toe) than those corresponding to the milder slope of 1:2.5 (C10 and C7). This occurred because the 1:2 slope tended to reduce the local mean velocity at the toe more than the corresponding turbulent fluctuations; a similar effect was also noticed with the riprap (see Section 6.2).

The results for the concrete blocks were analysed in a similar way to those for the riprap. In view of the satisfactory fit obtained for riprap with an Izbash-type equation, it was also decided to relate the parameter C to the turbulence intensity in the streamwise direction. Values of the bottom velocity at the threshold of block movement were measured at approximately 7% of the total flow depth but, due to the speed of failure, velocities at other depths could not be recorded (see Section 7.1). However, velocity profiles were measured at flow rates below the threshold of movement. By assuming that the shapes of the profile near the bed did not vary with discharge, the value of the bottom velocity at 10% of the water depth was estimated for each failure condition. The same method was applied to the turbulence intensity and the values obtained are shown in Table 22.

A plot was then produced of $C = 2g\ (s-1)\ D/V_b^2$, where D is the thickness of the blocks, against TI at 0.1 y_o above the toe (Fig 24). Since tests C29 and C30 had to be carried out using a miniature propeller meter, only mean flow velocities could be obtained so the values of TI were not available. In the figure dashed lines indicate the value of the constant C for these two tests, one of which (C30) was a normal turbulence test. The linear equation found in the analysis of riprap was also included as a solid line in Figure 24.

It can be seen in Figure 24 that the points corresponding to the concrete blocks on flat bed and on a 1:2.5 slope plot fairly close to but below the line found for riprap. Lower values of C were obtained for blocks on the 1:2 slope. The stability of blocks on a slope is partly dependent on the type of toe termination adopted. As mentioned before, it was decided to reproduce the restraint of block movement that occurs in prototype schemes by a small wooden batten fixed along the toe of the bank. In prototype protection schemes toe termination details can vary considerably. Blocks can be laid on a continuation of the slope below bed level or can be anchored at the toe for increased stability.

The results of the tests suggest that the equation found for riprap (equation (20)) can be reduced by a factor of 0.75 to apply to concrete blocks on a flat bed and on slopes of 1:2.5 (see Section 8.1.2). Tests with blocks on slope 1:2 seem to indicate that C in equation (20) should be reduced by a factor of approximately 0.5 but more data are needed to confirm these results. The safe design equation for concrete blocks can be given by equation (21) reduced by a factor of 0.75.

The recommendation of using a reduction factor in equation (20) supports the common notion that concrete blocks are usually more economical than riprap in terms of thickness; the same conclusion can be found in Pilarczyk's (1990) equation.

8.3 Relationship between the Froude number and the turbulence intensity

The values of TI measured in high turbulence tests depended directly on the strength of the hydraulic jump produced by the sluice gate. It is well established that the strength of a jump and the Froude number of the flow at the vena contracta (see Section 2, in Fig 1) are correlated. Therefore the Froude number at that section was calculated for some tests in order to relate its value with the measured value of TI in the streamwise direction. Values of Fr ranging between 3.4 and 5.1 were obtained which corresponded to turbulence intensities of 15 to 30%, approximately. Tests with normal turbulence (ie with no hydraulic jump) were performed with values of Fr of the order of 0.60-1.0 and corresponded to turbulence intensities below 10%.

These results suggest that values of TI downstream of control gates can be estimated from the value of the Froude number of the flow entering a hydraulic jump. When measurements of TI cannot be obtained, a simple estimate can be made from the following table:

Condition	Fr	TI (%)
Normal river flow (no jump)	< 1.0	5-10
	3.5	16
Hydraulic	4.0	20
jump	4.5	26
	5.0	30

Note that TI refers to a section downstream of the hydraulic jump where the energy of the jump is such that a concrete revetment (stilling basin, concrete apron) is no longer required, and riprap protection is sufficient. The above values apply only to gates, weirs and other structures where a jump is formed to establish a transition between supercritical and subcritical flows.

9 CONCLUSIONS AND RECOMMENDATIONS

(1) An extensive literature review was carried out on design formulae for riprap as a channel protection material downstream of hydraulic structures. An experimental study was then conducted to investigate the stability of riprap on a flat bed and on slopes of 1V:2.5H and 1V:2H in environments with various levels of turbulence. Tests were performed with six different stone sizes

and with normal turbulence levels (corresponding to uniform flow in a straight channel) and high turbulence levels (corresponding to conditions downstream of a hydraulic jump). The turbulence intensities varied between 5 and 30%, approximately.

(2) The following best-fit formula (eqn 20) for the stability of riprap on a flat bed and on bank slopes of 1:2 or flatter was found (developed from the well-known Izbash equation):

$$D_{n50} = C \frac{1}{s-1} \frac{V_b^2}{2g}$$

where

$C = 0.36$ for $TI \leq 10\%$

$C = 12.3\ TI - 0.87$ for $10\% < TI \leq 30\%$

$$TI = \frac{rms\ u}{V_b}$$ at 10% of the water depth.

This formula is expressed in terms of a representative bottom velocity V_b and corresponding turbulence intensity TI, taken at 10% of the water depth above the bed. For the case of banks, V_b and TI are measured at 10% of the water depth vertically above the toe. For safe design of riprap on a flat bed and bank slopes of 1:2 or flatter it is recommended to use eqn (21):

$$D_{n50} = (12.3TI - 0.20)\ \frac{1}{s-1}\ \frac{V_b^2}{2g}$$

for TI ≥ 5%.

(3) An alternative best-fit equation (eqn (25)) expressed in terms of the depth-averaged velocity U_d (which is more likely to be known than V_b) was found to be:

$$D_{n50} = L\ y_o^{0.22} \left(\frac{1}{s-1}\ \frac{U_d^2}{2g} \right)^{0.78}$$

where

$L = 0.13$ for TI ≤ 10%

$L = (3.75\ TI - 0.30)^{0.78}$ for 10% < TI ≤ 30%

This equation is valid for riprap on a flat bed and on slopes of 1:2.5 or flatter. For the case of banks, U_d is the depth-averaged velocity in the vertical above the toe of the bank.

For safe design equation (26) is recommended:

$$D_{n50} = \left[(3.75TI - 0.090)\ \frac{1}{s-1}\ \frac{U_d^2}{2g} \right]^{0.78} y_o^{0.22}$$

for TI ≥ 5%

Where suitable data are available, the equations in (2) are preferable because they are more accurate and also apply to steeper bank slopes.

(4) The performance of filters was investigated for riprap on a flat bed. Tests with a sand filter determined according to the usual Terzaghi rules destabilised the armour layer in highly turbulent environments. The use of conventional granular filters is therefore not recommended downstream of hydraulic structures where the levels of turbulence are likely to be high. Tests using a non-woven geotextile placed underneath a layer of riprap in the same conditions showed that the stability of the armour layer was similar to that of the riprap without the granular filter.

(5) Tests were carried out with solid concrete blocks of dimensions 0.030m x 0.030m x 0.008m and specific gravity 2.33 in similar conditions to those for riprap. The blocks were placed in chequer-board fashion (or stack bond). It was found that the equations for riprap (equations (20) and (21)) can be applied to concrete blocks if the thickness of the blocks is taken as 75% of D_{n50} ; this result applies for blocks on a flat bed or on slopes of 1:2.5 or flatter. Tests with blocks on a 1:2 slope indicated that the reduction factor would be approximately 0.5, but more data are needed to confirm this result. Comparative tests were carried out with staggered blocks (stretcher bond) to investigate the effect of this

layout on the stability of the blocks. For similar water depth the blocks were found to be stable under a slightly higher velocity (typically 5%) than blocks having the normal layout. This would correspond to a reduction in required block thickness of about 10%.

(6) The tests performed with high levels of turbulence also provided a relationship between the Froude number of the flow entering the hydraulic jump, and the turbulence intensity TI in the streamwise direction (see Section 8.3). TI is defined at 10% of the water depth. The relationship obtained can be adopted to estimate the value of TI to use in the proposed equations when measurements of TI are not available.

(7) The tests showed that concrete blocks can be used in high turbulence flows and can produce a saving in terms of quantity of material necessary for the protection scheme. However, unlike riprap, concrete blocks are liable to sudden progressive failures. Therefore greater care is needed in constructing and maintaining such a scheme.

10 ACKNOWLEDGEMENTS

The design and the setting up of the test rip was done by Mr I R Willoughby who also developed some of the software used in the data analysis. The experimental work was carried out by Ms M Escarameia and Mr S Mambretti. Mr R Atkins, in Mr R L Soulsby's section, developed the software used in the data acquisition and analysis. The

project was carried out by Mr R W P May and Ms M Escarameia in the Research Department headed by Dr W R White.

11 REFERENCES

ANWAR, H O and ATKINS, R (1980). Turbulence Measurements in Simulated Tidal Flow. Journal of Hydraulic Engineering, Proc ASCE, Vol 106, No 8, pp 1273-1289.

CAMPBELL, F B (1966). Hydraulic Design of Rock Riprap. Miscellaneous Paper No 2-777. US Army Engineer WES, USA

CHOW, V T (1973). Open-Channel Hydraulics. McGraw-Hill Book Company, Singapore.

CIRIA (1987). Protection and Provision for Safe Overtopping of Dams and Flood Banks. Report of Overseas Scientific & Technical Expert Mission. Department of Trade and Industry, UK.

Department of Transportation of the State of California (1970). Bank and Shore Protection in California Highway Practice. Caltrans, USA.

FARRADAY, R V and CHARLTON, F G (1983). Hydraulic Factors in Bridge Design. Hydraulics Research Station, Wallingford.

HEMPHILL, R W and BRAMLEY, M E (1989). Protection of River and Canal Banks. CIRIA, Butterworths, London.

IZBASH, S V and KHALDRE, Kh Yu (1970). Hydraulics of River Channel Closure. Butterworths, London.

JANSEN, P Ph, BENDEGOM, L van, BERG, J van den, VRIES, M de and ZANEN, A (1979). Principles of

River Engineering. The non-tidal alluvial river. Pitman, London.

KEOWN, M P, OSWALT, N R, PERRY, E B, DARDEAU Jr, E A (1977). Literature Survey and Preliminary Evaluation of Streambank Protection Methods. Technical report H-77-9, US Army Engineer WES, USA.

KIRKGOZ, M S (1989). Turbulent Velocity Profiles for Smooth and Rough Open Channel Flow. Journal of Hydraulic Engineering, ASCE, Vol 115, No 11, pp 1543-1561.

LOPARDO, R A, De LIO, J C and VERNET, G F (1984). Model-Prototype Comparisons on Pressure Fluctuations in Hydraulic Jump Energy Dissipators. IAHR Symposium on Scale Effects in Modelling Hydraulic Structures, Esslingen 1984, H KOBUS (ed.), ab 7.2.

MAYNORD, S T (1978). Practical Riprap Design. Miscellaneous Paper H-78-7. US Army Engineer WES, USA.

MAYNORD, S T, RUFF, J F, ABT, S R (1989). Riprap design. Journal of Hydraulic Engineering, ASCE, Vol 115, No 7, pp 937-949.

NARAYANAN, R (1978). Pressure Fluctuations Beneath Submerged Jumps. Journal of the Hydr. Div, Proc ASCE, Vol 104, No 7, pp 1331-1342.

NEZU, I and RODI, W (1986). Open-Channel Flow Measurements with a Laser Doppler Anemometer. Journal of Hydraulic Engineering, ASCE, Vol 112, No 5, pp 335-355.

PIANC (1987). Guidelines for the Design and Construction of Flexible Revetment Incorporating

Geotextiles for Inland Waterways. Supplement to bulletin No 57, Belgium.

PETERKA, A J (1964). Hydraulic Design of Stilling Basins and Energy Dissipators. US Department of the Interior, Bureau of Reclamation, Engineering Monograph No 25.

PETERSEN, M S (1986). River Engineering. Prentice-Hall, Englewood Cliffs, USA.

PILARCZYK, K W (1984). The Closure of Tidal Basins. Closing of estuaries, tidal inlets and dike breaches. Deft University Press, The Netherlands.

PILARCZYK, K W (1990). Stability Criteria for Revetments. Proc of the 1990 National Conference on Hydraulic Engineering, ASCE, edited by Chang H H and Hill J C, San Diego, USA.

POWELL K A, ALLSOP N W H and OWEN M W (1985). Design of Concrete Block Revetments Subject to Wave Action; a literature review. HR Wallingford Report No SR 54.

RAMOS, C M (1990). Dimensionamento de Pontes (in Portuguese) ITH30, LNEC, Lisbon.

RAUDKIVI, A J (1967). Loose Boundary Hydraulics (1st Edition). Pergamon Press, Oxford.

RAUDKIVI, A J (1990). Loose Boundary Hydraulics (3rd Edition). Pergamon Press, Oxford.

ROUSE, H (ed), (1950). Engineering Hydraulics. Proc of the Fourth Hydraulics Conference. Iowa Institute of Hydraulic Research, June 1949. John Wiley & Sons Inc, New York.

SEARCY, J K (1967). Use of riprap for bank protection. US Department of Transportation, Bureau of Public Roads, Washington DC, USA.

SPAN, H J Th et al (1981). A Review of Relevant Hydraulic Phenomena and of Recent Developments in Research, Design and Construction of Protective Works. XXVth International Navigation Congress, Vol 1, Edinburgh.

STEPHENSON, D (1979). Rockfill in Hydraulic Engineering. Elsevier, Amsterdam, The Netherlands.

TENNEKES, H and LUMLEY, J L (1972). A First Course in Turbulence. The MIT Press, Cambridge, USA.

WANG, J J (1991). Distribution of Turbulent Intensity in a Gravel-Bed Flume. Experiments in Fluids 11, Technical Note, pp 201-202, Springer International.

YUEN, C and FRASER, D (1979). Digital Spectral Analysis. Pitman Publishing Limited, London.

TABLES

TABLE 1. CHARACTERISTICS OF THE RIPRAP MATERIALS USED IN THE TESTS

Nominal Stone Size D_{50}(mm)	D_{15}(mm)	D_{85}(mm)	s	M_{15}(g)	M_{50}(g)	M_{85}(g)	M_{100}(g)	s_f
4.6A	3.90	5.60	2.74	0.16	0.20	0.50	0.68	0.52
9.7A	7.40	9.70	2.74	0.55	1.40	2.25	3.25	0.49
11.8A	10.10	14.30	2.74	2.38	3.25	4.25	5.75	0.56
7.3R	6.50	8.70	2.68	0.64	0.91	1.27	1.55	0.49
7.7R	5.80	9.60	2.57	0.10	0.58	1.30	3.30	0.47
9.3R	8.10	11.00	2.67	1.08	1.95	2.88	3.88	0.48

Notes: A indicates angular stones

R indicates round stones

TABLE 2. TEST RESULTS
RIPRAP ON BED. NORMAL TURBULENCE
ANGULAR STONE

Stone size : 4.6mm A   Test : T19   Water depth = 0.182m
Mean flow velocity = 0.845m/s   Fr = 0.632 $u_* = 0.0625$m/s

y/y_o	TI_u (%)	TI_v (%)	TI_w (%)	u (m/s)
0.096	11.26	6.38	3.67	0.55
0.151	10.19	5.40	3.73	0.62
0.179	9.60	4.95	3.41	0.64
0.209	9.73	4.68	3.32	0.67
0.371	7.32	2.89	2.36	0.78
0.536	4.97	2.16	1.94	0.84

Stone size : 9.7mm A   Test : T7   Water depth = 0.254m
Mean flow velocity = 1.043m/s   Fr = 0.661 $u_* = 0.0975$m/s

0.072	8.94	4.28	2.65	0.85
0.093	6.86	3.78	2.45	0.96
0.113	5.40	3.24	2.19	1.04
0.134	2.70	2.47	1.70	1.11

Stone size : 11.8mm A   Test : T18   Water depth = 0.255m
Mean flow velocity = 1.172m/s   Fr = 0.742 $u_* = 0.0595$m/s

0.051	10.35	6.39	3.47	0.83
0.090	8.80	5.25	3.28	0.92
0.130	7.86	4.48	3.16	0.97
0.169	6.71	3.81	2.66	1.02
0.248	5.80	3.00	2.13	1.10
0.444	3.58	2.04	1.79	1.19
0.640	3.29	2.12	2.17	1.19

TABLE 3. TEST RESULTS
RIPRAP ON BED. NORMAL TURBULENCE
ROUND STONE

Stone size : 7.3mm R   Test : T30   Water depth = 0.243m
Mean flow velocity = 0.908m/s   Fr = 0.588 u_* = 0.0733m/s

y/y_o	TI_u (%)	TI_v (%)	TI_w (%)	u (m/s)
0.072	12.14	7.39	3.79	0.62
0.093	11.46	6.64	3.79	0.66
0.113	11.12	6.24	3.67	0.69
0.134	11.08	5.79	3.52	0.72
0.154	10.08	5.29	3.38	0.76
0.278	6.48	3.73	2.36	0.88
0.401	4.34	2.84	1.92	0.93
0.730	2.80	2.67	2.55	0.96

Stone size : 7.7mm R   Test : T4   Water depth = 0.199m
Mean flow velocity = 0.809m/s   Fr = 0.579 U_* = 0.0496m/s

0.088	11.53	5.51	3.54	0.59
0.138	10.54	4.62	3.25	0.65
0.188	10.57	4.23	3.03	0.70
0.339	6.19	2.69	2.07	0.81
0.590	3.30	2.07	1.73	0.86

Stone size : 9.3mm R   Test : T38   Water depth = 0.239m
Mean flow velocity = 1.117m/s   Fr = 0.730 U_* = 0.097m/s

0.073	13.12	6.56	4.36	0.68
0.094	12.68	6.45	4.36	0.72
0.115	11.22	5.48	3.89	0.78
0.136	10.38	5.06	3.62	0.82
0.157	9.29	4.63	3.49	0.85
0.282	5.74	3.15	2.33	1.00
0.492	2.93	2.10	1.80	1.09
0.701	2.63	2.08	2.03	1.10

TABLE 4. TEST RESULTS
RIPRAP ON BED. HIGH TURBULENCE
STONE SIZE 4.6mm A

Test : T20 Water depth = 0.336m Mean flow velocity = 0.453m/s
Fr = 0.249 u_* = 0.0157m/s

y/y_o	TI_u (%)	TI_v (%)	TI_w (%)	u (m/s)
0.043	14.80	14.44	5.51	0.40
0.058	14.03	14.27	5.71	0.41
0.073	14.39	13.17	5.98	0.43
0.088	14.29	14.05	6.33	0.43
0.103	14.35	13.69	6.57	0.44
0.192	13.05	12.21	7.11	0.47
0.281	13.72	11.36	7.53	0.48
0.490	12.77	10.90	7.87	0.50
0.638	12.43	11.54	7.53	0.51

Test : T21 Water depth = 0.245m Mean flow velocity = 0.600m/s
Fr: 0.387 u_* = 0.0313m/s

0.059	13.18	10.94	4.51	0.48
0.080	12.26	10.04	4.72	0.51
0.100	12.08	9.72	4.77	0.52
0.120	11.58	9.72	4.72	0.53
0.141	11.94	9.12	4.80	0.55
0.263	10.78	8.72	4.88	0.59
0.386	9.94	7.87	5.06	0.62
0.549	8.60	7.10	4.83	0.64
0.712	8.83	6.98	4.82	0.64

Test : T22 Water depth = 0.264m/s Mean flow velocity = 0.551m/s
Fr = 0.342 u_* = 0.0221m/s

0.055	13.99	13.05	5.59	0.43
0.074	14.41	12.86	5.76	0.45
0.093	13.48	11.96	5.87	0.46
0.112	13.73	12.02	6.01	0.47
0.131	14.32	12.84	6.53	0.48
0.244	12.81	10.71	6.31	0.52
0.358	11.67	10.74	6.85	0.54
0.509	11.76	10.33	7.07	0.55
0.737	11.93	9.65	6.49	0.57

TABLE 4 (Cont'd). TEST RESULTS
RIPRAP ON BED. HIGH TURBULENCE
STONE SIZE 4.6mm A

Test : T23 Water depth = 0.173m Mean flow velocity = 0.564m/s
Fr = 0.433 $u_* = 0.0331$m/s

y/y_o	TI_u (%)	TI_v (%)	TI_w (%)	u (m/s)
0.090	14.54	12.21	4.94	0.41
0.118	14.33	12.94	5.50	0.42
0.147	15.12	11.95	5.35	0.44
0.176	14.15	11.60	5.28	0.46
0.205	13.71	11.43	5.60	0.48
0.379	12.86	9.68	5.07	0.53
0.552	10.83	8.29	4.46	0.57
0.783	10.31	8.01	3.91	0.57

Test : T24 Water depth = 0.152m Mean flow velocity = 0.517m/s
Fr = 0.423 $u_* = 0.0262$m/s

0.102	15.47	15.79	6.40	0.37
0.135	14.91	14.32	5.93	0.39
0.168	14.92	13.80	6.53	0.39
0.201	14.06	12.89	6.05	0.41
0.234	14.03	12.97	6.60	0.42
0.365	13.23	10.93	6.02	0.45
0.497	11.90	10.27	5.36	0.47
0.628	11.67	9.03	4.99	0.49

TABLE 5. TEST RESULTS
RIPRAP ON BED. HIGH TURBULENCE
STONE SIZE 9.7mm A

Test : T5 Water depth = 0.350m Mean flow velocity = 0.665m/s
Fr = 0.359 $u_* = 0.0485$m/s

y/y_0	TI_u (%)	TI_v (%)	TI_w (%)	u (m/s)
0.044	15.39	11.68	5.03	0.64
0.073	14.51	11.01	5.09	0.70
0.101	13.27	10.44	5.13	0.74
0.187	12.28	9.48	5.40	0.80
0.330	11.78	8.67	5.80	0.83

Test : T6 Water depth = 0.248m Mean flow velocity = 0.757m/s
Fr = 0.485 $u_* = 0.0778$m/s

0.070	12.34	7.69	3.29	0.68
0.111	11.11	6.93	3.30	0.77
0.151	9.71	6.74	3.14	0.83
0.272	7.60	5.65	3.19	0.91
0.474	6.98	5.22	3.65	0.92

Test : T8 Water depth = 0.155m Mean flow velocity = 0.740m/s
Fr = 0.599 $u_* = 0.0891$m/s

0.113	12.03	7.00	3.85	0.56
0.177	11.09	6.04	3.38	0.66
0.241	10.31	5.58	3.45	0.73
0.434	7.81	4.18	2.92	0.82
0.628	6.55	3.57	3.06	0.86

TABLE 5 (Cont'd). TEST RESULTS
RIPRAP ON BED. HIGH TURBULENCE
STONE SIZE 9.7mm A

Test : T9 Water depth = 0.178m Mean flow velocity = 0.738m/s
Fr = 0.559 $u_* = 0.0847$m/s

y/y_o	TI_u (%)	TI_v (%)	TI_w (%)	u m/s
0.098	11.12	6.86	3.82	0.61
0.154	10.45	5.54	3.33	0.71
0.211	9.18	4.75	3.01	0.77
0.379	6.11	3.92	2.47	0.86
0.548	4.90	3.47	2.25	0.89

Test : T10 Water depth = 0.152m Mean flow velocity = 0.753m/s
Fr = 0.616 $u_* = 0.0597$m/s

0.115	12.61	8.74	3.95	0.66
0.180	11.04	6.37	3.32	0.70
0.246	11.04	6.69	3.91	0.76
0.443	8.05	4.70	3.25	0.86
0.639	6.20	4.09	2.91	0.87

Test : T11 Water depth = 0.364m Mean flow velocity = 0.629m/s
Fr = 0.333 $u_* = 0.0490$ m/s

0.048	13.72	10.29	4.75	0.57
0.076	13.48	10.48	5.08	0.63
0.103	12.81	10.20	5.02	0.67
0.186	12.04	8.67	4.98	0.74
0.323	11.21	7.88	5.40	0.76

TABLE 6. TEST RESULTS
RIPRAP ON BED. HIGH TURBULENCE
STONE SIZE 11.8mm A

Test : T12 Water depth = 0.261m Mean flow velocity = 0.646m/s
Fr = 0.404 u_* = 0.0357m/s

y/y_o	TI_u (%)	TI_v (%)	TI_w (%)	u (m/s)
0.048	16.42	13.13	6.14	0.52
0.067	16.10	12.46	6.11	0.54
0.086	15.65	11.84	6.12	0.57
0.105	15.60	11.61	6.07	0.60
0.125	14.70	10.77	5.92	0.60
0.239	13.16	9.75	5.98	0.66
0.354	13.60	9.35	5.68	0.71
0.584	12.77	8.23	5.95	0.74

Test : T15 Water depth = 0.263m Mean flow velocity = 0.683 m/s
Fr = 0.426 u_* = 0.0491m/s

0.048	15.26	12.50	5.76	0.52
0.067	15.17	12.25	5.76	0.55
0.086	14.34	11.16	5.24	0.59
0.105	14.32	10.83	5.42	0.62
0.124	13.87	10.64	5.13	0.63
0.238	12.56	8.79	4.76	0.72
0.352	11.74	7.76	4.84	0.76
0.429	11.35	7.84	5.07	0.79

Test : T16 Water depth = 0.342m Mean flow velocity = 0.655m/s
Fr = 0.358 u_* = 0.0481m/s

0.51	17.90	15.00	7.04	0.59
0.066	17.37	13.72	6.51	0.62
0.080	16.98	13.03	6.44	0.64
0.095	17.10	13.88	6.48	0.66
0.110	16.58	13.18	6.55	0.67
0.168	15.27	11.64	6.84	0.75
0.227	14.70	11.16	6.54	0.78
0.285	14.66	10.34	6.60	0.80
0.402	13.77	10.24	6.99	0.83

TABLE 6 (Cont'd). TEST RESULTS
RIPRAP ON BED. HIGH TURBULENCE
STONE SIZE 11.8mm A

Test : T17 Water depth = 0.179m Mean flow velocity = 0.677m/s
Fr = 0.512 u_* = 0.0594m/s

0.098	23.31	20.98	7.60	0.49
0.126	23.56	20.43	7.54	0.53
0.154	22.61	17.97	7.80	0.55
0.182	21.67	18.00	7.73	0.58
0.209	21.31	17.09	7.88	0.61
0.265	20.72	16.38	7.56	0.63
0.377	18.31	12.78	6.81	0.74
0.489	15.61	10.50	6.00	0.79
0.656	13.41	8.15	5.27	0.87

TABLE 7. TEST RESULTS
RIPRAP ON BED. HIGH TURBULENCE
STONE SIZE 7.3mm R

Test : T25 Water depth = 0.157m Mean flow velocity = 0.405m/s
Fr = 0.327 u_* = 0.0387m/s

y/y_o	TI_u (%)	TI_v (%)	TI_w (%)	u (m/s)
0.111	31.60	28.31	12.21	0.26
0.143	28.85	29.48	12.78	0.28
0.175	29.76	27.80	13.03	0.29
0.207	29.68	27.71	14.38	0.30
0.239	31.81	28.13	14.35	0.31
0.430	25.03	22.14	14.12	0.37
0.621	24.77	19.74	12.10	0.41
0.748	21.73	17.63	9.53	0.45

Test : T26 Water depth = 0.208m Mean flow velocity = 0.513m/s
Fr = 0.359 u_* = 0.0317m/s

0.084	23.14	24.17	9.64	0.28
0.132	25.44	24.77	11.38	0.31
0.180	22.13	22.78	10.78	0.34
0.325	20.12	16.86	10.98	0.38
0.469	19.74	15.19	10.19	0.42
0.565	18.69	13.32	9.14	0.46
0.805	19.72	13.17	8.44	0.50

Test : T27 Water depth = 0.222m Mean flow velocity = 0.622m/s
Fr = 0.421 u_* = 0.0432m/s

0.063	15.22	12.42	5.73	0.45
0.086	13.98	11.34	5.25	0.49
0.108	14.38	10.72	5.44	0.52
0.131	13.33	11.06	5.15	0.53
0.153	13.02	10.87	5.23	0.55
0.288	10.92	9.13	4.79	0.62
0.423	10.43	8.86	4.86	0.66
0.604	9.27	7.37	4.56	0.67
0.784	10.45	7.63	4.27	0.67

TABLE 7 (Cont'd). TEST RESULTS
RIPRAP ON BED. HIGH TURBULENCE
STONE SIZE 7.3mm R

Test : T28 Water depth = 0.280m Mean flow velocity = 0.617m/s
Fr = 0.372 u_* = 0.0442m/s

y/y_o	TI_u (%)	TI_v (%)	TI_w (%)	u (m/s)
0.063	15.65	13.18	5.59	0.475
0.080	14.68	12.66	5.85	0.494
0.098	14.48	13.25	5.85	0.521
0.116	14.26	12.22	5.91	0.539
0.134	13.32	12.39	6.17	0.558
0.241	12.42	10.47	5.86	0.615
0.348	11.57	9.64	5.88	0.644
0.491	10.82	9.77	6.24	0.659
0.777	10.46	8.66	5.64	0.665

Test : T29 Water depth = 0.339m Mean flow velocity = 0.553m/s
Fr = 0.304 u_* = 0.0414m/s

0.052	16.68	15.81	6.48	0.432
0.066	16.92	16.41	6.48	0.466
0.081	16.06	15.68	6.49	0.477
0.096	17.15	14.84	6.75	0.494
0.111	15.44	14.23	6.78	0.516
0.199	14.66	12.59	6.99	0.555
0.347	14.33	12.65	7.52	0.586
0.789	13.65	11.60	8.09	0.579

TABLE 8. TEST RESULTS
RIPRAP ON BED. HIGH TURBULENCE
STONE SIZE 7.7mm R

Test : T1 Water depth = 0.126m Mean flow velocity = 0.461m/s
Fr = 0.415 $u_* = 0.0534$m/s

y/y_o	TI_u (%)	TI_v (%)	TI_w (%)	u (m/s)
0.139	19.79	14.12	6.23	0.510
0.298	16.63	10.87	6.07	0.614
0.537	14.81	7.60	5.50	0.690

Test : T2 Water depth = 0.241m Mean flow velocity = 0.633m/s
Fr = 0.412 $u_* = 0.0548$m/s

0.058	13.97	12.19	4.62	0.479
0.141	13.82	9.97	4.81	0.601
0.265	12.00	8.56	4.34	0.687
0.679	9.73	6.59	4.10	0.744

TABLE 9. TEST RESULTS
RIPRAP ON BED. HIGH TURBULENCE
STONE SIZE 9.3mm R

Test : T33 Water depth = 0.217m Mean flow velocity = 0.571m/s
Fr = 0.392 u_* = 0.0254m/s

y/y_o	TI_u (%)	TI_v (%)	TI_w (%)	u (m/s)
0.081	19.15	17.31	7.98	0.371
0.104	17.84	17.32	7.80	0.389
0.127	17.90	17.76	8.13	0.401
0.150	18.51	16.81	8.91	0.409
0.173	18.11	16.48	8.46	0.421
0.311	18.80	15.59	8.55	0.458
0.449	18.01	14.04	8.29	0.492
0.634	17.52	11.93	7.64	0.537

Test : T34 Water depth = 0.248m Mean flow velocity = 0.640m/s
Fr = 0.410 u_* = 0.0486m/s

0.091	16.67	12.94	6.92	0.451
0.111	14.53	13.11	6.40	0.462
0.131	15.44	11.47	6.48	0.505
0.151	15.88	11.87	6.56	0.510
0.272	14.03	10.62	6.10	0.589
0.393	12.70	9.75	5.63	0.631
0.554	11.73	8.48	5.47	0.664
0.756	10.56	7.85	5.19	0.676

Test : T35 Water depth = 0.311m Mean flow velocity = 0.646m/s
Fr = 0.370 u_* = 0.0398m/s

0.043	16.00	14.55	6.59	0.495
0.059	16.30	13.22	6.57	0.537
0.076	16.34	13.42	6.67	0.548
0.092	16.57	12.67	6.74	0.572
0.108	16.26	12.06	6.59	0.589
0.204	14.11	10.13	6.45	0.652
0.365	13.69	9.88	6.79	0.695
0.686	11.99	8.76	6.74	0.729

TABLE 9 (Cont'd). TEST RESULTS
RIPRAP ON BED. HIGH TURBULENCE
STONE SIZE 9.3mm R

Test : T36 Water depth = 0.267m Mean flow velocity = 0.746m/s
Fr = 0.461 $u_* = 0.0600$m/s

y/y_o	TI_u (%)	TI_v (%)	TI_w (%)	u (m/s)
0.066	15.89	10.13	5.37	0.546
0.084	14.51	10.49	5.22	0.578
0.103	14.62	9.69	5.19	0.608
0.122	14.00	9.47	5.07	0.634
0.140	14.34	9.28	5.24	0.654
0.253	11.98	7.71	4.80	0.747
0.440	9.48	6.56	4.45	0.816
0.627	9.08	5.91	4.56	0.833
0.702	8.43	5.94	4.48	0.832

Test : T37 Water depth = 0.249m Mean flow velocity = 0.876m/s
Fr = 0.561 $u_* = 0.0667$m/s

0.070	13.68	8.18	4.99	0.662
0.090	13.33	7.28	4.75	0.701
0.110	12.23	7.42	4.81	0.731
0.131	11.23	6.94	4.57	0.764
0.151	10.94	6.64	4.43	0.789
0.271	8.06	5.18	3.57	0.885
0.472	5.98	4.19	3.07	0.938
0.429	5.50	3.89	3.16	0.938

TABLE 10. TEST RESULTS
GRANULAR FILTER
STONE 4.6mm A + SAND BASE

Test : T41 Water depth = 0.188m Mean flow velocity = 1.069m/s
Fr = 0.651 u_* = 0.0573m/s Normal turbulence

y/y_o	TI_u (%)	TI_v (%)	TI_w (%)	u (m/s)
0.093	12.80	7.32	4.67	0.49
0.146	12.18	6.36	4.36	0.55
0.173	11.53	5.51	4.30	0.58
0.199	11.15	5.53	3.99	0.60
0.359	9.50	3.12	2.71	0.74
0.519	5.51	2.08	1.84	0.82
0.731	3.75	1.94	1.82	0.83

Test : T39 Water depth = 0.150m Mean flow velocity = 0.600m/s
Fr = 0.409 u_* = 0.0470m/s

0.117	26.65	25.92	8.80	0.41
0.150	27.53	23.29	9.88	0.43
0.183	28.81	25.48	10.95	0.42
0.217	26.68	21.29	9.54	0.46
0.250	25.16	21.35	9.09	0.47
0.383	24.60	18.65	10.91	0.50
0.517	22.03	13.25	9.47	0.58
0.650	21.80	12.65	8.82	0.60

Test : T40 Water depth = 0.172m Mean flow velocity = 0.727m/s
Fr = 0.462 u_* = 0.0561m/s

0.102	20.11	26.01	8.04	0.37
0.131	21.97	23.74	8.33	0.40
0.160	21.53	23.92	8.85	0.42
0.189	22.20	21.97	8.97	0.45
0.218	23.97	23.09	9.59	0.46
0.392	20.29	17.73	9.51	0.55
0.567	19.15	14.40	8.18	0.61
0.799	17.01	11.29	5.72	0.68

TABLE 10 (Cont'd). TEST RESULTS
GRANULAR FILTER
STONE 4.6mm A + SAND BASE

Test : T42 Water depth = 0.254m Mean flow velocity = 0.846m/s
Fr = 0.443 u_* = 0.0395m/s

y/y_o	TI_u (%)	TI_v (%)	TI_w (%)	u (m/s)
0.069	13.35	10.90	4.89	0.53
0.089	13.33	10.81	5.23	0.56
0.108	12.74	10.12	5.06	0.57
0.128	12.56	9.68	5.09	0.59
0.148	12.99	9.70	5.26	0.61
0.266	12.95	8.73	5.42	0.66
0.384	12.03	7.88	4.70	0.72
0.541	10.76	7.36	5.04	0.73
0.699	10.57	6.91	5.01	0.74

TABLE 11. TEST RESULTS
SYNTHETIC FILTER
STONE 4.6mm A + GEOTEXTILE TERRAM NP4 + SAND BASE

Test : T44 Water depth = 0.185m Mean flow velocity = 0.893m/s
Fr = 0.663 u_* = 0.0770m/s Normal Turbulence

y/y_o	TI_u (%)	TI_v (%)	TI_w (%)	u (m/s)
0.095	12.45	7.43	3.71	0.54
0.149	11.57	6.28	3.64	0.61
0.176	11.89	5.63	3.60	0.64
0.203	11.14	5.27	3.46	0.66
0.365	8.68	3.27	2.64	0.80
0.527	5.72	2.57	2.33	0.86
0.743	4.12	2.41	2.98	0.87

Test : T45 Water depth = 0.247m Mean flow velocity = 0.609m/s
Fr = 0.391 u_* = 0.0314m/s

0.055	12.58	11.06	4.56	0.46
0.075	12.47	10.66	4.63	0.50
0.095	12.72	10.57	4.89	0.51
0.115	12.38	10.67	5.14	0.53
0.136	12.24	10.92	5.46	0.53
0.257	11.43	9.39	5.12	0.59
0.379	10.66	8.24	5.01	0.62
0.540	10.06	7.70	5.19	0.64
0.702	9.64	7.74	5.06	0.63

Test : T46 Water depth = 0.173m Mean flow velocity = 0.568m/s
Fr = 0.436 u_* = 0.0255m/s

0.084	12.78	14.00	5.16	0.41
0.113	13.68	13.44	5.19	0.42
0.142	12.93	13.15	5.67	0.44
0.171	12.80	12.58	5.74	0.45
0.199	12.58	11.50	5.86	0.46
0.373	12.55	10.23	5.79	0.52
0.546	11.90	8.46	5.13	0.55
0.777	11.27	8.36	4.55	0.55

TABLE 11 (Cont'd). TEST RESULTS
SYNTHETIC FILTER
STONE 4.6mm A + GEOTEXTILE TERRAM NP4 + SAND BASE

Test : T47 Water depth = 0.151m Mean flow velocity = 0.493m/s
Fr = 0.405 $u_* = 0.0328$m/s

y/y_o	TI_u (%)	TI_v (%)	TI_w (%)	u (m/s)
0.116	16.25	18.18	6.61	0.36
0.149	15.73	18.13	7.20	0.38
0.182	16.92	20.26	7.44	0.39
0.215	16.34	17.80	7.07	0.41
0.248	15.99	16.23	7.40	0.42
0.381	14.70	14.25	7.35	0.45
0.513	13.76	11.50	7.19	0.49
0.646	13.88	11.27	6.04	0.50

TABLE 12. TEST RESULTS
RIPRAP ON SLOPE 1:2
STONE SIZE 4.6mmA

Test : S6 Water depth = 0.209m Mean flow velocity = 1.176m/s
Fr = 0.556 Fr2 = 0.643 Normal Turbulence

MID CHANNEL $u_* = 0.0477m/s$

y/y_o	TI_u (%)	TI_v (%)	TI_w (%)	u (m/s)
0.084	9.79	6.63	5.32	0.536
0.132	8.49	6.24	5.29	0.560
0.227	7.98	4.73	4.53	0.629
0.323	6.32	3.32	3.43	0.689
0.562	2.26	1.58	1.90	0.753

BANK

0.167	12.38	7.92	5.50	0.447
0.262	11.76	7.24	5.99	0.451

Test : S5 Water depth = 0.323m Mean flow velocity = 0.625m/s
Fr = 0.345 Fr2 = 0.415

TOE $u_* = 0.0453m/s$

0.054	20.75	21.28	10.56	0.285
0.085	16.32	13.87	9.14	0.371
0.147	14.75	12.24	9.69	0.412
0.209	13.83	11.71	10.35	0.433
0.364	14.43	9.45	10.87	0.487
0.673	12.66	6.70	7.48	0.605

BANK

0.108	19.15	14.06	9.54	0.408
0.170	18.01	12.97	9.73	0.440
0.231	16.95	11.46	9.89	0.464
0.417	14.53	8.74	9.16	0.529

TABLE 12 (Cont'd). TEST RESULTS
RIPRAP ON SLOPE 1:2
STONE SIZE 4.6mm A

Test : S4 Water depth = 0.241m Mean flow velocity = 0.709m/s
Fr = 0.452 Fr2 = 0.529

TOE $u_* = 0.0847$m/s

0.073	17.59	12.57	8.77	0.355
0.114	16.31	10.86	8.38	0.395
0.197	15.72	9.37	8.46	0.439
0.280	14.72	8.15	8.10	0.486
0.405	13.39	6.62	7.29	0.546
0.737	7.90	3.80	4.14	0.662

BANK

0.146	19.91	12.31	8.22	0.386
0.229	15.86	10.67	8.01	0.427
0.313	14.76	9.98	8.03	0.457

Test : S3 Water depth = 0.171m Mean flow velocity = 0.737m/s
Fr = 0.560 Fr2 = 0.637

TOE $u_* = 0.0602$m/s

0.102	14.91	9.16	6.07	0.426
0.161	14.86	9.19	6.36	0.442
0.278	12.25	7.47	6.00	0.500
0.395	10.63	5.33	5.49	0.541
0.687	8.57	6.31	4.50	0.578

Test : S2A Water depth = 0.185m Mean flow velocity = 0.748m/s
Fr = 0.546 Fr2 = 0.626

TOE $u_* = 0.0449$m/s

0.095	18.93	11.17	6.99	0.429
0.149	17.75	9.89	7.37	0.476
0.257	14.91	7.84	7.40	0.531
0.365	13.92	6.50	6.92	0.575
0.527	10.24	4.90	5.76	0.624

TABLE 12 (Cont'd). TEST RESULTS
RIPRAP ON SLOPE 1:2
STONE SIZE 4.6mm A

Test : S4 Water depth = 0.241m Mean flow velocity = 0.709m/s
Fr = 0.452 Fr2 = 0.529

TOE $u_* = 0.0847$m/s

0.073	17.59	12.57	8.77	0.355
0.114	16.31	10.86	8.38	0.395
0.197	15.72	9.37	8.46	0.439
0.280	14.72	8.15	8.10	0.486
0.405	13.39	6.62	7.29	0.546
0.737	7.90	3.80	4.14	0.662

BANK

0.146	19.91	12.31	8.22	0.386
0.229	15.86	10.67	8.01	0.427
0.313	14.76	9.98	8.03	0.457

Test : S3 Water depth = 0.171m Mean flow velocity = 0.737m/s
Fr = 0.560 Fr2 = 0.637

TOE $u_* = 0.0602$m/s

0.102	14.91	9.16	6.07	0.426
0.161	14.86	9.19	6.36	0.442
0.278	12.25	7.47	6.00	0.500
0.395	10.63	5.33	5.49	0.541
0.687	8.57	6.31	4.50	0.578

Test : S2A Water depth = 0.185m Mean flow velocity = 0.748m/s
Fr = 0.546 Fr2 = 0.626

TOE $u_* = 0.0449$m/s

0.095	18.93	11.17	6.99	0.429
0.149	17.75	9.89	7.37	0.476
0.257	14.91	7.84	7.40	0.531

TABLE 13. TEST RESULTS
RIPRAP ON SLOPE 1:2
STONE SIZE 9.7mmA

Test : S10 Water depth = 0.251m Mean flow velocity = 0.930m/s
Fr = 0.586 Fr2 = 0.686 Normal Turbulence

TOE $u_* = 0.0495$ m/s

y/y_o	TI_u (%)	TI_v (%)	TI_w (%)	u (m/s)
0.058	8.50	3.48	2.95	0.798
0.098	7.56	3.07	2.87	0.855
0.177	4.65	2.10	2.29	0.954
0.257	2.55	1.57	1.79	0.997
0.376	1.40	1.31	1.32	1.014
0.616	1.30	1.09	1.44	1.005

BANK

0.115	10.98	5.79	4.95	0.547
0.194	9.38	5.46	5.03	0.571
0.271	9.19	5.15	5.14	0.567

Test : 57 Water depth = 0.159m Mean flow velocity = 1.159m/s
Fr = 0.912 Fr2 = 1.031

TOE $u_* = 0.0461$m/s

0.091	10.85	4.96	3.53	0.786
0.154	9.16	4.32	3.22	0.854
0.280	7.38	3.14	3.06	0.932
0.406	5.62	2.78	2.52	0.972
0.594	3.81	2.09	2.42	0.996

Test : S8 Water depth = 0.247m Mean flow velocity = 0.820m/s
Fr = 0.519 Fr2 = 0.608

TOE $u_* = 0.0674$m/s

0.071	15.29	8.48	5.77	0.540
0.111	14.97	7.94	5.95	0.594
0.192	14.00	6.90	5.35	0.669
0.273	13.07	5.48	4.99	0.732
0.395	10.77	4.67	4.42	0.800
0.638	6.89	3.38	3.07	0.916

TABLE 13 (Cont'd). TEST RESULTS
RIPRAP ON SLOPE 1:2
STONE SIZE 9.7mmA

BANK

0.141	15.01	8.62	6.22	0.484
0.222	13.40	7.87	6.71	0.511
0.302	12.71	7.22	6.72	0.530

Test : S9 Water depth = 0.349m Mean flow velocity = 0.650m/s
Fr = 0.347 Fr2 = 0.419

y/y_o	TI_u (%)	TI_v (%)	TI_w (%)	u (m/s)
0.050	14.41	11.99	5.99	0.427
0.079	13.13	11.49	6.67	0.446
0.136	12.13	10.03	7.02	0.487
0.193	12.69	9.64	7.86	0.522
0.337	12.79	8.11	8.51	0.562
0.681	12.02	5.44	5.64	0.741

BANK

0.100	17.55	10.75	8.50	0.484
0.157	16.99	10.26	8.57	0.518
0.214	17.09	9.26	8.15	0.548
0.386	15.59	6.87	7.74	0.612

Test : S11 Water depth = 0.157m Mean flow velocity = 1.098m/s
Fr = 0.869 Fr2 = 0.982

TOE $u_* = 0.0445m/s$

0.073	13.94	6.69	4.72	0.705
0.137	13.00	5.63	4.27	0.774
0.264	10.24	4.23	4.12	0.866
0.392	7.82	3.37	3.88	0.910
0.583	5.61	2.98	3.46	0.922

TABLE 14. TEST RESULTS
RIPRAP ON SLOPE 1:2
STONE SIZE 11.8mmA

Test : S15 Water depth = 0.252m Mean flow velocity = 1.089m/s
Fr = 0.683 Fr2 = 0.802 Normal Turbulence

TOE $u_* = 0.0747$m/s

y/y_o	TI_u (%)	TI_v (%)	TI_w (%)	u (m/s)
0.058	5.67	3.14	2.35	0.923
0.097	4.63	2.40	2.25	1.012
0.177	3.12	1.51	1.49	1.146
0.256	1.75	1.32	1.10	1.192
0.534	1.60	0.91	1.26	1.195

Test : S13 Water depth = 0.190m Mean flow velocity = 0.985m/s
Fr = 0.710 Fr2 = 0.815

TOE $u_* = 0.0564$m/s

0.071	9.87	4.82	3.17	0.757
0.124	7.86	4.09	2.99	0.885
0.229	6.04	3.80	2.83	0.954
0.334	5.59	3.08	2.74	0.999
0.492	4.65	2.47	2.51	1.039

Test : S14 Water depth = 0.264m Mean flow velocity = 0.839m/s
Fr = 0.513 Fr2 = 0.606

TOE $u_* = 0.0688$m/s

0.066	15.58	8.91	5.50	0.587
0.104	14.23	8.25	5.21	0.654
0.180	12.49	6.92	4.97	0.744
0.256	11.13	5.95	4.89	0.819
0.445	7.91	4.78	4.52	0.910

BANK

0.102	14.28	8.03	5.50	0.596
0.178	14.44	7.22	5.57	0.639
0.216	13.96	6.87	5.49	0.653

TABLE 14 (Cont'd). TEST RESULTS
RIPRAP ON SLOPE 1:2
STONE SIZE 11.8mmA

Test : S16 Water depth = 0.337m Mean flow velocity = 0.729m/s
Fr = 0.395 Fr2 = 0.476

TOE $u_* = 0.0794$m/s

0.052	19.62	14.21	7.90	0.362
0.082	15.36	12.55	7.06	0.484
0.141	14.39	10.43	6.87	0.576
0.200	13.33	8.88	6.63	0.632
0.349	12.48	6.69	6.75	0.732
0.645	9.18	5.63	5.51	0.887

BANK

0.074	25.11	14.05	9.71	0.390
0.133	17.31	11.45	8.81	0.511
0.192	18.32	10.28	8.77	0.536
0.251	17.32	9.30	8.29	0.575

TABLE 15. TEST RESULTS
RIPRAP ON SLOPE 1:2.5
STONE SIZE 4.6mmA

Test : S30 Water depth = 0.181m Mean flow velocity = 0.781m/s
Fr = 0.586 Fr2 = 0.723 Normal Turbulence

TOE $u_* = 0.0464$m/s

y/y_o	TI_u (%)	TI_v (%)	TI_w (%)	u (m/s)
0.075	9.94	3.58	2.81	0.749
0.130	7.94	2.83	2.41	0.815
0.185	6.28	2.16	2.04	0.860
0.351	2.38	1.31	1.47	0.928
0.517	1.69	1.15	1.72	0.914

BANK

0.121	3.92	1.62	1.81	0.880
0.190	2.92	1.47	1.76	0.893
0.259	2.14	1.39	1.67	0.903

Test : S26 Water depth = 0.186m Mean flow velocity = 0.681m/s
Fr = 0.505 Fr2 = 0.623

TOE $u_* = 0.0190$m/s

0.073	11.68	6.51	4.44	0.614
0.127	11.33	5.59	4.18	0.636
0.234	9.36	4.90	4.73	0.677
0.341	8.27	4.23	4.93	0.689
0.503	7.67	3.43	4.46	0.702

BANK

0.117	15.87	7.60	5.53	0.496
0.185	15.51	6.55	5.28	0.536
0.252	14.29	5.55	5.24	0.571
0.386	12.53	4.58	4.30	0.624

Test : S27 Water depth = 0.176m Mean flow velocity = 0.731m/s
Fr = 0.556 Fr2 = 0.683

TOE $u_* = 0.0231$m/s

0.076	7.55	4.04	3.19	0.711
0.133	6.34	3.47	3.23	0.758
0.247	4.85	2.96	3.51	0.779
0.361	4.66	2.77	3.72	0.780

TABLE 15 (Cont'd). TEST RESULTS
RIPRAP ON SLOPE 1:2.5
STONE SIZE 4.6mmA

BANK

0.096	8.13	5.59	3.70	0.604
0.167	7.52	4.80	3.55	0.650
0.238	7.06	1.31	3.74	0.682
0.379	6.53	3.10	3.67	0.720

Test : S28 Water depth = 0.258m Mean flow velocity = 0.651m/s
Fr = 0.409 Fr2 = 0.519

TOE $u_* = -$

y/y_o	TI_u (%)	TI_v (%)	TI_w (%)	u (m/s)
0.068	6.26	4.72	2.71	0.712
0.107	6.18	4.65	2.94	0.715
0.145	6.46	4.85	3.70	0.712
0.223	6.45	5.15	4.59	0.702
0.378	6.35	5.15	6.15	0.686
0.533	6.45	3.87	5.55	0.697

BANK

0.085	12.32	10.56	5.00	0.438
0.133	12.06	9.80	5.45	0.467
0.182	11.45	9.39	5.93	0.498
0.279	12.24	7.52	6.10	0.553

Test : S28A Water depth = 0.258m Mean flow velocity = 0.649m/s
Fr = 0.408 Fr2 = 0.517

TOE $u_* = -$

0.068	5.92	4.61	2.53	0.723
0.107	5.97	4.65	2.94	0.727
0.145	6.26	4.69	3.56	0.721
0.223	6.47	5.09	4.63	0.706
0.378	6.15	4.89	5.85	0.689
0.533	6.07	3.96	5.66	0.695

BANK

0.066	11.92	10.97	5.80	0.448
0.114	11.30	10.11	6.35	0.477
0.163	12.32	9.16	6.63	0.507
0.260	12.09	6.84	6.47	0.561

TABLE 15 (Cont'd). TEST RESULTS
RIPRAP ON SLOPE 1:2.5
STONE SIZE 4.6mmA

Test : S29   Water depth = 0.332m   Mean flow velocity = 0.629m/s
Fr = 0.349 Fr2 = 0.450

TOE $u_* = -$

0.053	7.86	5.96	3.28	0.713
0.083	7.81	5.86	3.88	0.707
0.113	8.51	6.33	5.38	0.691
0.203	9.34	6.96	6.89	0.665
0.354	9.79	7.70	9.33	0.625
0.602	9.61	5.99	6.95	0.687

BANK

0.066	12.96	11.10	5.71	0.456
0.104	12.93	11.14	6.79	0.476
0.142	12.41	10.66	7.52	0.494
0.255	11.73	9.91	8.82	0.530

TABLE 16. TEST RESULTS
RIPRAP ON SLOPE 1:2.5
STONE SIZE 9.7mmA

Test : S25 Water depth = 0.247m Mean flow velocity = 1.063m/s
Fr = 0.678 Fr2 = 0.856 Normal Turbulence

TOE $u_* = 0.0486$m/s

y/Y_o	TI_u (%)	TI_v (%)	TI_w (%)	u (m/s)
0.055	7.07	3.58	2.93	0.891
0.095	5.00	2.70	2.56	0.968
0.176	3.65	2.14	1.87	1.054
0.257	2.62	1.75	1.55	1.096
0.379	1.42	1.31	1.35	1.119
0.621	1.21	1.10	1.33	1.103

BANK

0.068	6.90	3.40	2.62	0.947
0.119	4.50	2.34	2.26	1.025
0.220	3.04	1.61	1.63	1.109
0.321	1.59	1.28	1.18	1.151

Test : S21 Water depth = 0.162m Mean flow velocity = 0.733m/s
Fr = 0.586 Fr2 = 0.716

TOE $u_* = 0.0359$m/s

0.108	10.54	6.66	4.55	0.572
0.170	10.54	6.29	4.55	0.604
0.293	9.70	5.03	4.53	0.659
0.417	8.13	4.18	4.33	0.691

BANK

0.135	13.38	6.57	4.55	0.538
0.212	11.95	5.24	3.68	0.603
0.288	10.79	4.45	3.79	0.656

Test : S22 Water depth = 0.150m Mean flow velocity = 1.108m/s
Fr = 0.913 Fr2 = 1.108

TOE $u_* = 0.0318$m/s

0.083	11.28	5.25	3.38	0.710
0.150	9.59	4.23	3.25	0.806
0.283	8.37	4.19	3.80	0.838
0.417	7.28	3.50	4.02	0.854
0.617	6.20	2.48	3.32	0.882

TABLE 16 (Cont'd). TEST RESULTS
RIPRAP ON SLOPE 1:2.5
STONE SIZE 9.7mmA

BANK

0.104	9.67	3.50	2.87	0.836
0.188	7.41	3.04	2.55	0.886
0.270	6.73	2.64	2.48	0.914

Test : S23 Water depth = 0.250m Mean flow velocity = 0.877m/s
Fr = 0.560 Fr2 = 0.708

TOE $u_* = 0.0414$m/s

y/Y_o	TI_u (%)	TI_v (%)	TI_w (%)	u (m/s)
0.054	9.75	5.01	2.40	0.816
0.094	7.35	4.56	2.71	0.900
0.174	5.80	4.36	3.45	0.938
0.257	5.87	4.42	4.12	0.929
0.374	5.40	4.29	4.67	0.911
0.610	5.23	3.11	3.82	0.921

BANK

0.088	13.59	5.59	4.70	0.726
0.138	11.82	4.94	4.25	0.788
0.188	11.42	4.64	4.14	0.822
0.288	9.35	3.55	3.67	0.8812

Test : S24 Water depth = 0.354m Mean flow velocity = 0.878m/s
Fr = 0.468 Fr2 = 0.607
TOE $u_* = 0.0258$m/s

y/Y_o	TI_u (%)	TI_v (%)	TI_w (%)	u (m/s)
0.038	8.40	5.83	3.06	0.862
0.066	8.10	5.86	3.78	0.912
0.123	6.18	5.61	4.46	0.938
0.179	5.72	5.25	5.23	0.941
0.321	6.18	5.57	6.58	0.926
0.660	6.71	4.45	4.62	0.981

TABLE 16 (Cont'd). TEST RESULTS
RIPRAP ON SLOPE 1:2.5
STONE SIZE 9.7mmA

BANK

0.062	15.69	9.01	6.25	0.611
0.097	15.28	8.15	5.88	0.660
0.133	15.26	7.86	6.06	0.696
0.239	13.66	6.42	6.27	0.788
0.345	10.91	5.66	5.50	0.878

TABLE 17. TEST RESULTS
RIPRAP ON SLOPE 1:2.5
STONE SIZE 11.8mmA

Test : S20 Water depth = 0.229m Mean flow velocity = 1.291m/s
Fr = 0.860 Fr2 = 1.080 Normal Turbulence

TOE $u_* = 0.0892$m/s

y/y_o	TI_u (%)	TI_v (%)	TI_w (%)	u (m/s)
0.076	6.33	3.70	2.78	0.896
0.120	4.58	2.73	2.45	0.998
0.207	3.21	1.67	1.59	1.135
0.295	1.75	1.20	1.09	1.190
0.688	1.30	1.07	1.23	1.184

BANK

0.096	4.63	2.53	2.37	1.008
0.150	4.21	1.96	2.14	1.079
0.205	3.46	1.51	1.66	1.160
0.260	2.53	1.25	1.34	1.203

Test : S17 Water depth = 0.194m Mean flow velocity = 1.105m/s
Fr = 0.801 Fr2 = 0.993

TOE $u_* = 0.0685$m/s

0.064	9.01	-	2.66	0.762
0.116	7.26	-	3.18	0.884
0.219	3.64	-	3.05	0.972
0.322	2.98	-	4.02	0.976
0.477	3.53	-	5.84	0.954

BANK

0.113	10.35	-	4.27	0.528
0.177	11.47	-	4.67	0.596
0.242	9.82	-	4.52	0.658
0.371	9.17	-	4.56	0.749
0.565	7.49	-	4.06	0.825

TABLE 17 (Cont'd). TEST RESULTS
RIPRAP ON SLOPE 1:2.5
STONE SIZE 11.8mmA

Test : S18 Water depth = 0.263m Mean flow velocity = 0.899m/s
Fr = 0.559 Fr2 = 0.709

TOE $u_* = 0.0398$m/s

0.048	7.67	4.75	2.66	0.846
0.086	5.87	4.03	2.94	0.915
0.162	3.72	3.70	3.42	0.968
0.238	3.46	3.72	4.42	0.959
0.428	4.43	5.06	6.31	0.925

BANK

0.083	12.31	6.91	3.97	0.691
0.130	11.58	6.10	3.79	0.746
0.178	11.27	7.95	4.99	0.658
0.225	10.81	7.33	5.11	0.692
0.320	9.91	6.07	4.96	0.756

Test : S19 Water depth = 0.341m Mean flow velocity = 0.797m/s
Fr = 0.435 Fr2 = 0.563

TOE $u_* = 0.0255$m/s

0.034	8.66	6.06	2.78	0.784
0.063	7.18	6.48	3.24	0.855
0.122	5.29	5.97	4.12	0.893
0.180	5.40	5.80	5.00	0.888
0.327	6.88	5.96	6.40	0.867
0.620	7.41	5.08	5.71	0.899

BANK

0.064	15.91	8.04	5.65	0.605
0.101	15.28	7.78	5.69	0.648
0.137	15.14	7.45	6.16	0.679
0.174	14.66	7.38	5.97	0.708
0.247	13.59	6.51	5.92	0.773

TABLE 18. TEST RESULTS
CONCRETE BLOCKS

FLAT BED

Test : C27 Water depth = 0.264m Mean flow velocity = 0.688m/s
Fr = 0.428

y/y_o	TI_u (%)	TI_v (%)	TI_w (%)	u (m/s)
0.066	16.28	11.89	6.25	0.461

Test : C29* Water depth = 0.240m Mean flow velocity = 0.806m/s
Fr = 0.525

0.042	-	-	-	0.541
0.125	-	-	-	0.613

Test : C30* Water depth = 0.266m Mean flow velocity = 1.013m/s
Fr = 0.627 Normal turbulence

0.038	-	-	-	0.517
0.150	-	-	-	0.667

SLOPE 1:2 (TOE)

Test : C15 Water depth = 0.259m Mean flow velocity = 1.382m/s
Fr1 = 0.867 Fr2 = 1.023 Normal turbulence

0.068	7.44	4.71	2.48	0.937

Test : C17 Water depth = 0.269m Mean flow velocity = 0.804m/s
Fr1 = 0.495 Fr2 = 0.586

0.065	16.79	8.64	4.54	0.521

Test : C22 Water depth = 0.260m Mean flow velocity = 1.082m/s
Fr1 = 0.677 Fr2 = 0.799

0.067	16.75	-	-	0.564

Test : C23 Water depth = 0.198m Mean flow velocity = 1.315m/s
Fr1 = 0.944 Fr2 = 1.089

0.088	8.47	-	-	1.014

TABLE 18 (Cont'd). TEST RESULTS
CONCRETE BLOCKS

SLOPE 1:2.5 (TOE)

Test : C8 Water depth = 0.312m Mean flow velocity = 0.845m/s
Fr1 = 0.483 Fr2 = 0.622 Normal turbulence

y/y_o	TI_u (%)	TI_v (%)	TI_w (%)	u (m/s)
0.056	6.88	3.43	2.44	0.772

Test : C7 Water depth = 0.259m Mean flow velocity = 0.809m/s
Fr1 = 0.508 Fr2 = 0.646

0.068	8.20	4.40	3.01	0.792

Test : C10 Water depth = 0.265m Mean flow velocity = 0.908m/s
Fr1 = 0.563 Fr2 = 0.717

0.066	9.02	5.70	3.05	0.787

Test : C13 Water depth = 0.262m Mean flow velocity = 0.975m/s
Fr1 = 0.608 Fr2 = 0.774 Staggered blocks

0.066	5.93	5.51	3.55	0.813

* Test using miniature propellor current meter

TABLE 19. TEST RESULTS
RIPRAP ON BED
VALUES OF Dn_{50}, TI_u (10%), V_b (10%) and U_d

Dn_{50} (m)	TI_u (10%) (%)	V_b (10%) (m/s)	U_d (m/s)
0.0042	11.26	0.548	0.740
	14.35	0.438	0.460
	12.08	0.523	0.579
	13.50	0.462	0.522
	14.54	0.412	0.490
	15.47	0.369	0.379
0.0080	6.7	0.548	1.052
	12.81	0.740	0.820
	12.61	0.750	0.863
	11.12	0.558	0.735
	11.03	0.606	0.793
	11.42	0.657	0.759
	13.27	0.666	0.713
0.0106	8.60	0.680	1.106
	15.61	0.590	0.684
	14.33	0.610	0.737
	16.90	0.660	0.804
	23.31	0.490	0.716
0.0070	11.27	0.680	0.853
	31.76	0.260	0.301
	23.50	0.290	0.414
	14.30	0.504	0.612
	14.48	0.521	0.546
	17.10	0.500	0.543
0.0090	12.68	0.730	0.975
	17.84	0.389	0.464
	15.50	0.456	0.601
	16.30	0.580	0.667
	14.62	0.600	0.729
	12.68	0.716	0.860

TABLE 20. TEST RESULTS
RIPRAP ON SLOPE 1:2.5 (TOE)
VALUES OF Dn_{50}, TI_u (10%), V_b (10%) and U_d

Dn_{50} (m)	TI_u (10%) (%)	V_b (10%) (m/s)	U_d (m/s)
0.0042	8.20	0.770	0.880
	8.16	0.695	0.662
	6.04	0.725	0.694
	6.16	0.712	0.693
	11.51	0.625	0.679
	6.80	0.729	0.766
0.0080	4.95	0.960	1.073
	6.80	0.927	0.943
	7.00	0.905	0.911
	10.86	0.742	0.836
	10.54	0.572	0.674
0.0106	5.60	0.950	1.132
	6.00	0.880	0.877
	5.40	0.858	0.916
	7.80	0.843	0.937

TABLE 21. TEST RESULTS
RIPRAP ON SLOPE 1:2 (TOE)
VALUES OF Dn_{50}, TI_u (10%), V_b (10%), and U_d

Dn_{50} (m)	TI_u (10%) (%)	V_b (10%) (m/s)	U_d (m/s)
0.0042	9.20	0.542	0.634
	16.50	0.380	0.970
	14.90	0.426	0.871
	18.90	0.432	0.553
0.0080	7.60	0.855	0.980
	13.54	0.730	0.854
	12.80	0.462	0.609
	12.00	0.570	0.803
	10.50	0.790	0.954
0.0106	4.60	1.012	1.180
	15.04	0.505	0.791
	14.40	0.650	0.898
	8.00	0.827	0.984

TABLE 22. TEST RESULTS
CONCRETE BLOCKS
VALUES OF V_b (10%) and TI_u (10%)

Test	V_b (10%) (m/s)	TI_u (10%) (%)
Flat bed		
C25	0.487	15.8
C29	0.593	-
C30	0.640	-
Slope 1:2.5		
C7	0.841	6.6
C10	0.811	8.9
C13	0.878	4.2
Slope 1:2		
C15	1.090	7.4
C17	0.482	16.4
C22	0.595	17.2
C23	1.016	8.5

FIGURES

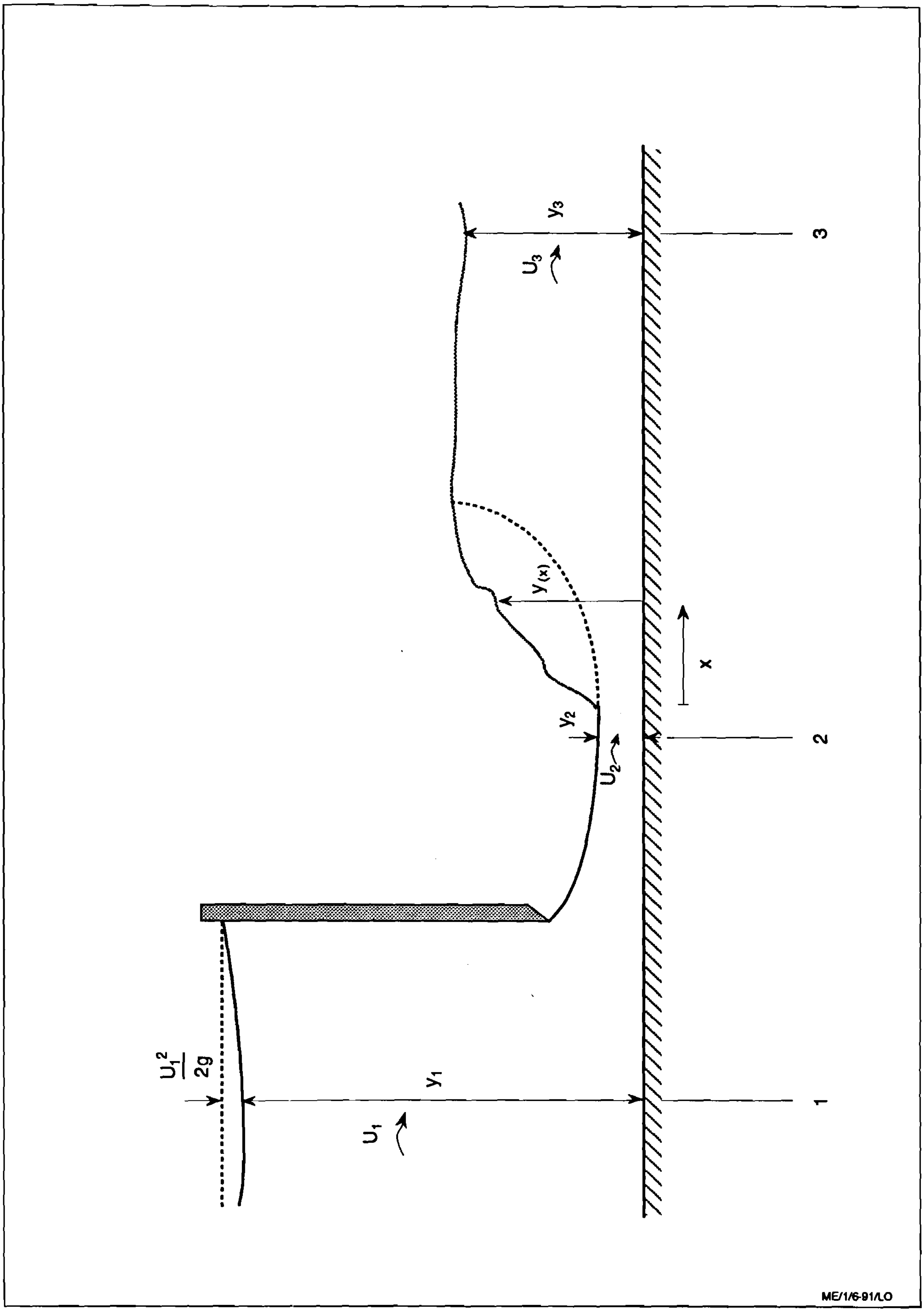

Fig 1 Schematic diagram of a hydraulic jump generated by a sluice-gate

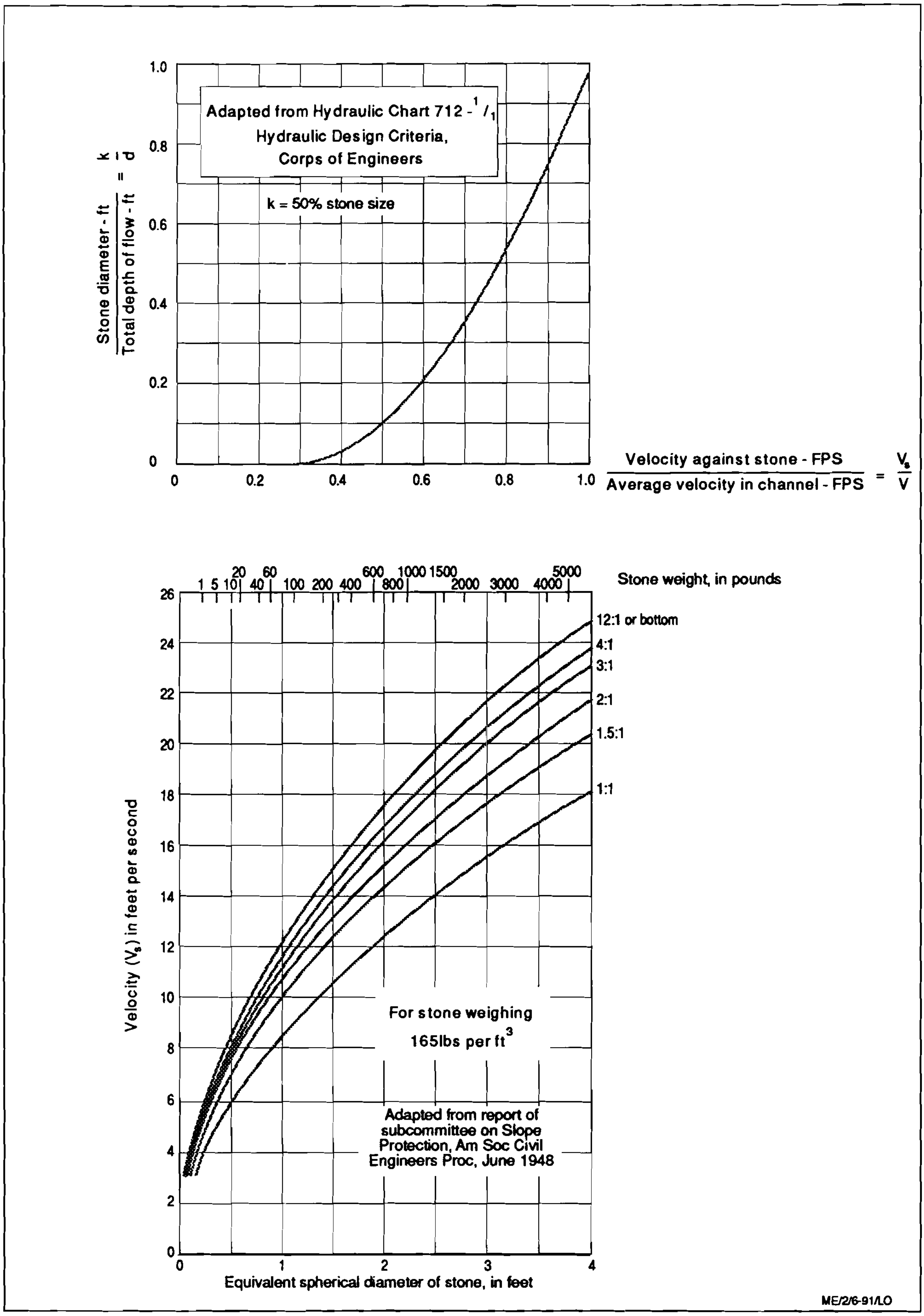

Fig 2 Charts for sizing stone protection on banks under parallel current attack (from Searcy, 1967)

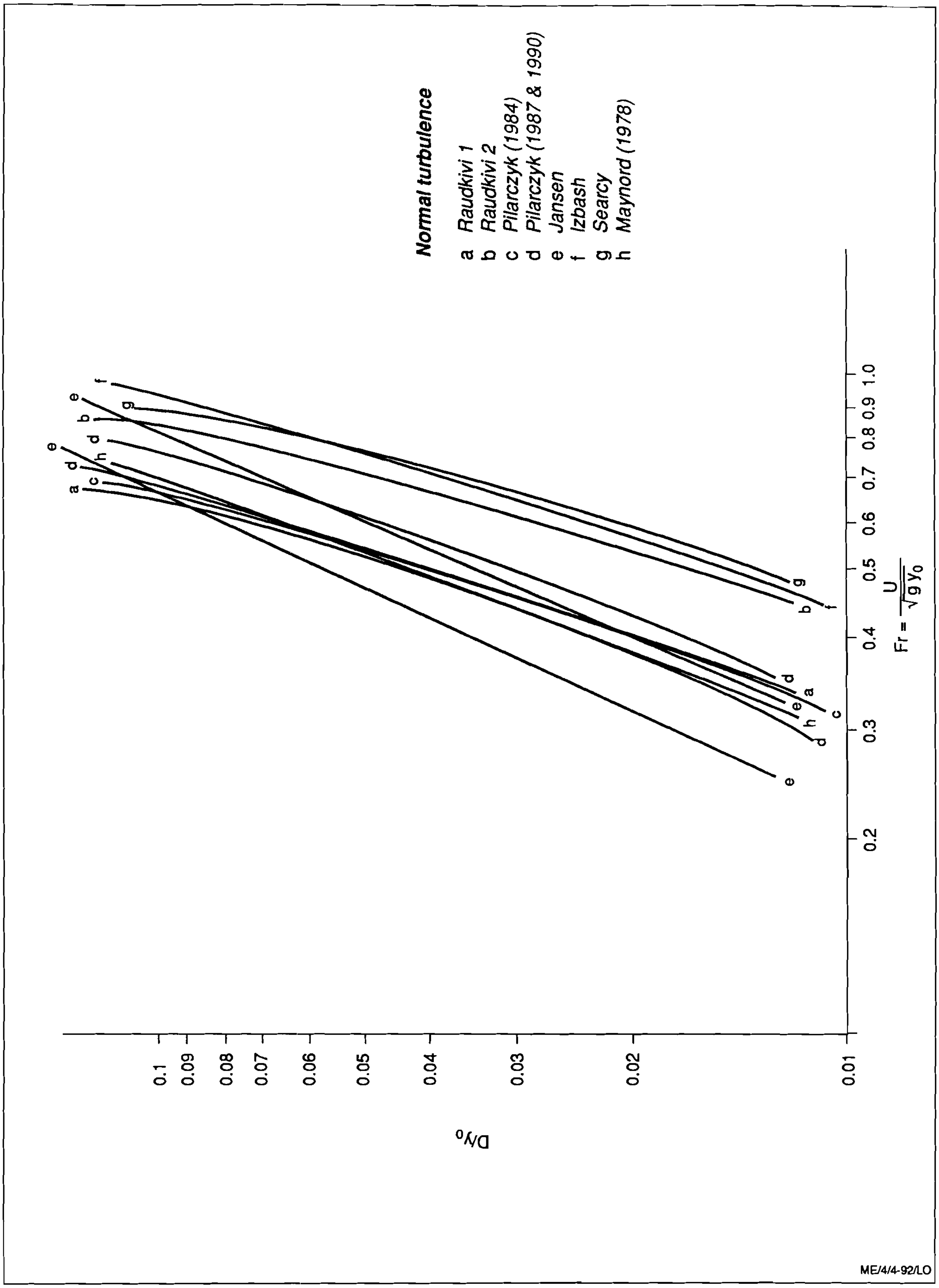

Figure 3 Comparison of different equations relating D/y_0 to the Froude number: normal turbulence

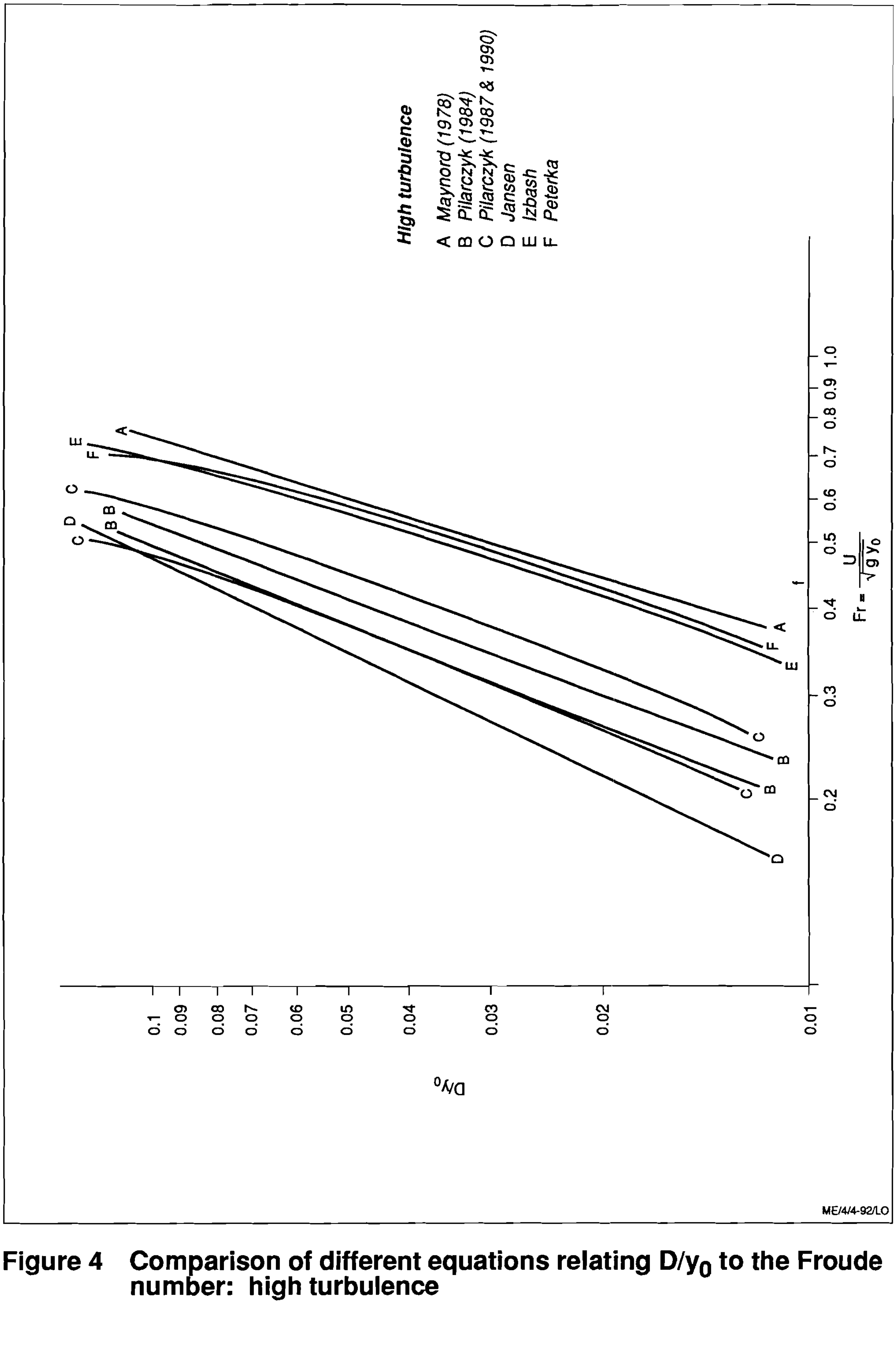

Figure 4 Comparison of different equations relating D/y_0 to the Froude number: high turbulence

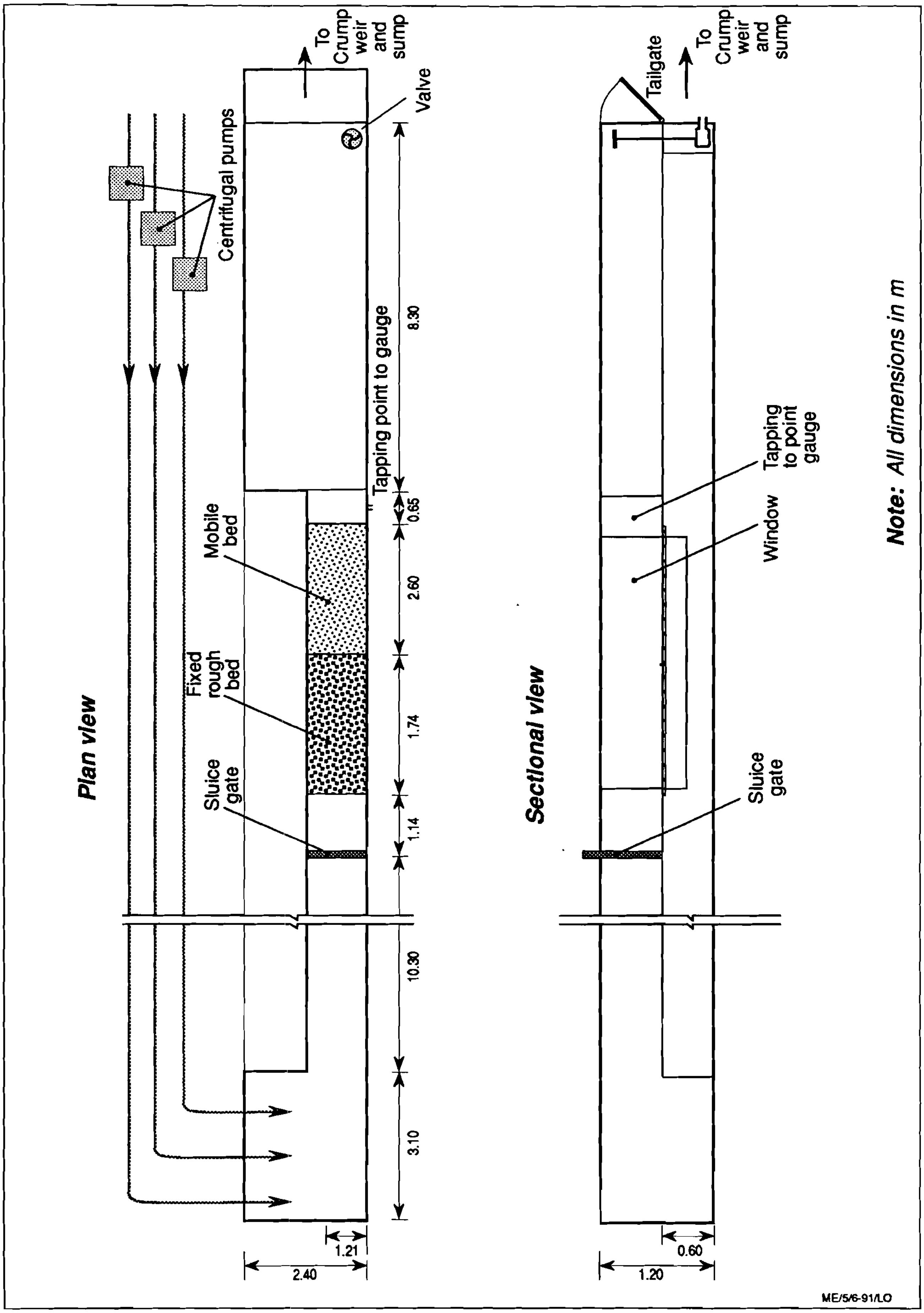

Fig 5 General layout of test rig

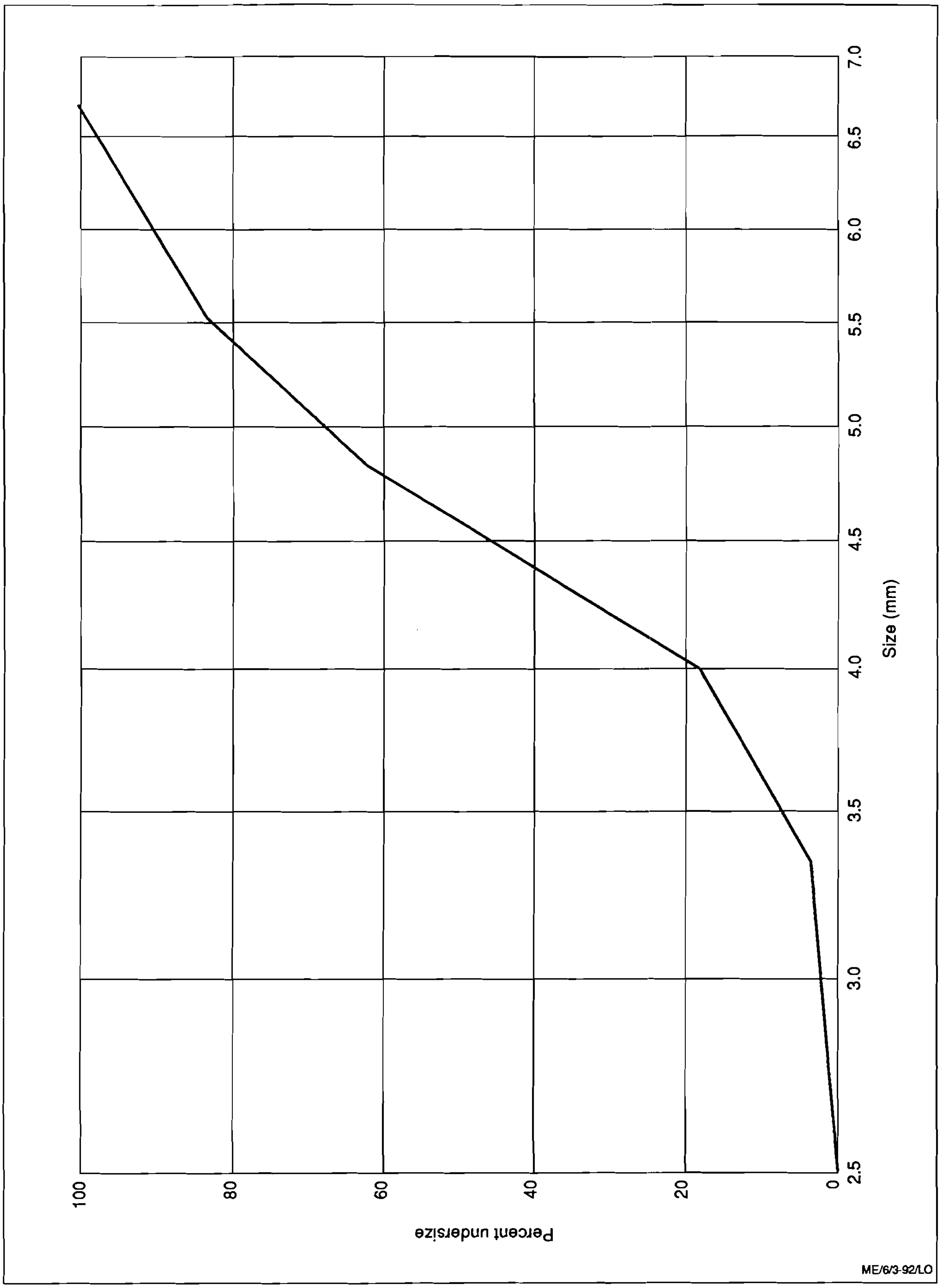

Figure 6 Grading curve – stone size 4.6mmA

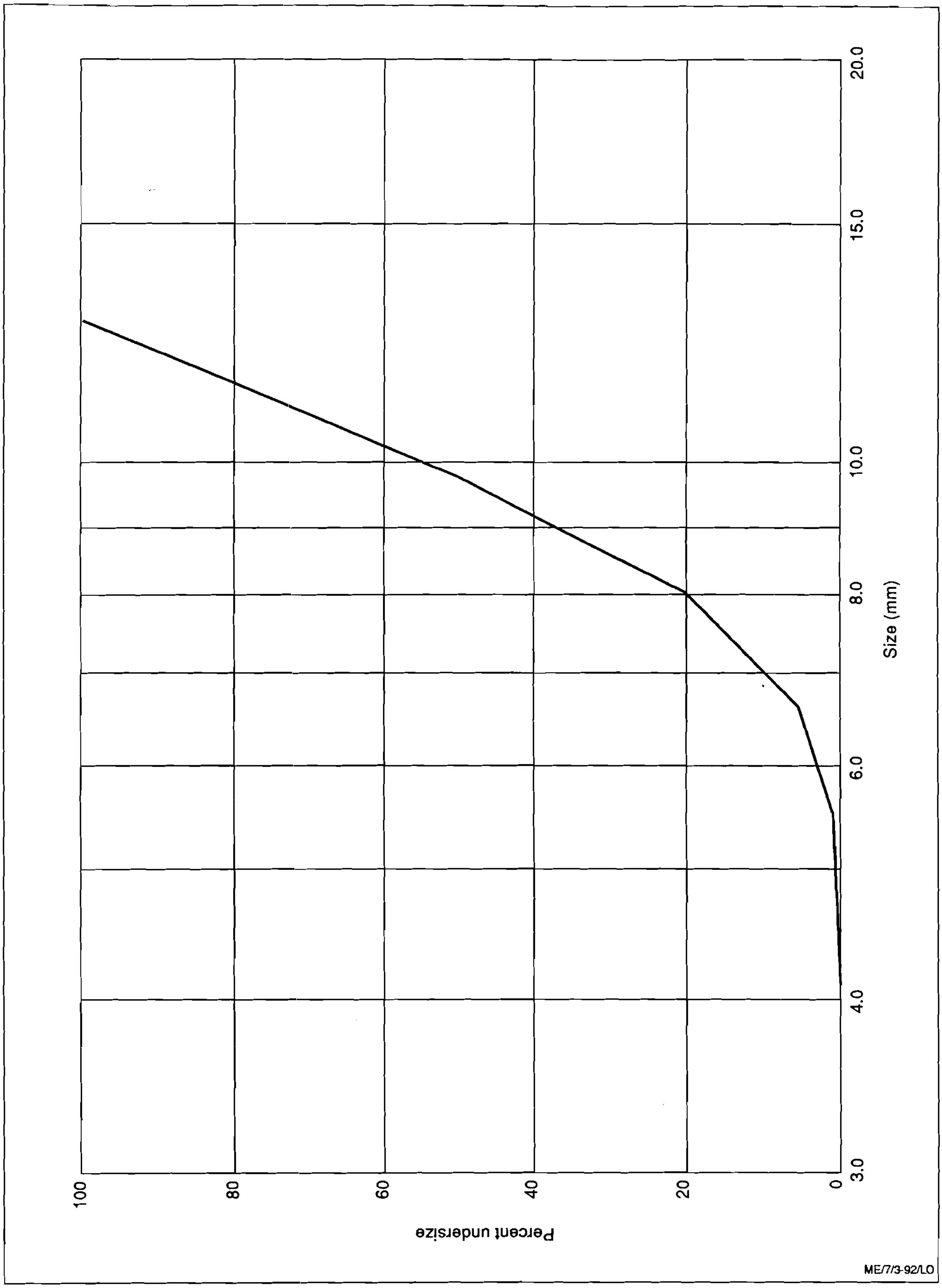

Figure 7 Grading curve – stone size 9.7mmA

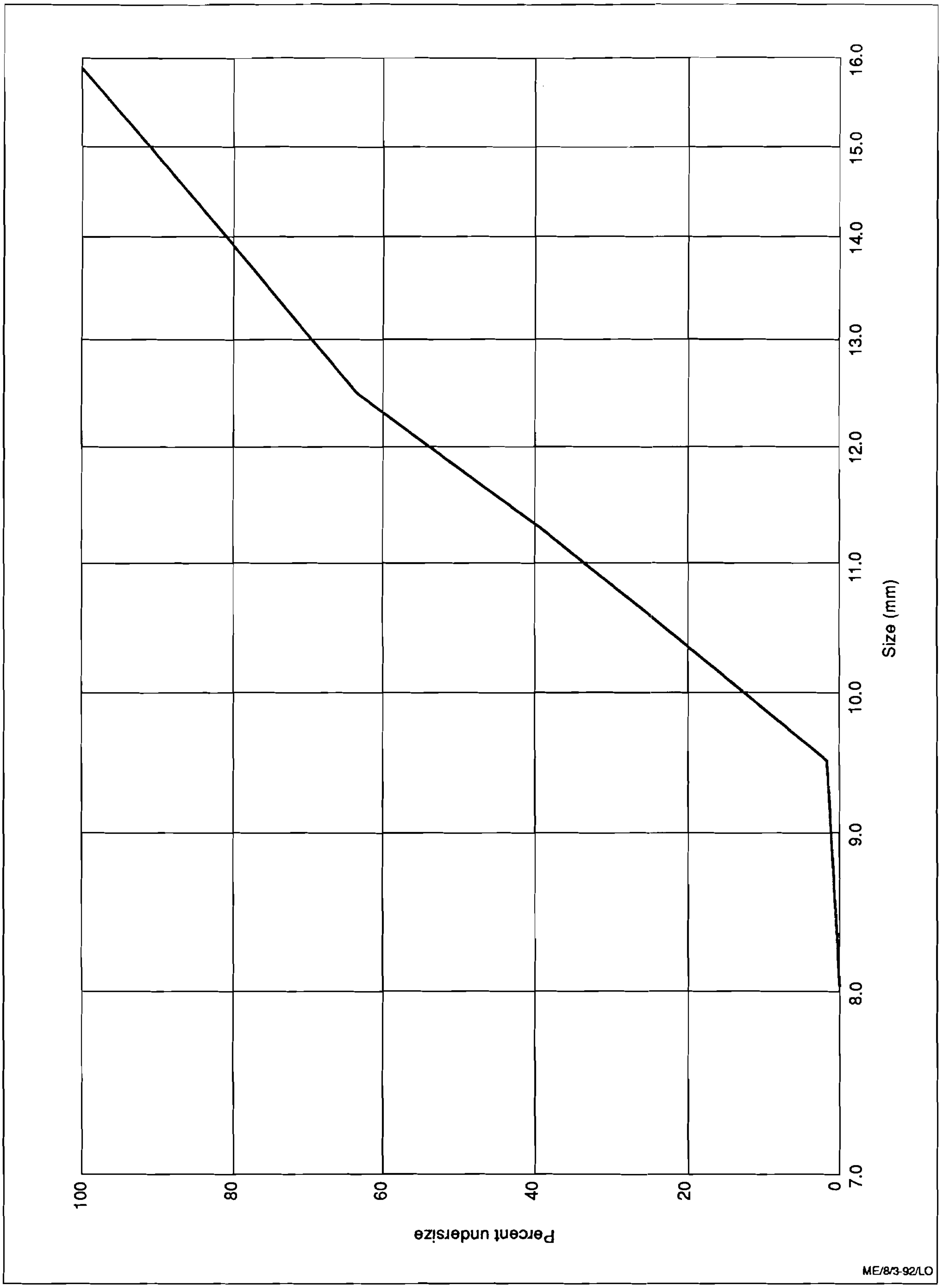

Figure 8 Grading curve – stone size 11.8mmA

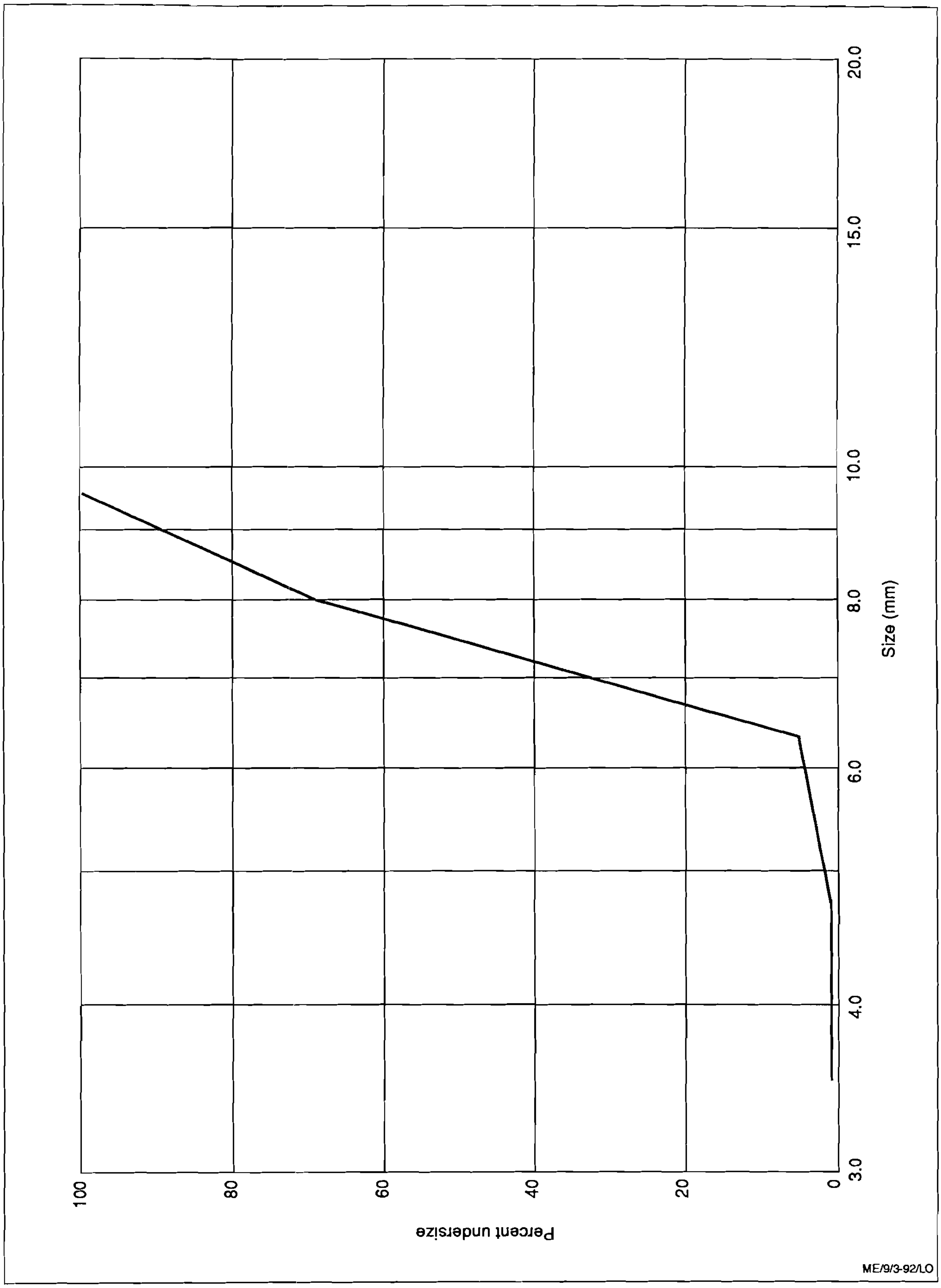

Figure 9 Grading curve – stone size 7.3mmR

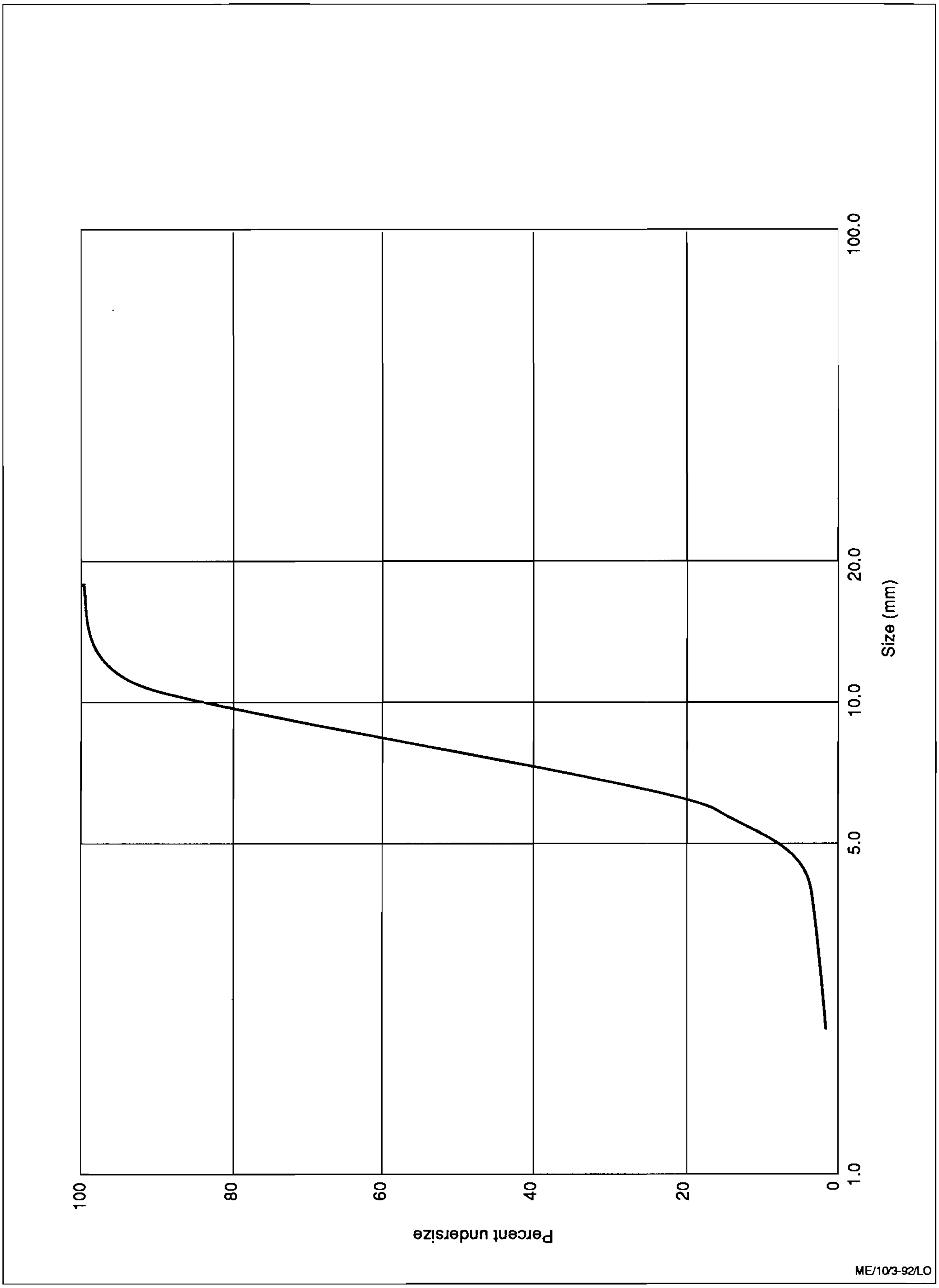

Figure 10 Grading curve – stone size 7.7mmR

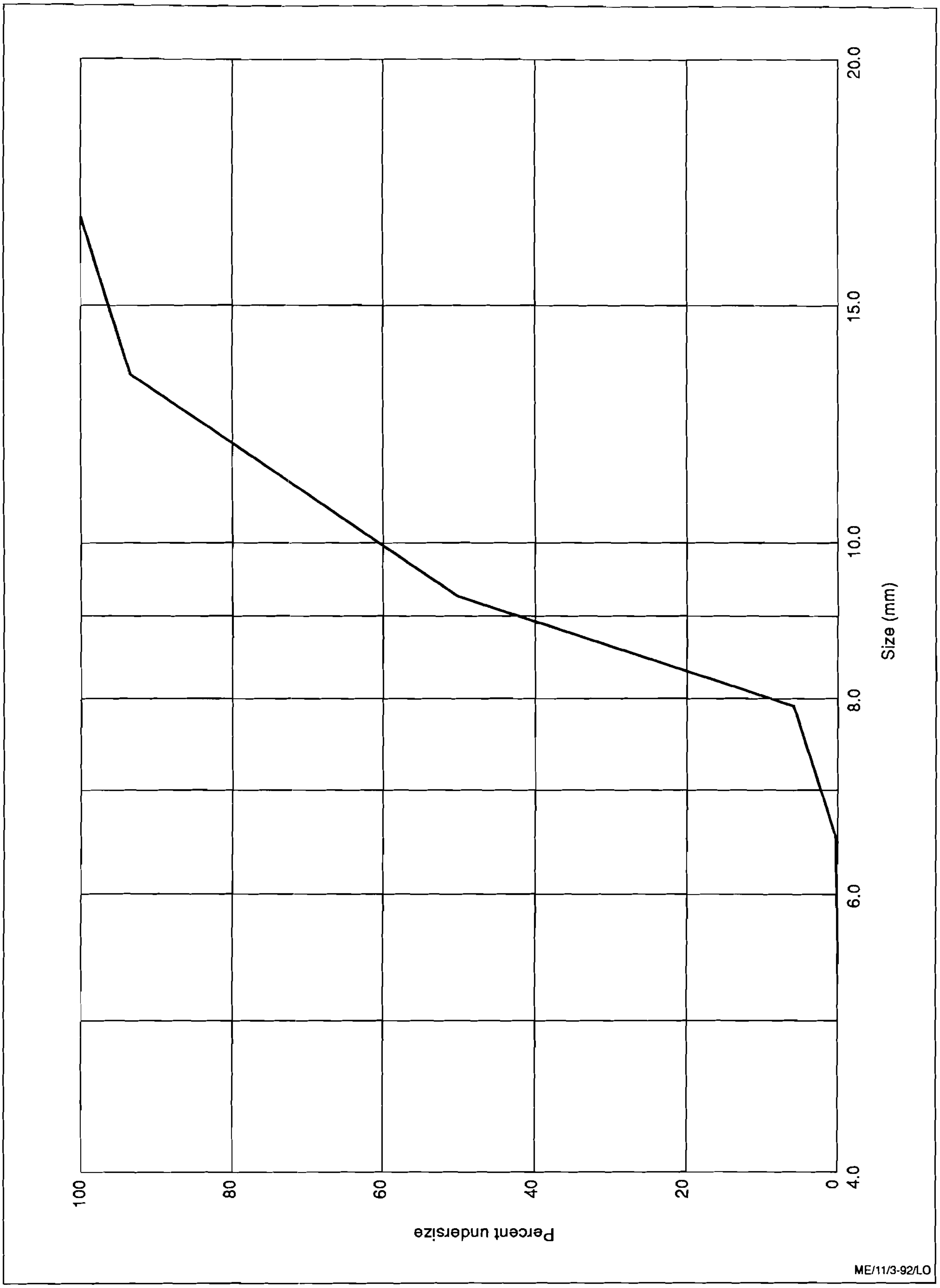

Figure 11 Grading curve – stone size 9.3mmR

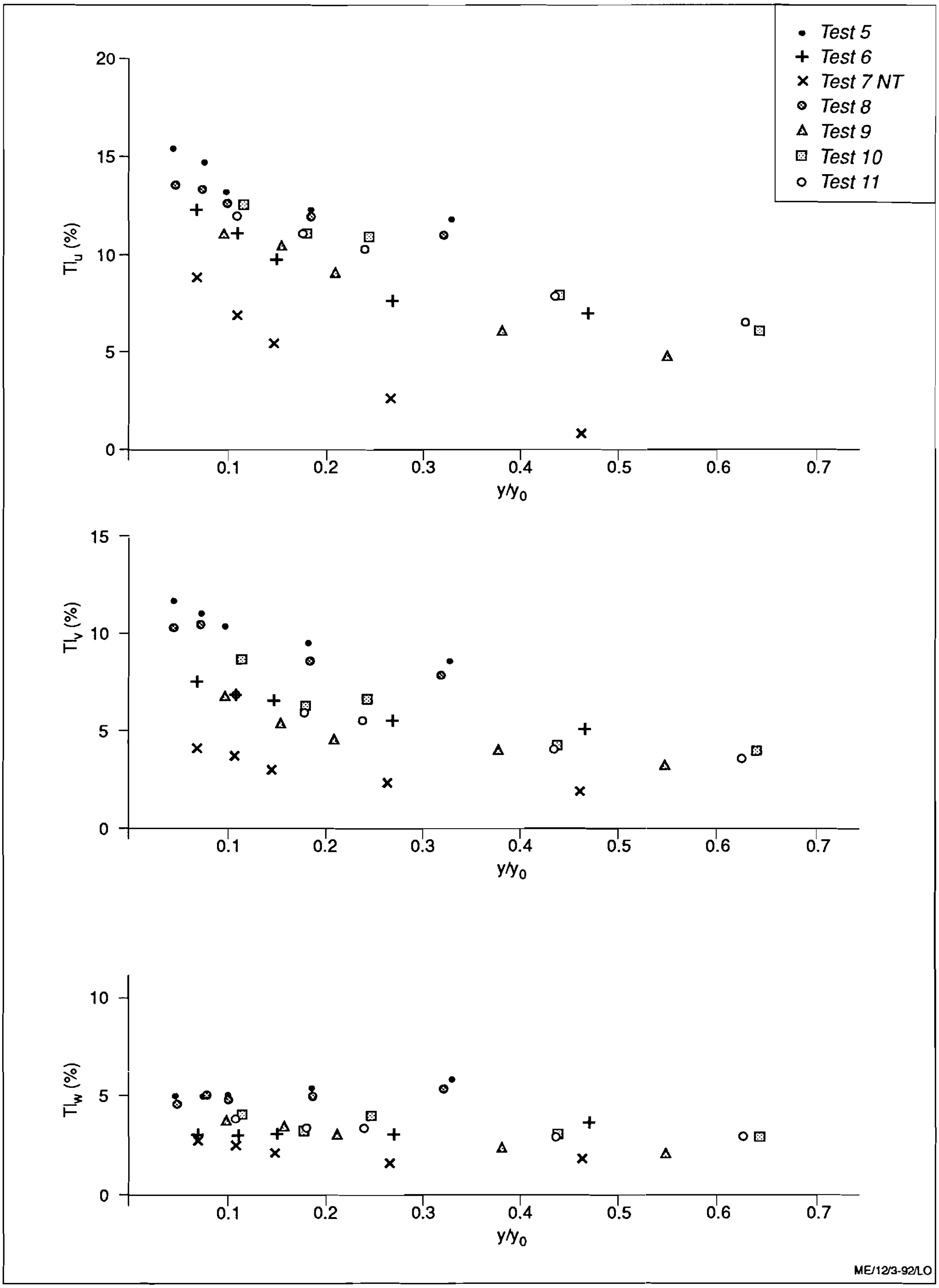

Figure 12 Longitudinal, transverse and vertical turbulence intensity profiles – stone size 9.7mmA

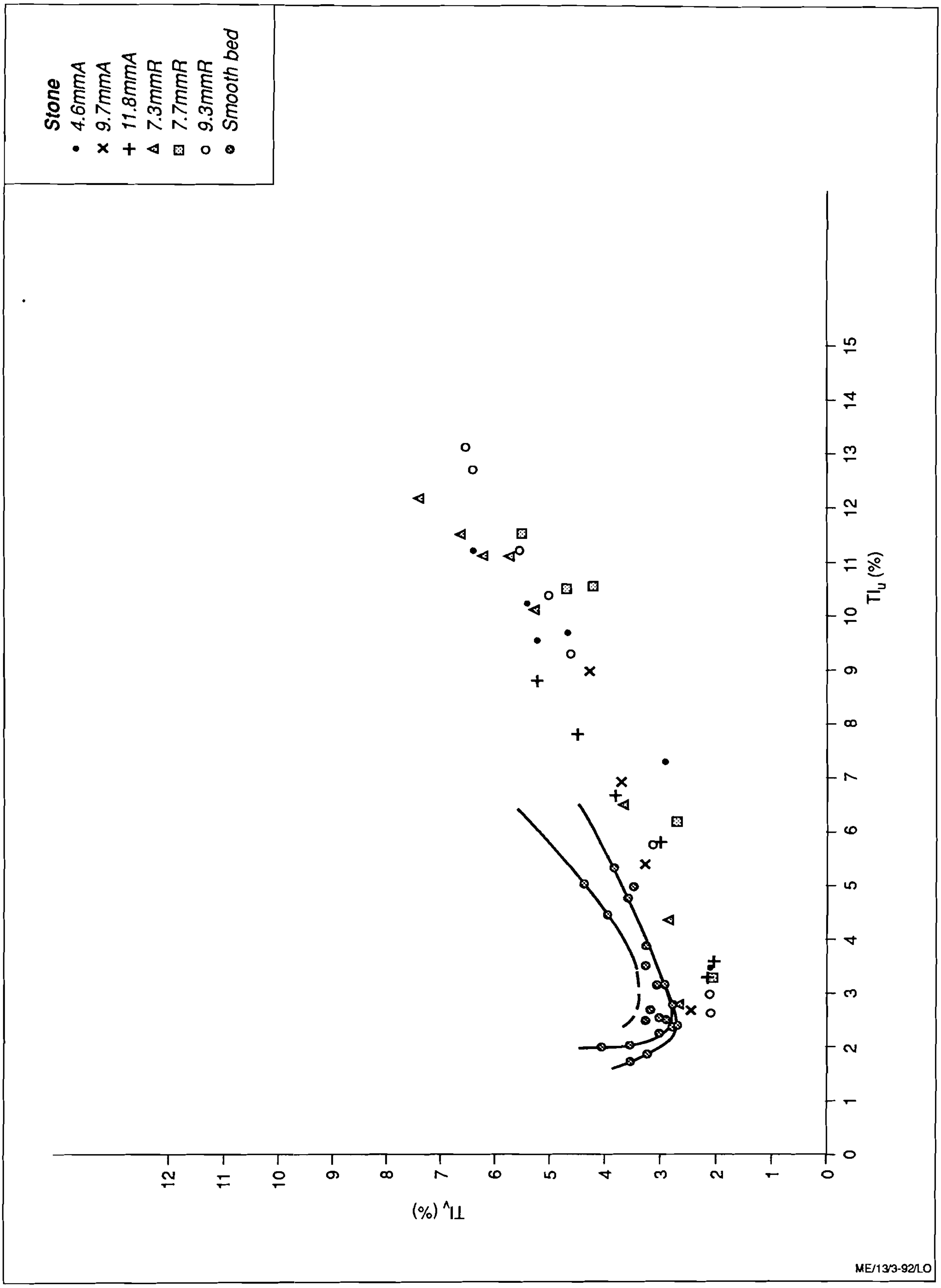

Figure 13 Relationship between longitudinal and transverse turbulence intensities – normal turbulence

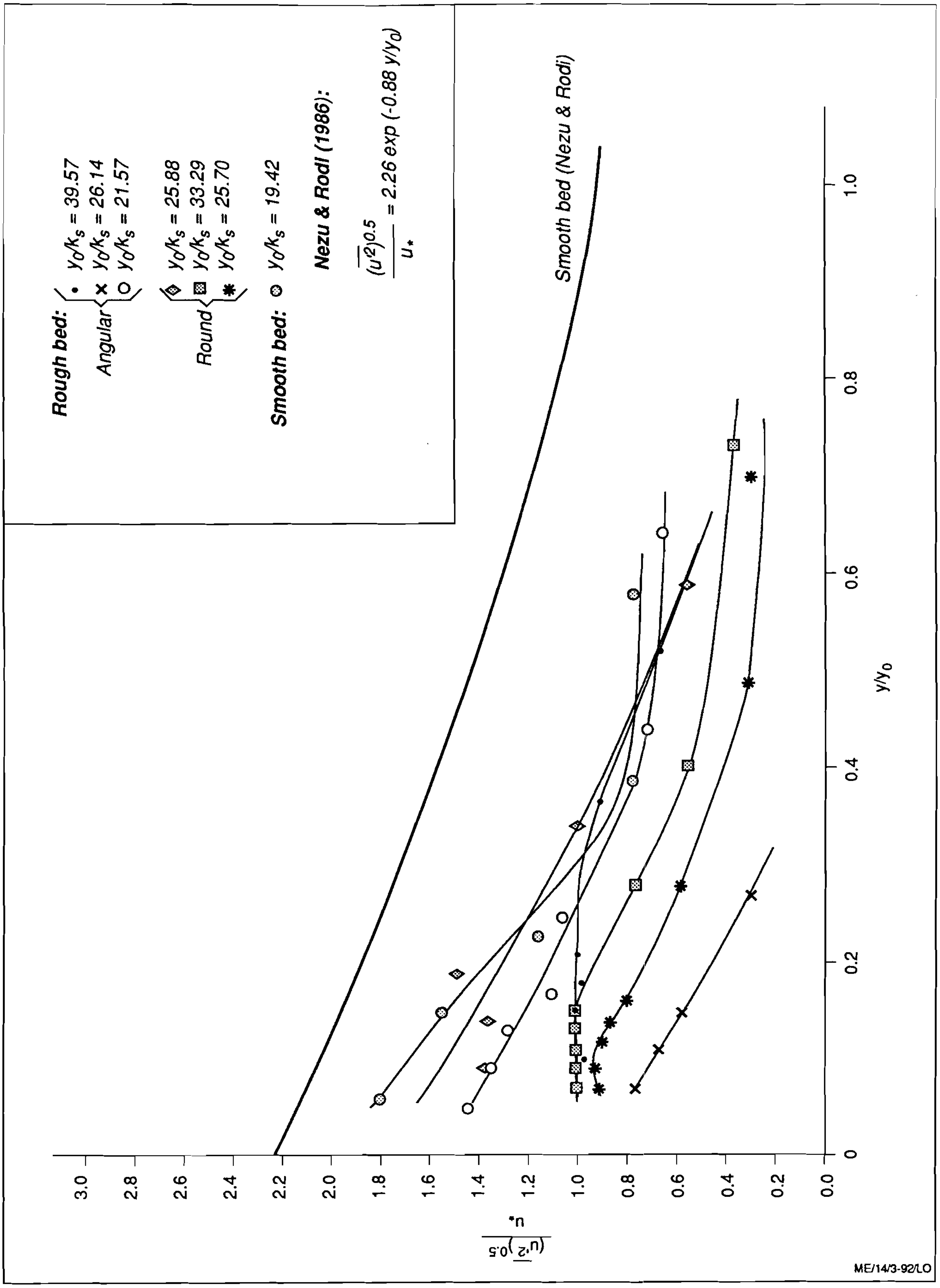

Figure 14 Distribution of $(\overline{u'^2})^{0.5}/u_*$ with nondimensional depth – normal turbulence

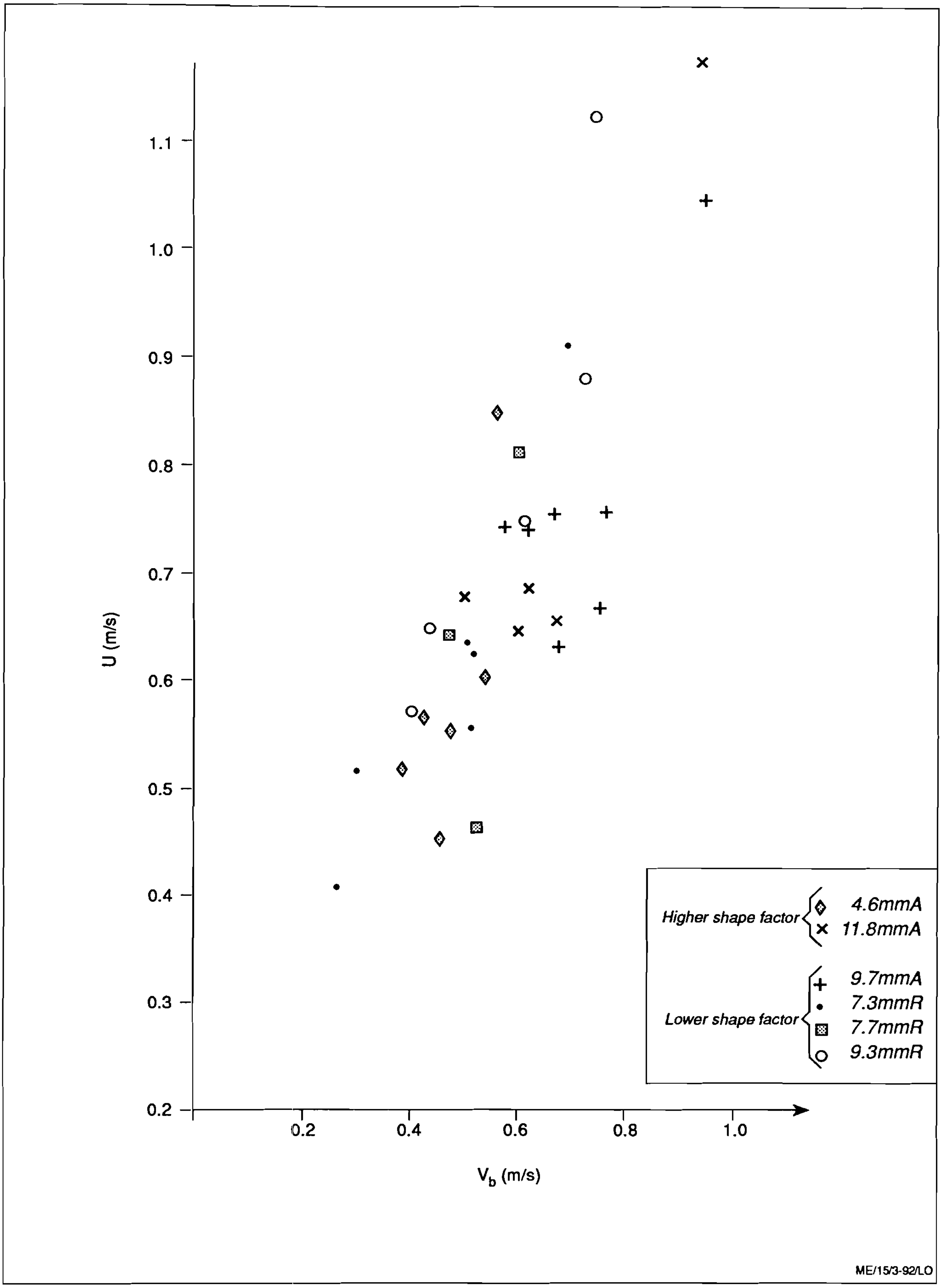

Figure 15 Effect of the shape factor on the relationship between bottom and mean velocities

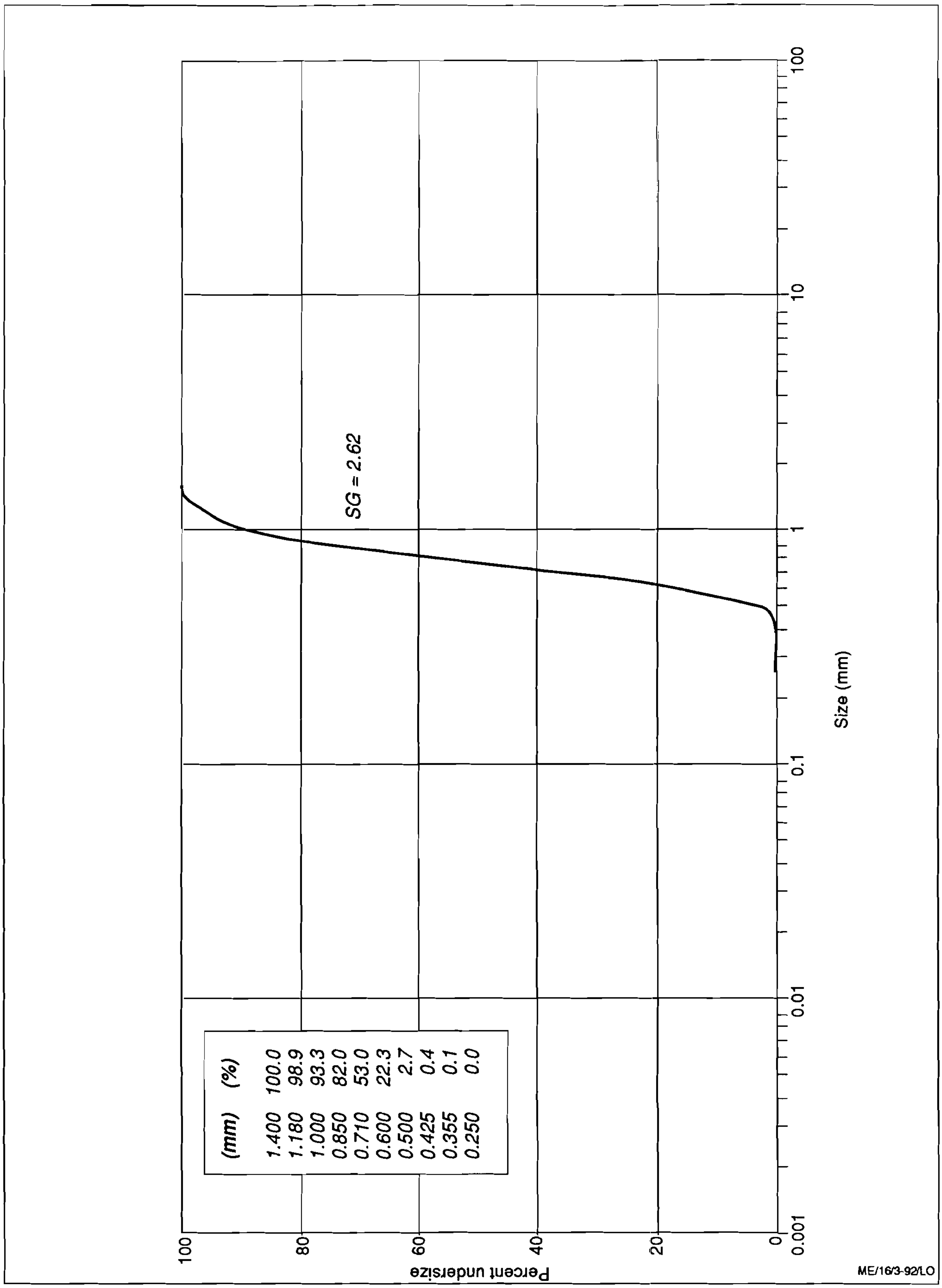

Figure 16 Grading curve of sand used in tests of filters

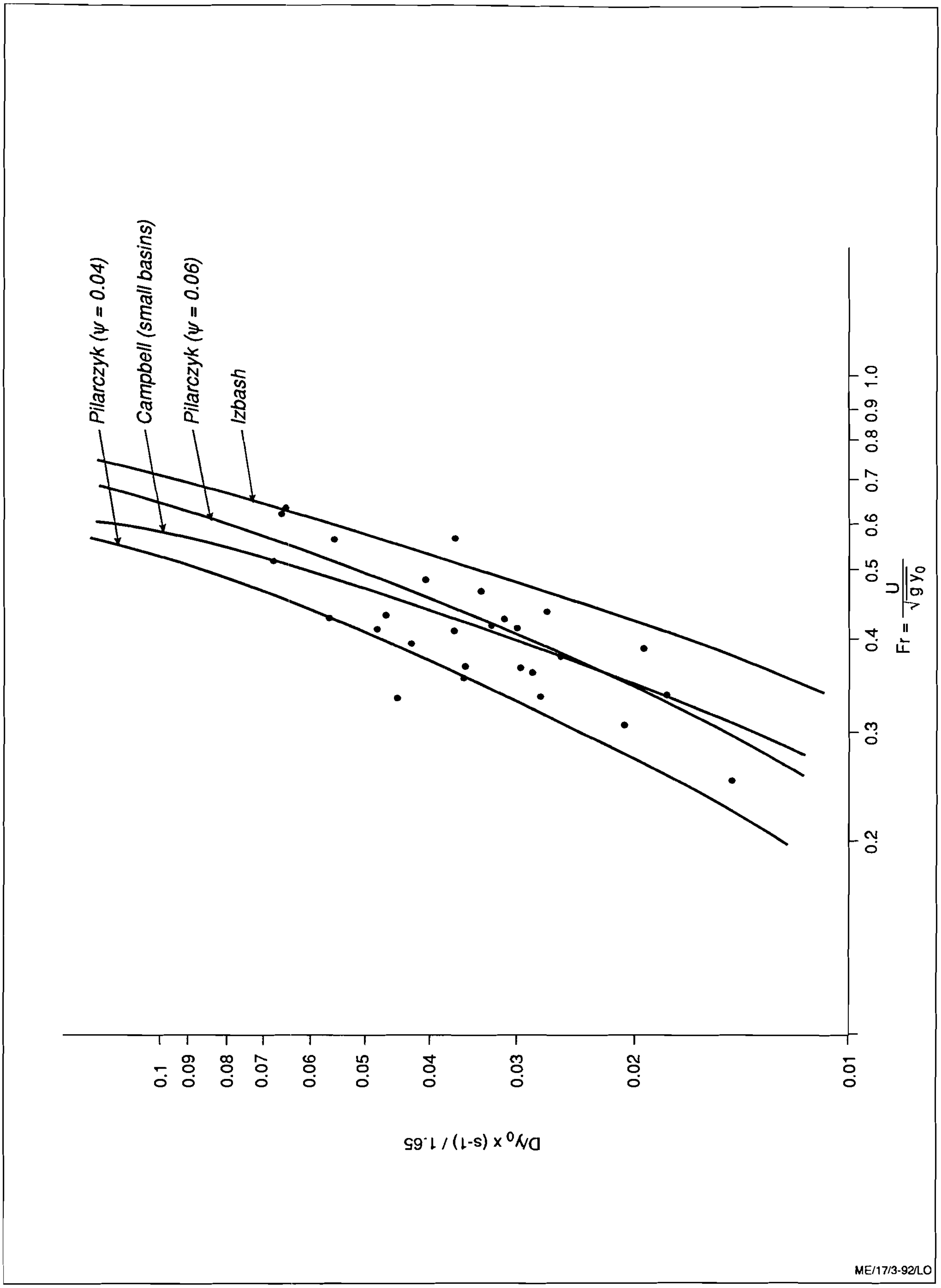

Figure 17 Comparison of equations proposed by Izbash, Campbell and Pilarczyk with the results for riprap on flat bed

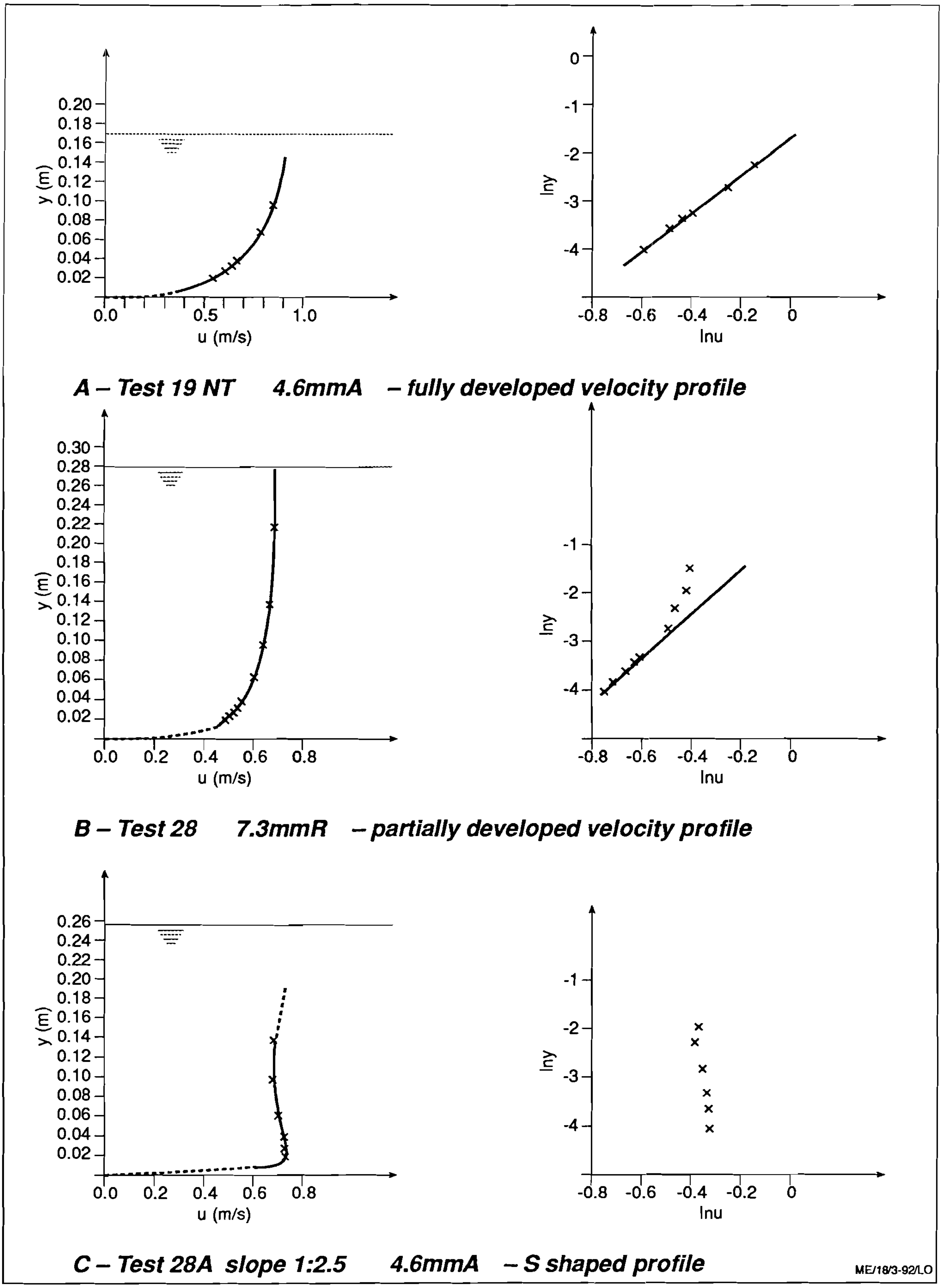

Figure 18 Types of velocity profiles

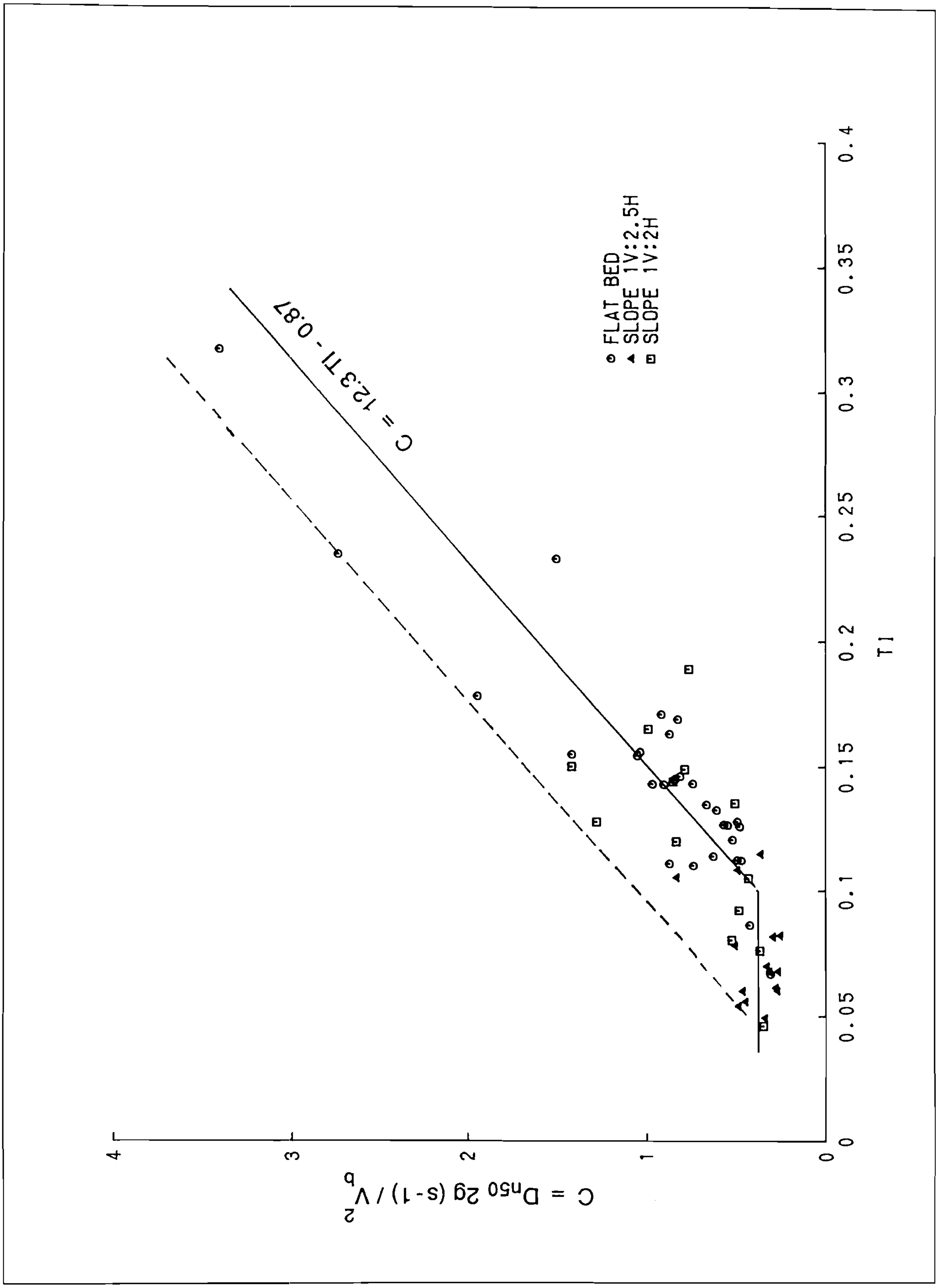

Figure 19 Relationship between C and the turbulence intensity for riprap

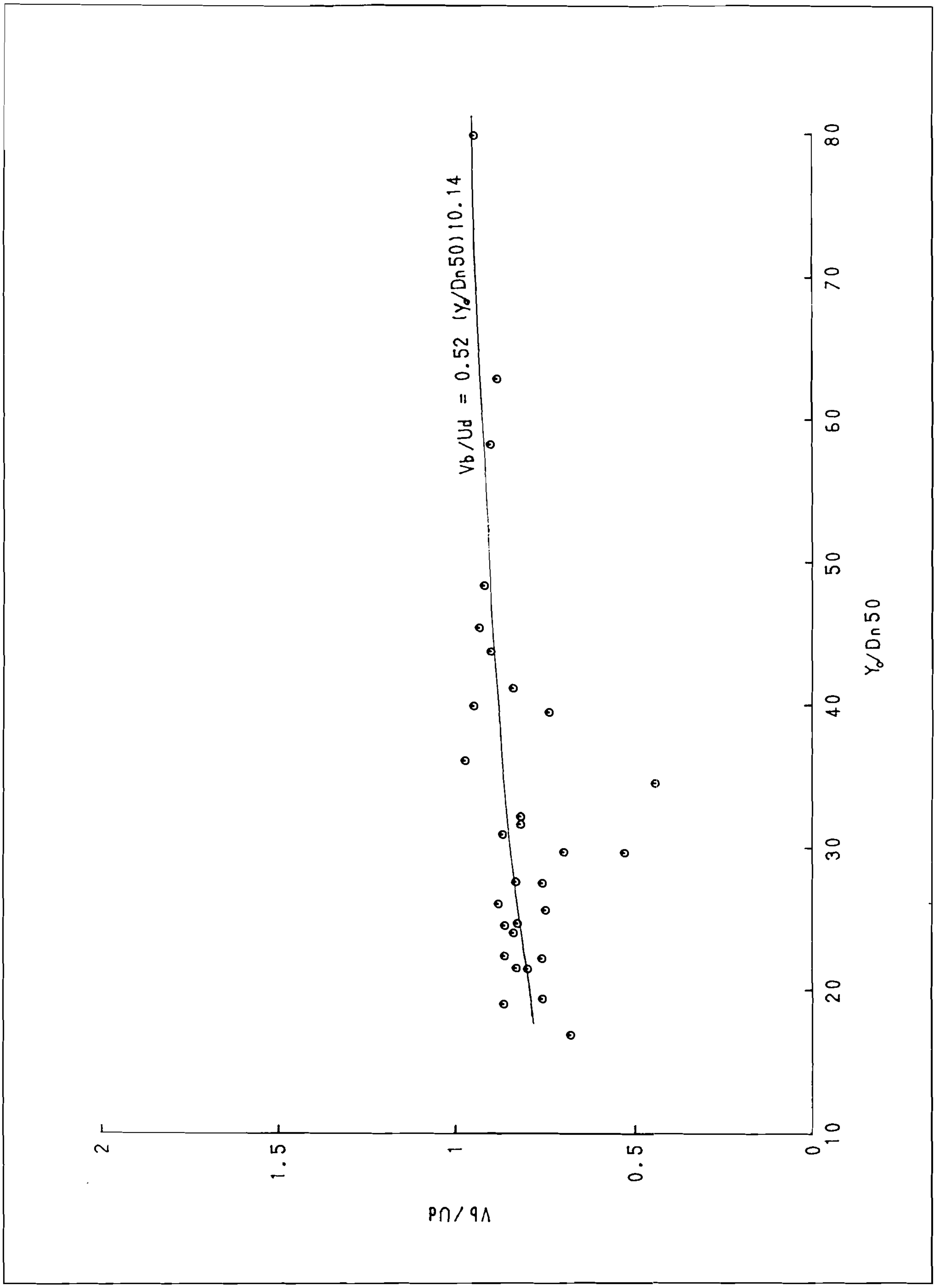

Figure 20 Relationship between bed velocity and depth averaged velocity – riprap on flat bed

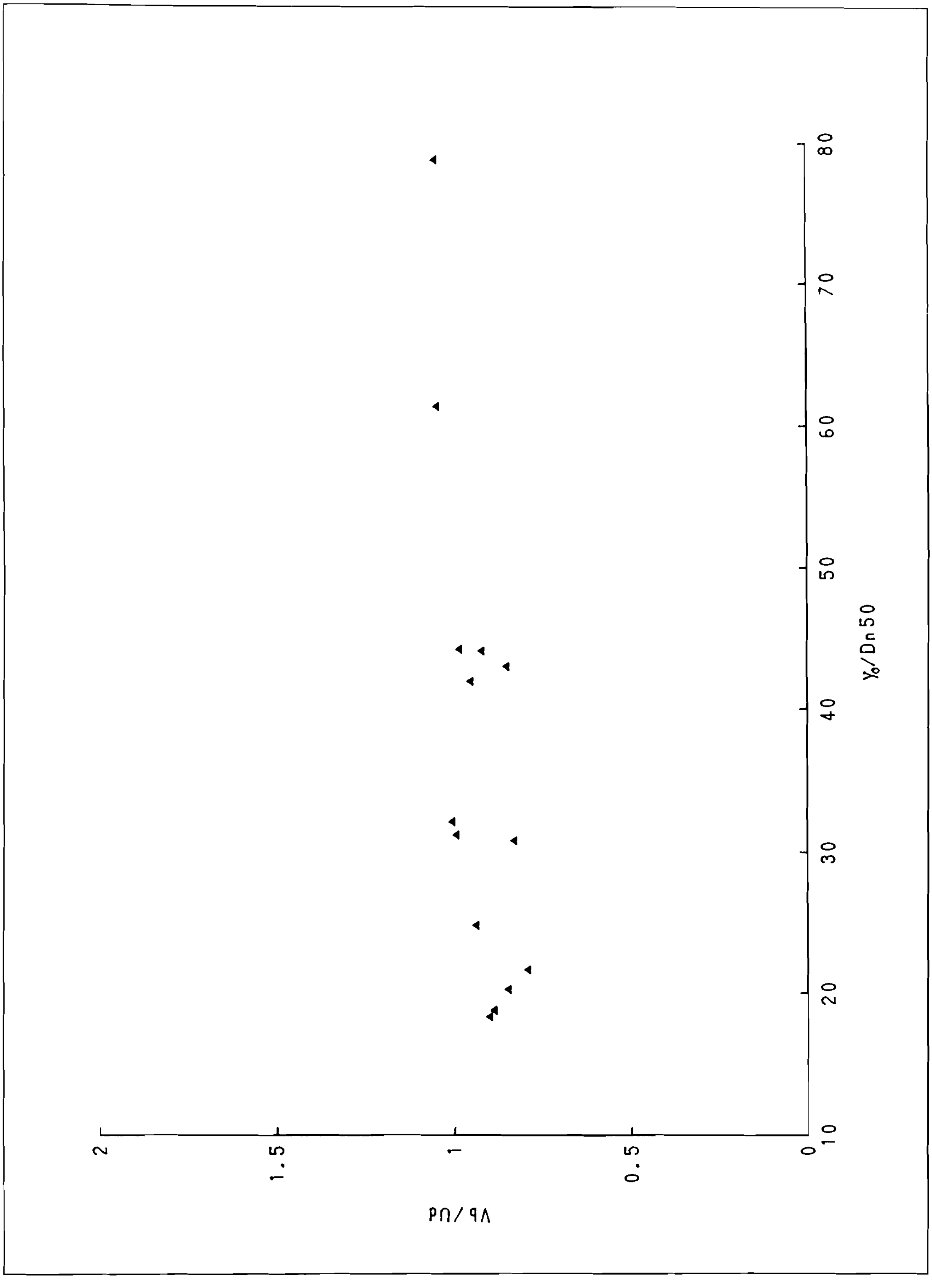

Figure 21 Relationship between bed velocity and depth averaged velocity – riprap on slope 1:2.5

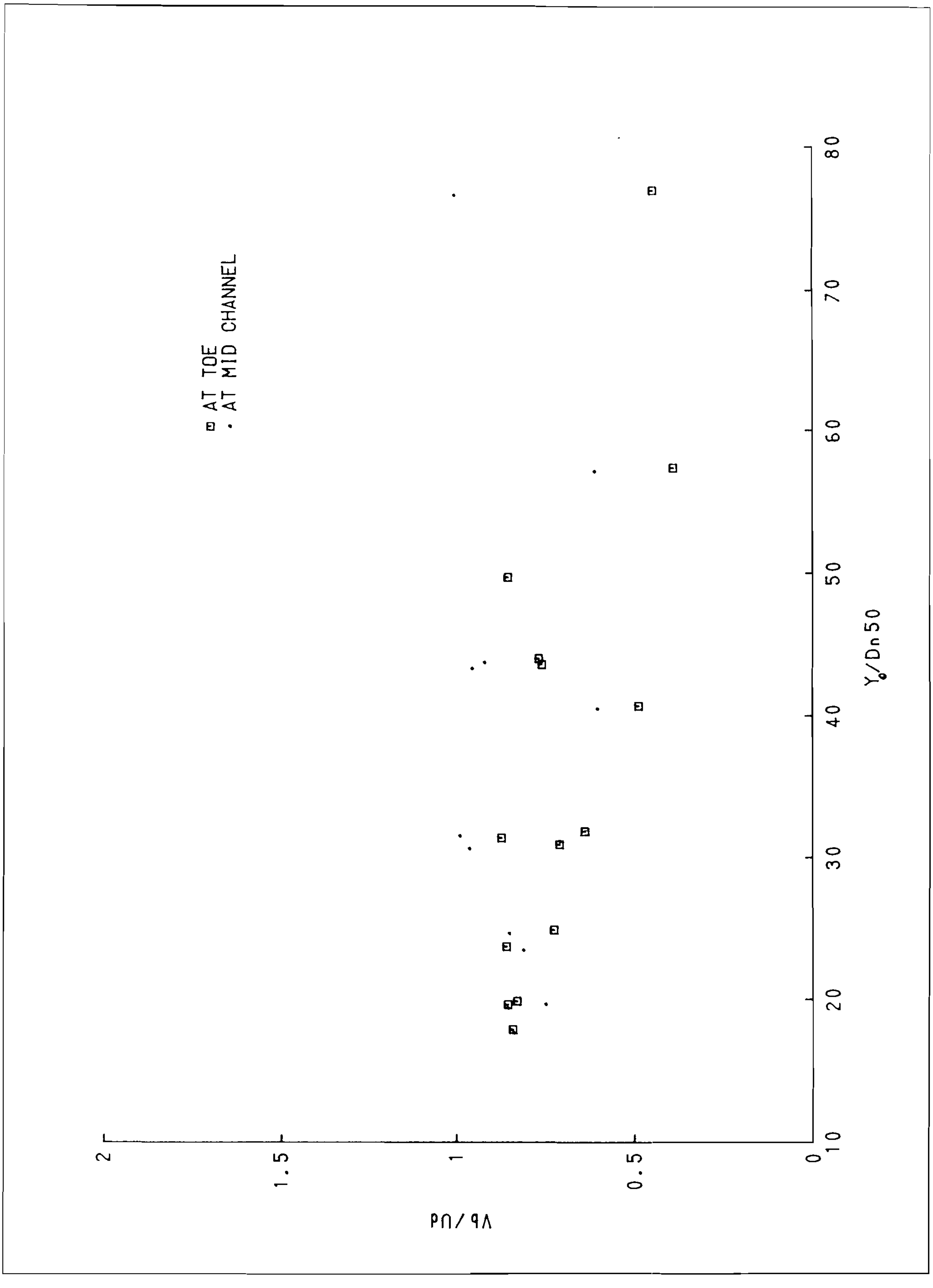

Figure 22 Relationship between bed velocity and depth averaged velocity – riprap on slope 1:2

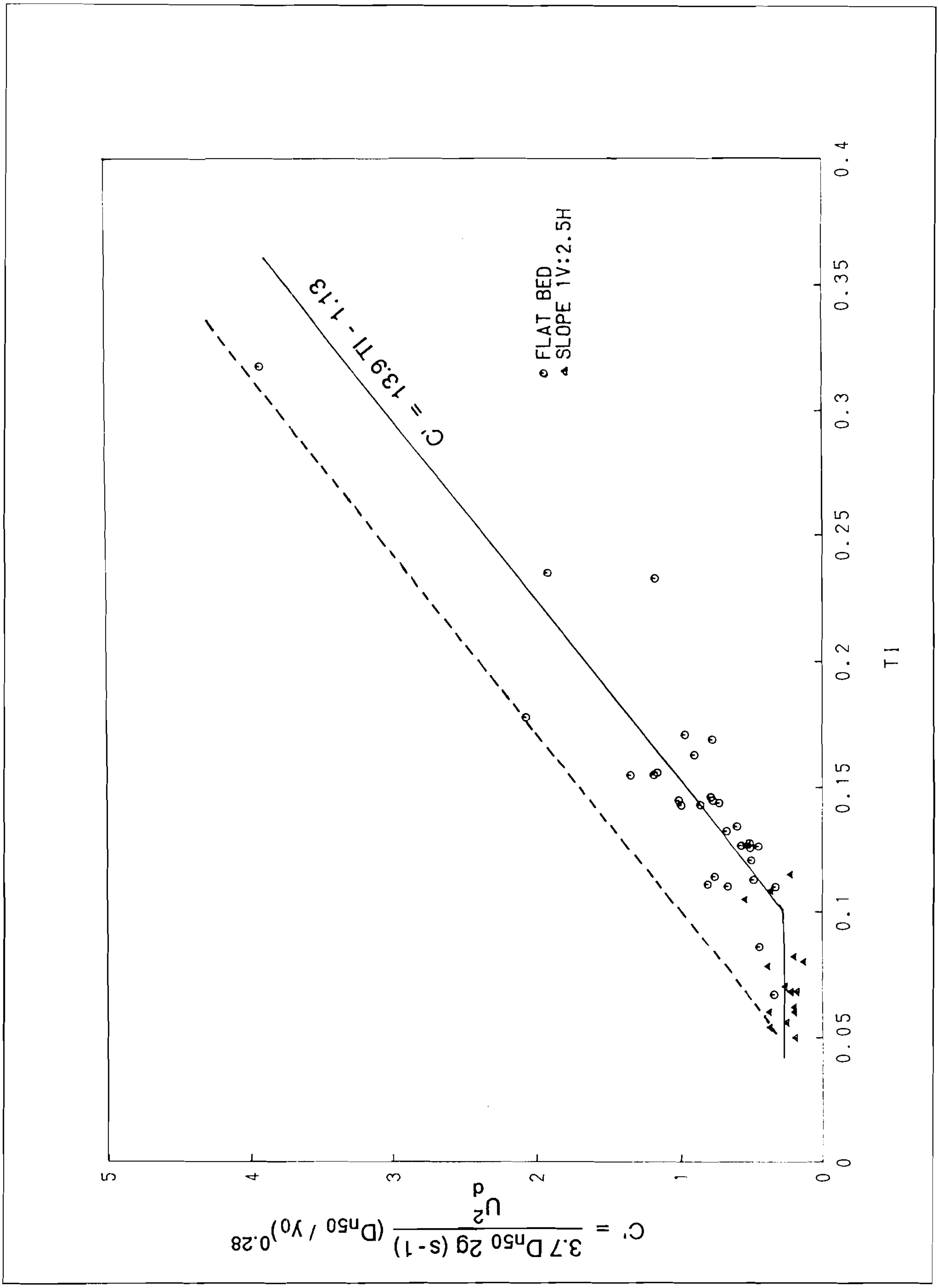

Figure 23 Relationship between C'and the turbulence intensity for riprap

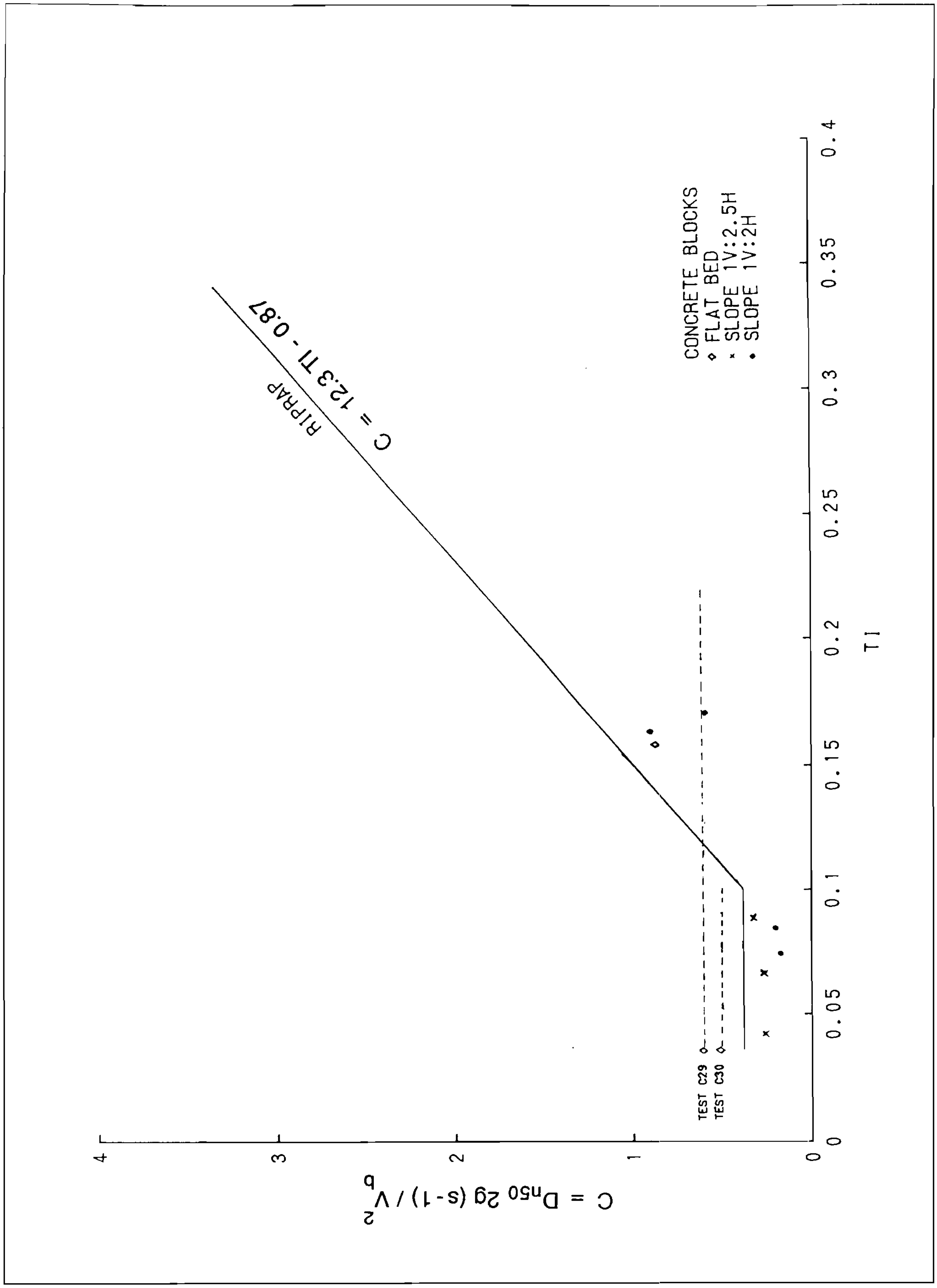

Figure 24 Relationship between C and TI for riprap and concrete blocks

PLATES

Plate 1 Test rig with stone size 9.7mmA

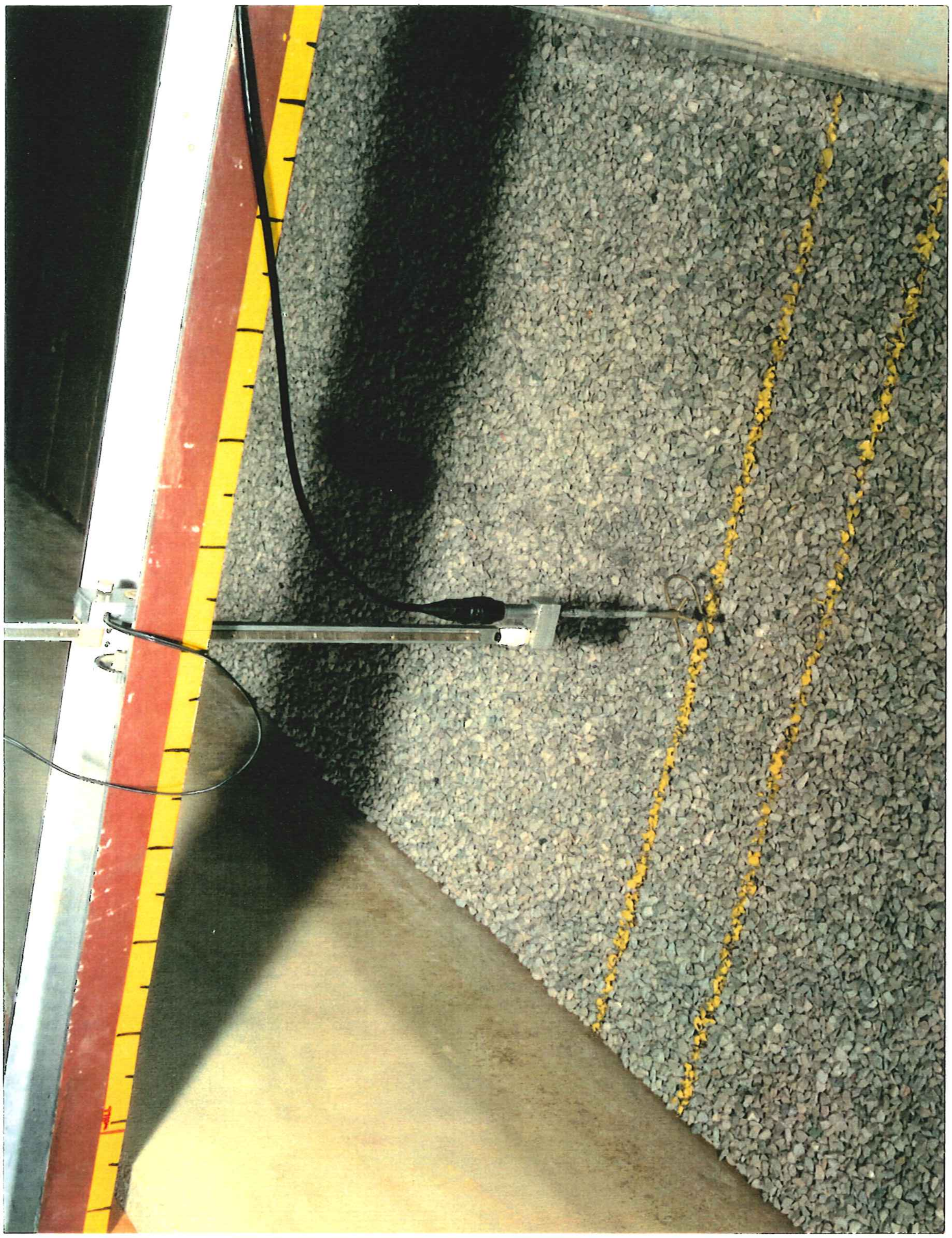

Plate 2 View of the ultrasonic current meter

Plate 3 Riprap on bed. Test with stone 11.8mmA,
$Q = 0.271m^3/s$ and $y_o = 0.342m$

Plate 4 Riprap on bed. Test with stone 11.8mmA, $Q = 0.271m^3/s$ and $y_o = 0.342m$. Detail of the probe and mobile bed

Plate 5 Concrete blocks on flat bed before a test

Plate 6 Concrete blocks on flat bed after a test

Plate 7 Concrete blocks on bank with slope 1:2

Plate 8 Concrete block on bank with slope 1:2.5.

Staggered

APPENDICES

APPENDIX A

Description and specifications of the ultrasonic Minilab current meter

DESCRIPTION OF COMPONENTS

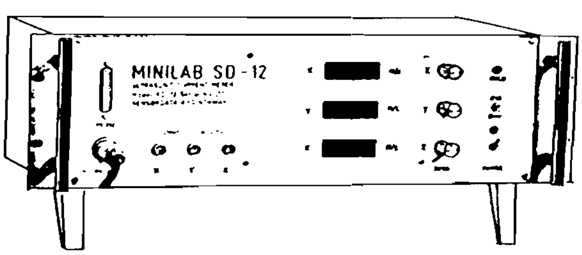

Display Unit 3000

19 inch rack cabinett containing power supply, processing circuits, digital displays and terminals for analogue and RS – 232C formated signals.
Dimensions of cabinett 435 x 132 x 245 mm.

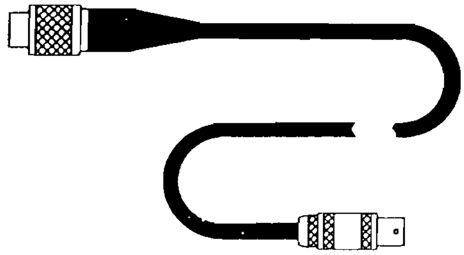

Instrument Cable 3003

Polyurethane cable with waterproof termination.
Connects probe house to display unit.
Standard length is 10 meter. Other practical lengths may be specified.

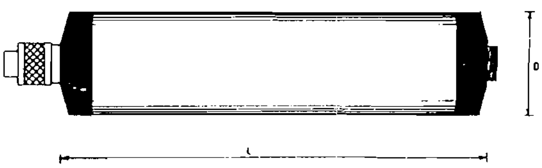

Probe House 3001

Tubular housing (D = 60 mm, L = 400 mm) which contains acoustic preprocessing circuits. The probe house is waterproof. It can be connected directly to the probe thus functioning as a stiff probe handle, or it can be indirectly connected to the probe via the probe extension cable. The connector on top of probe house mates with the waterproof connector on the instrument cable 3003.

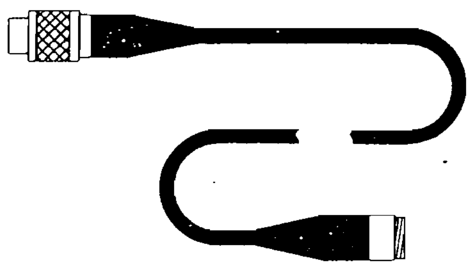

Probe Extension Cable 3002

Polyurethane cable for flexible connection between probe and probe house. Length: 4 meter.

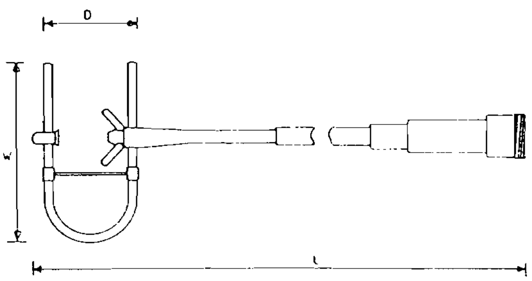

3 Axis Probe 3004

Consists of 3 orthgonal pairs of 2 x 5 mm piezoelectric 4 MHz trandusers mounted on stem. The net acoustic path length is 30 mm. The stem is terminated with underwater connector which mates with the connector of the probe cable and the probe house.
Dimensions: W: 91 mm, D: 49 mm, L: 300, 600 or 750 mm (chooseable).

SYSTEM SPECIFICATIONS

Range	: 0 to + / – 1 m/s (Gain x 1) 0 to + / – 10 m/s (Gain x 10)
Resolution	: 1 mm/s
Response time	: 1/30 s
Number of axes	: 3 (X, Y and Z)
Analogue outputs	: 0 to + / – 10V
RS-232C output	: 300 – 19200 baud, ASCII Coded BCD, 1 start bit, 8 data bits (unit m/sec), 1 stop bit, even or odd parity (selectable).

Cable length	: 10 meter standard (other lengths may be specified)
Maximum fluid temperature	: 100 centigrades
Power	: 115 or 230V, 50 – 60 Hz, 50 W
Dimensions	: See description above
Weight	: Display Unit: 4,7 kg Instrument Cable: 1,1 kg Probe House: 2 kg Probe Extension Cable: 0,5 kg
Packing	: Instrument case (plywood)
Gross weight	: 16 kg

APPENDIX B

Calculation of bed shear stress from measured mean velocity profiles

APPENDIX B

Calculation of bed shear stress from measured mean velocity profiles

It is well established that the turbulent boundary layer can be subdivided into an inner and an outer regions. In the inner region it is possible to distinguish two different layers: the bed layer, dominated by viscous forces, and the fully turbulent layer, where the velocity distributions can be described by a logarithmic law. In the outer region the velocity profiles are no longer controlled by the fluid viscosity or the roughness of the wall but depend on the nature of the free-stream flow if the boundary layer does not occupy the whole depth of the flow.

For flows over rough surfaces the thickness of the viscous bed layer is usually very small. In the present study the somewhat bulky nature of the ultrasonic probe did not allow measurements to be taken very close to the bed. Therefore, only data from outside the viscous bed layer were used in the calculation of the shear stresses. The velocity law in the inner region derives from the semi-empirical theory of pipe resistance developed by Nikuradse, and further developed by Prandtl, and has the following form:

$$\frac{u}{u_*} = \frac{1}{K} \ln \frac{y}{z} + A$$

$$\text{or} \quad \frac{u}{u_*} = \frac{1}{K} \ln \left(\frac{A' y}{z}\right) \qquad \text{(B.1)}$$

where

u	mean velocity at height y
u_*	shear velocity
K	von Karman constant (usually taken as 0.4)
y	height above the bed
$z/A'=z_0$	"reference height", a concept introduced to establish the height where the mean velocity is zero
A, A'	constants for a given set of conditions.

In the outer region of the boundary layer the velocity profiles can be described by the velocity-defect law:

$$\frac{u_m - u}{u_*} = -\frac{1}{K} \ln \frac{y}{\delta} \qquad (B.2)$$

where

u_m maximum value of velocity in the profile

δ thickness of the boundary layer.

A comprehensive experimental study of turbulent velocity profiles over rough boundaries using a laser-doppler anemometer was carried out recently by Kirkgoz (1989). It showed that, for the same range of roughness as used in the present study, the velocity-defect law did not describe the velocity distributions as well as the logarithmic law. Based on these findings and on what was mentioned before concerning the bed viscous layer, it was decided to calculate the bed shear stress according to the logarithmic law in eqn (B.1).

The velocity profile equation can thus assume the following form:

$$u = \frac{u_*}{K} \ln y - \frac{u_*}{K} \ln (z_o)$$

or, adopting the general equation for a straight line

$$u = m \ln y + E$$

Linear regression through the measured points u and ln y will give a fitted gradient m and an intercept E, where

$$m = u_*/K$$

or

$$u_* = m K \quad and \quad E = - \frac{u_*}{K} \ln (z_o)$$

from which

$$z_o = \exp (- \frac{E}{m})$$

The bed shear stress, τ, may then be evaluated from

$$\tau = \rho \, u_*^2$$

where ρ is the density of water.